

**INTEGRITY ASSESSMENT FOR AGING STRUCTURES —
EVALUATING AND IMPROVING THE EFFECTIVENESS OF
ULTRASONIC TESTING**

FINAL REPORT

TEES Projects 32525-51790, 5179MA, 5179MB

by

L.D. Lutes, T.L. Kohutek, B.K. Ellison, and K.F. Konen

**Texas Engineering Experiment Station
Texas A&M University
College Station, Texas**

December 1999

ACKNOWLEDGMENTS

This project was funded by two companies involved in the recovery of oil and gas and a federal agency responsible for regulation of that industry. The technical representatives of these organizations are an essential part of the research team. The authors hereby express their appreciation to them for their financial support and technical input throughout this project. The following is a list of the financial sponsors and their representatives:

Minerals Management Services
Dr. Charles Smith
Ms. Amy White
Engineering and Technology
381 Elden Street
Herndon, VA 20170-4021
703-787-1665

Shell Deepwater Development, Inc.
Mr. Kris A. Digre
P.O. Box 576
Houston, TX 77001-0576
713-544-4104

Mobil Technology Company,
Mr. Christopher P. Burke
Dr. S.N. Raju Pakalapati
13777 Midway Road
Dallas, TX 75244-4390
972-851-7156

In addition to those listed above, the authors hereby recognize the very substantial assistance received from the firm of J. Ray McDermott, Inc. Thanks is expressed for not only allowing the research assistants to perform field studies within the facilities of the firm, but also providing technical assistance during the performance of those field studies. The primary contact was:

Mr. Larry Verzwylt
J. Ray McDermott, Inc.
Fabrication Division
Morgan City, LA

TABLE OF CONTENTS

LIST OF FIGURES	iv
LIST OF TABLES	vii
EXECUTIVE SUMMARY	viii
CHAPTER I. INTRODUCTION / BACKGROUND	1
1.1 Objectives	1
1.2 Present Status of the Problem	1
1.3 Motivation for Research	4
1.4 Overview of Present Research	6
CHAPTER II. EQUIPMENT AND PROCEDURES	8
2.1 Experimental Studies	8
2.2 Specimen Coordinates and Nomenclature	13
2.3 Statistical Studies	13
CHAPTER III. EFFECT OF THICKNESS ON STRENGTH	21
3.1 Uniform Loss of Wall Thickness	21
3.2 Unsymmetric Loss of Wall Thickness	24
3.3 Determination of Controlling Condition	28
CHAPTER IV. FIELD STUDY	32
4.1 Description of Site	32
4.2 Description of Specimens	33
4.3 Specimen Analysis – UT Thickness Data	39
CHAPTER V. LONGITUDINAL VARIATIONS OF THICKNESS	51
5.1 Member 01 (Forest I, Diagonal)	52
5.2 Member 02 (Forest II, Diagonal)	54
5.3 Member 03 (Santa Fe, Diagonal)	57
5.4 Member 04 (Forest I, Horizontal)	61
5.5 Member 05 (Forest II, Horizontal)	63
5.6 Member 06 (Santa Fe, Horizontal)	65
5.7 Summary of Observations	66
CHAPTER VI. CIRCUMFERENTIAL VARIATIONS OF THICKNESS	69
6.1 Plots and ANOVA Results	69
6.2 Further Analysis of θ Dependence	74
CHAPTER VII. ISSUES RELATED TO TESTING PROTOCOL	83
7.1 Review of Corrosion Trends	83
7.2 Effect of Sample Size on Detection of Strength Loss	87
7.3 Summary	92
CHAPTER VIII. SUMMARY AND RECOMMENDATIONS	94
8.1 Summary	95
8.3 Recommendations	95
8.2 Recommendations	98
REFERENCES	100

LIST OF FIGURES

<u>Figure No.</u>	<u>Page</u>
1.1 New Anode.....	3
1.2 Spent Anode	3
2.1 Dual Transducer Sound Paths.....	10
2.2 Specimen Coordinates.....	13
3.1 Worst-Case Unsymmetric Corrosion.....	26
3.2 Values of P_{unsym} / P_{sym} for $P_{unsym} < P_{sym}$	30
4.1 Gulf of Mexico Structure Locations	35
4.2 Circumferential Ray Location	35
4.3 Forest Jacket Schematic Drawing.....	36
4.4 Forest I Jacket.....	37
4.5 Forest II Jacket.....	37
4.6 Forest Jacket Orientation (Plan View)	37
4.7 Santa Fe Lean-to Structure Schematic Drawing.....	38
4.8 Santa Fe Jacket Orientation (Plan View)	39
4.9 Member 01 (Facing Ray E).....	40
4.10 Member 01 (Marine Growth Removed at Ring)	40
4.11 Member 01 Schematic Drawing	40
4.12 Member 02 Schematic Drawing	40
4.13 Member 03 (Facing Ray A).....	41
4.14 Member 03 Schematic Drawing	41
4.15 Member 03 Subsection Schematic Drawing	42
4.16 Member 04 (Full-length).....	44
4.17 Member 04 (Corrosion at Grate, View from Deck).....	45

LIST OF FIGURES (Continued)

<u>Figure No.</u>	<u>Page</u>
4.18 Member 04 (Heavy Corrosion, View toward Deck).....	45
4.19 Member 04 Schematic Drawing (View toward Deck).....	45
4.20 Member 04 Railing System Detail.....	46
4.21 Member 05 (Full-length).....	46
4.22 Member 05 Dent (View toward Deck).....	47
4.23 Member 05 Dent (View from Center of Structure)	47
4.24 Member 05 Schematic Drawing (View toward Deck).....	47
4.25 Member 06 (View from Deck)	48
4.26 Member 06 Schematic Drawing (View toward Deck).....	48
5.1 Longitudinal Relationships for Member 01, Showing All Rings	54
5.2 Longitudinal Relationships for Member 01, Showing Rings 4-14 (Average over All Rays).....	54
5.3 Longitudinal Relationships for Member 02, Showing All Rings	56
5.4 Longitudinal Relationships for Member 02, Showing Rings 4-13 (Average over All Rays).....	56
5.5 Longitudinal Relationships for Member 03, Showing All Rings	58
5.6 Longitudinal Relationships for Member 03, Showing Rings 1-7.....	59
5.7 Longitudinal Relationships for Member 03, Showing Rings 8-16.....	59
5.8 Longitudinal Relationships for Member 03, Showing Rings 1-7 (Average over All Rays).....	60
5.9 Longitudinal Relationships for Member 03, Showing Rings 8-16 (Average over All Rays).....	60
5.10 Longitudinal Relationships for Member 04, Showing All Rings	62

LIST OF FIGURES (Continued)

<u>Figure No.</u>	<u>Page</u>
5.11 Longitudinal Relationships for Member 04, Showing Rings 2-9 (Average over All Rays).....	62
5.12 Longitudinal Relationships for Member 05, Showing All Rings	64
5.13 Longitudinal Relationships for Member 05, Showing Rings 3-9 (Average over All Rays).....	64
5.14 Longitudinal Relationships for Member 06, Showing All Rings	65
5.15 Longitudinal Relationships for Member 01, Showing All Rings (Average over All Rays).....	66
5.16 Wall Loss in Forest Structure (Schematic).....	68
5.17 Wall Loss in Santa Fe Structure (Schematic).....	68
6.1 Circumferential Relationships for Member 01, Average over Rings 1-3 and Average over Rings 4-14	70
6.2 Circumferential Relationships for Member 02, Average over Rings 4-13 ..	71
6.3 Circumferential Relationships for Member 03, Average over Rings 1-7	71
6.4 Circumferential Relationships for Member 03, Average over Rings 8-16 ..	72
6.5 Circumferential Relationships for Member 04, Average over Rings 2-9	72
6.6 Circumferential Relationships for Member 05, Average over Rings 3-9	73
6.7 Circumferential Relationships for Member 06, Average over All Rings	73
6.8 General Notation for Thickness Comparisons.....	75
7.1 Summary of Corrosion Trends, Forest Jacket	85
7.2 Summary of Corrosion Trends, Santa Fe Jacket	86
7.3 Thickness Comparison Summary	87
7.4 Sample Size to Give Prescribed Error Bound	92

LIST OF TABLES

<u>Table No.</u>	<u>Page</u>
2.1 Effect of Sample Size ($\alpha = 0.05$)	20
4.1 Jacket Structure Histories	33
4.2 Member Descriptions	34
4.3 UT Thickness Measurements for Member 01	42
4.4 UT Thickness Measurements for Member 02	43
4.5 UT Thickness Measurements for Member 03	43
4.6 UT Thickness Measurements for Member 04	49
4.7 UT Thickness Measurements for Member 05	49
4.8 UT Thickness Measurements for Member 06	50
5.1 Summary of Results for Longitudinal Variation of Thickness	67
6.1 Summary of ANOVA Results for Circumferential Relationships	74
6.2 Mean Thickness Values for Grouped Data, Using All Rings	76
6.3 Mean Thickness Values for Grouped Data, Grouping Only Rings with the Same Nominal Thickness	77
6.4 Summary of <i>t</i> -test Results for Circumferential Relationships	80
7.1 Thickness Bounds from Reduced Samples ($\alpha = 0.05$)	89

EXECUTIVE SUMMARY

This report documents the work performed and the results obtained in the joint industry project (JIP), "Integrity Assessment for Aging Structures — Evaluating and Improving The Effectiveness of Ultrasonic Testing." The project was funded by the Minerals Management Service of the Department of the Interior, Mobil Technology Company, and Shell Deepwater Development, Inc., and was conducted by the Texas Engineering Experiment Station at Texas A&M University. The Principal Investigator was Loren D. Lutes, P.E., Ph.D., and the project was co-directed by Terry L. Kohutek, P.E., Ph.D.

The basic objectives of this project were:

- determination of the feasibility of using ultrasonic thickness (UT) measurements for assessment of corroded members in offshore structures,
- identification of any common patterns of corrosion in these members, which might be used in designing a more effective assessment protocol, and
- determination of the amount of data needed for meaningful assessment.

Ultrasonic (UT) measurements of thickness in an earlier JIP study gave evidence that the corrosion in members within offshore structure may not be randomly distributed. However, no information was available concerning the precise orientation of the studied bracing members, and such information is essential to the development of any procedure for making use of the corrosion patterns. Thus, the current study focused on obtaining additional thickness measurements either within offshore structures, or on members for which the precise *in situ* orientation was known. In addition, it was necessary to acquire state-of-the-art UT equipment for making in-place thickness measurements.

A Panametrics 26DL Plus device was selected for the current project, and extensive studies were performed to verify the adequacy of the device, as well as to train

the student research assistants in its use. Subsequently, this device was used to make extensive studies on six bracing members in-place within jacket structures that had recently been salvaged from their offshore environment in the Gulf of Mexico. The structures were in the offshore fabrication yards of J. Ray McDermott, Inc. in Morgan City, Louisiana. The six members chosen for study were located within three structures, with one diagonal member and one horizontal member analyzed in each structure. The diagonal members passed through the mean water level, and the horizontal members were within the splash zone.

Several statistical tests were used to determine the extent and usefulness of any patterns in the data obtained in the field study. These tests included analysis of variance, linear regression, and a *t*-test, as well as various types of plots that could reveal patterns in the data. In addition, analyses were performed to find the relationship between loss of wall thickness and the remaining compressive strength of a corroded member. These analyses included consideration of Euler buckling, inelastic buckling, and onset of yielding in a member with unsymmetrical corrosion.

The strength analyses performed in this study demonstrate that it is acceptable to use the API design formulas to predict member strength, even if the corrosion is not symmetrical. Since the API formulas for symmetric members are sufficiently conservative, there is no need to seek patterns of corrosion in the application of UT testing to actual structures. Rather, one should seek a conservative (i.e., lower bound) estimate of the remaining wall thickness of the member, then use the API formulas to predict strength for a member with that value of wall thickness, proceeding as if the thickness were the same everywhere. Thus, the importance of patterns of corrosion is that they might be used in designing the testing protocol, concentrating measurements at locations where the maximum corrosion is to be expected.

No conclusive evidence was found for useful variations of corrosion along the length of the members, even though the statistical analyses did show very small probabilities that the some of the longitudinal thickness variations could be strictly random. Since the trends were inconsistent, or contradictory, it is concluded that one should take measurements along the length of each member, including measurements near each end, in order to avoid the possibility of only taking measurements at a location with minimal corrosion.

The variation of corrosion around the circumference of the members was found to be quite small, but to have a consistency that may be useful in designing a testing protocol. In particular, it was found that each of the six members had more corrosion on the side located on the outer perimeter of the structure than it did on the side toward the center of the structure. This observed trend also agrees with an opinion held within at least some segments of the offshore industry, and may be related to the exposure to waves when the structures are in place in the Gulf of Mexico.

Tests were also performed to determine whether corrosion was negatively correlated with the proximity to a sacrificial anode, but no such correlation was observed. Apparently the anodes were sufficiently close together on these structures that there were no areas experiencing excessive corrosion because of lack of cathodic protection.

Statistical analyses were also used in an effort to determine the sample size needed to obtain reliable predictions of the strength loss due to corrosion in tubular members. In particular, a plot was developed to indicate the sample size that would produce a prescribed error bound for the mean thickness of a member with a particular observed value of the standard deviation of thickness. It was found that using only five or six measurement points can often give results which may be quite adequate in practice, but additional measurements may be needed if the standard deviation of the measurements is large. Since this standard deviation is generally unknown prior to UT testing, a two-stage procedure is recommended. Following the first five or six tests, one

can calculate the standard deviation and use the plot provided to determine whether more measurements are required in order to achieve the desired accuracy.

Based on the results of this research, it is apparent that UT is a feasible tool for assessment of wall thickness in aging offshore structures. It was found that the random errors in the results obtained from such an instrument are small enough to allow reliable measurements of wall thickness. In particular, the standard deviation values for repeated measurements at a given location on a given specimen were less than 0.001 inches for clean bar stock and less than 0.01 inches for badly corroded members. The measurement error is expected to be within these bounds for members of interest within existing structures. Further, with proper knowledge of the instrumentation, readings may be taken quickly and efficiently. The strength analyses showed that there is no need to identify corrosion patterns within the member being assessed, and it was found that estimation of only the average wall thickness can often be done quite reliably with relatively few data points. The pattern observed in the members studied reinforced an existing opinion that it is prudent to concentrate the UT measurements on the side of the member most exposed to waves from the open sea, in order to obtain a conservative estimate of the wall thickness. The measurements should be distributed over the length of the member, since corrosion can have a significant longitudinal variation that cannot be predicted *a priori*.

It is recommended that UT be seriously considered as a method of assessing the extent of corrosion in members in aging structures. This could be done in inspections of structures *in situ* in the sea, or in determining the condition of members within a structure being rehabilitated onshore before being put back into service.

CHAPTER I

INTRODUCTION / BACKGROUND

1.1 Objectives

This project concerns the use of ultrasonic testing for assessing the integrity of aging offshore structures. Specifically, the research discussed herein has three main objectives:

- determination of the feasibility of using ultrasonic thickness (UT) measurements for assessment of corroded members in offshore structures,
- identification of any common patterns of corrosion in these members that might be used in designing a more effective assessment protocol, and
- determination of the amount of data needed for meaningful assessment.

In addition, analyses will be presented to relate the compressive strength of a corroded member to its loss of wall thickness. These analyses will include consideration of Euler buckling, inelastic buckling, and onset of yielding in a member with unsymmetric corrosion.

1.2 Present Status of the Problem

The offshore industry began about 50 years ago in the Gulf of Mexico, with the first steel template-type structures installed in 1947 (Hennegan et al. 1993). Production and development in the North Sea began soon thereafter. Many of these structures have been in operation far beyond their intended lives, which are typically 20-25 years (Bea et al. 1988). Such being the case, there are new challenges in the area of maintenance and reevaluation of adequacy of these existing structures. The number of structures facing these new challenges is significant. At present, there are over 7,000 offshore structures around the world, with more than 3,800 of them located in the Gulf of Mexico (Wisch et al. 1993). Hennegan et al. (1993) summarized this challenge:

"Operators, owners, and regulatory bodies face a difficult challenge: to safeguard life and resources, yet provide an environment in which oil and gas reserves can be developed and profitably produced. The collapse of oil prices in the 1980's has put tremendous pressure on producers to eliminate waste. Inspection and intervention

programs have been heavily scrutinized and pressured to cut costs. All inspection programs in today's environment should be as inexpensive as possible while meeting the needs of the assessment and requalification practices."

Several factors contribute to this new challenging environment. Reassessment of offshore structures is sometimes due to violent climatic activity, such as Hurricanes Hilda and Betsy in the 1960's and Andrew in 1992. Public policy concerning environmental and life safety issues has also changed over the years, directly influencing the need for improved integrity assessment. Additionally, new technology has allowed the discovery and exploitation of new oil fields, bringing increased investments in the use of existing structures on the order of several hundred million dollars. The age of most structures is perhaps the major factor. Of the platforms in the Gulf of Mexico, 1,157 of them were installed prior to 1974 (James K. Dodson Co. 1993).

There are various types of damage inflicted on aging structures. These include deflected members, dents, tears, cracks, holes, deformed shapes, unusual deflections, missing members, and corroded members (Hennegan et al. 1993). Corrosion problems can result in significantly reduced wall thickness, and therefore must be monitored on aging offshore structures. Since cathodic protection is in common usage, most monitoring techniques involve measurements of anode consumption and electrical potential measurements (Lotsberg 1993). If anodes are not depleted and the potential is still sufficient, then further inspection is usually not carried out. Typical in-place anodes are shown in Figs. 1.1 and 1.2. Fig. 1.1 shows a new anode, while Fig. 1.2 shows an older anode with the marine growth and other deposits removed. If no anodes remain, or if the potential is not in an acceptable range, then visual and/or other forms of inspection are employed, possibly including UT inspection.

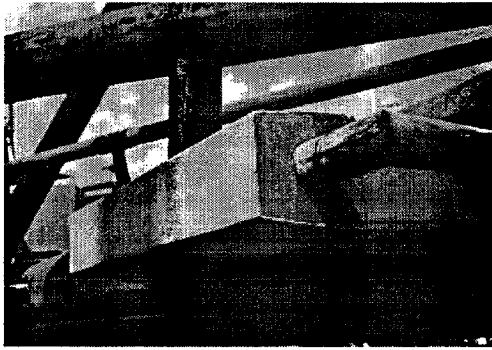


FIG. 1.1. New Anode

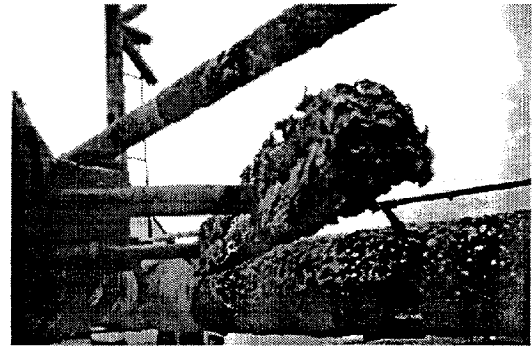


FIG. 1.2. Spent Anode

To take these measurements, a company may send a diver out to an offshore structure to take UT measurements near the splash zone. This "is the most critical area of protection due to alternate wet and dry conditions" (Rubio 1999). Indeed, studies have shown that corrosion here may be up to four or five times greater than in any other section of the platform (Lewis and Mercer 1984). Defined as extending roughly from the -15-foot elevation to +15-foot elevation relative to the mean sea level (Holdsworth and Townley 1999), the splash zone is often difficult to access. It is often the site of damage, and must be inspected both above and below the water as thoroughly as possible (Hennegan et al. 1993). Cathodic protection is not available or not effective in this zone, since there is not continual submersion, and the constant wetting with turbulent oxygenated seawater provides ideal corrosion conditions. The inspection procedure is dangerous and expensive, and it is often difficult to obtain UT thickness readings in such circumstances, even in the best of weather conditions. Such monitoring has often been avoided in the past, such as in the United Kingdom where there are pressures to reduce inspection because it can represent up to 40% of operating costs (Winkworth 1993). If UT measurements are taken, the number may be very limited because of the difficulties involved. Thus, there are serious questions concerning the cost effectiveness of the UT procedure.

Lotsberg (1993) has pointed out that improvements are needed in splash zone coatings for the construction phase, for permanent use, and for repair painting. Loss of wall thickness due to corrosion in the splash zone has become less of a problem in recent years due to increased use of such corrosion protection, which has resulted from increased research on the problem. New corrosion resistant membranes are sometimes placed on the members in the splash zone area. Pemex Exploration and Production has used a protective epoxy coating called "RE-32" in the Bay of Campeche with satisfactory results (Rubio 1999). Ameron International provides a similar spray-applied epoxy cladding called "Tideguard" that may be applied either in the fabrication yard or on a structure in-place in the sea. However, most current in-place members have survived their design lives without such recent advances, suffering corrosion and subsequent loss of wall thickness, and must therefore be monitored and reevaluated.

Another possible application of the current research concerns the requalification of structures that have been removed and brought ashore for refurbishment. It is possible that UT measurements might provide an economical and useful tool for determining the structural adequacy of the members within such a structure. Use of UT in this situation does not face all of the difficulties inherent to *in situ* measurements. In particular, such shipyard measurements would not require a diver and could be performed without concern for waves or other adverse sea conditions. Thus, it would generally be feasible to obtain much more extensive sets of UT measurements when they were performed on shore, suggesting that the current study should not necessarily be limited to the use of small sample sizes.

1.3 Motivation for Research

As described earlier, it is typically feasible to take only a few UT measurements on a splash-zone member in-place within a structure in the sea, and these measurements are made in less than ideal conditions. There have often been questions concerning the adequacy of the number of measurements and the accuracy of these measurements.

Additionally, it has been difficult to establish an appropriate level of confidence for these integrity assessments. Such questions, along with the challenges presented in Section 1.2, have prompted the current research (with the objectives stated at the beginning of this chapter). In addition to assessing the general usefulness of UT measurements, there has been an attempt to devise means of improving the effectiveness of ultrasonic thickness testing. The concept of this study developed from the results of a joint industry project (JIP) that was carried out at Texas A&M University (TAMU) from 1989 to 1990 (Moehlman 1990).

In 1989, several offshore companies shipped a total of nineteen salvaged tubular members to TAMU for various tests, including observation of buckling strength, buckled shape, and post-buckling behavior. These members had been removed near the splash zone from a number of structures, and exhibited different levels of corrosion and other damage such as holes, bends, and dents. They varied from 17 to 40 feet in length, and from 10.75 to 18 inches in diameter. Column buckling tests were performed on all members. Because of variability of wall thickness, some of the specimens failed locally without exhibiting global column buckling behavior. Strain gages were placed on each member at regularly spaced intervals to aid in the analysis, and UT measurements were made at these locations. The strain gage locations were at 30 locations - every 60° around the circumference at each of five locations along the length. A cursory analysis of these thickness measurements suggested the existence of certain non-random patterns in corrosion and wall thickness in the members.

Patterns seemed sometimes to occur around the circumference of a member and sometimes along the member's length. However, variability of wall thickness over the surface of a typical member was not the primary objective of that study. Furthermore, the UT devices used in that study were much less reliable than currently available equipment. Overall, it was concluded that more extensive research was needed to determine if indeed there is any useful correlation to the patterns of corrosion. Such

information was deemed to be important inasmuch as it might possibly be of use in developing an efficient protocol for assessing corroded members in aging platforms. In particular, a non-random, repeatable corrosion pattern in the members could lead to the *a priori* identification of the location on some other member which is likely to have the maximum corrosion and the minimum wall thickness. A measuring protocol could then be established in which divers would concentrate their measurements in the most vulnerable positions. The efficiency and cost benefits of such integrity assessment tasks might be greatly increased. For example, if the data were to show that reduction in wall thickness is greatest near the top of horizontal in-service members, then divers could gain the most useful information by concentrating their UT measurements on this portion of the members.

1.4 Overview of Present Research

This project has been a joint effort, with funding from the Mineral Management Service (MMS) of the Department of the Interior, from Shell Deepwater Development, Inc., and from Mobil Technology Company. The main goals have been to obtain and use new UT thickness data from existing offshore structures to evaluate and improve the effectiveness of UT measurements as an assessment tool.

The members from the 1989 study were all structural bracing members from the splash zone. However, they came with no specific information regarding their original orientation and location within the structure. Therefore, these members had limited use in the present research. They were used, though, for sample measurements in the process of gaining familiarity with the new measuring equipment, determining reproducibility of measurements, etc. Although UT testing is quick, reproducible, and relatively inexpensive, it is very important that the operator has "proper training in the use and limitations of the equipment" (Potter 1994). The old members were very useful in the very important process of calibration of the UT device (Konen 1999).

The contents of the current report can be summarized as follows: Chapter II describes the tools used in the research, including the UT measurement device and the statistical tools used in the search for meaning in the data. Chapter III presents an analysis of the strength of corroded members, in order to determine the effects of various types of corrosion and to establish the type of corrosion which would be most damaging. This study includes analysis of Euler (elastic) buckling and inelastic buckling of a member with symmetrical corrosion and of the onset of yielding in a member with severely nonsymmetrical corrosion. Chapter IV gives descriptions of the six members that were thoroughly investigated within offshore structures being rehabilitated in a shipyard in Louisiana, and Chapters V and VI describe the results of extensive statistical studies of the data obtained. Chapter VII then investigates the possibilities of using the statistical results in the development of an improved protocol for testing of members within structures, either in the sea, or removed to shore. Finally, Chapter VIII gives a summary of the research and recommendations for future applications of the results.

More details on some aspects of this study are available in two Master of Science theses produced by the research assistants on the project (Ellison 1999, Konen 1999).

CHAPTER II

EQUIPMENT AND PROCEDURES

The "tools" used in this study were both experimental and statistical, since the object was to measure wall thickness values for members within offshore structures and to analyze these data in order to draw conclusions about the significance of the loss of wall thickness due to corrosion. Section 2.1 gives details on the ultrasonic (UT) thickness-measuring device which was used, Section 2.2 summarizes nomenclature and notation, and Section 2.3 describes several statistical procedures which were used in analyzing data.

2.1 Experimental Studies

Ultrasonic Thickness Measuring Device

The acquisition of a state-of-the-art ultrasonic device to meet the needs of this research was key to success of this project. After much consultation and investigation, the Panametrics Model 26DL Plus instrument was chosen for its many useful features. These features include:

Waveform display and capture

This function allows a visual analysis of the reflected sonic wave and identification of any interference with the idealized form, which can be useful in determining possible types of error in a measurement. The wave display uses one hundred data points over the scale of the graph, which was typically set at 0.50 inches for this study. The device performs an internal calculation that relates the time of the return signal to the measured thickness and automatically displays the thickness value.

Internal data storage

This feature saves time by eliminating the need to manually record every measurement as it is taken. The storage capacity is 3072 thickness readings or

682 waveforms. The capacity is large enough to allow taking of a complete set of data without having to stop and download it to a computer.

Computer connection

Manual copying of data from one source to another can introduce error. The computer connection, via serial cable, allowed data to be transferred quickly into a computer for analysis.

Resolution of 0.001 in.

The variations in wall thickness were expected to be small, therefore a device with a small resolution was needed. One one-thousandth of an inch resolution is standard for this type of device. As will be discussed later in this section, this resolution proved to be adequate for the study.

Dual element transducer

The device has a dual-element transducer allowing greater accuracy of measurement on the uneven surfaces encountered during this research. The reason for a dual-element is to provide one element for sending signals and another for receiving the reflected signals. Dual-element transducers are preferred over single element transducers because they are more sensitive to echoes from the base of corroded pits. As shown in Figure 2.1, the transmitting and receiving elements are placed at a slight angle to each other, instead of parallel, so that the signal sent from the transmitter will reflect off of the back surface of the specimen and return to the receiver. Since the signals fan out from the transmitter, the signal paths cross resulting in a pseudo-focussing effect. This effect helps provide optimum performance with corroded specimens because it is more sensitive to the base of pits on the opposite surface, resulting in a better measurement of the minimum remaining wall thickness. Corrosion pits on the measurement surface can result in echoes that interfere with resolution. The dual element transducer is more likely to ignore these false echoes, thus resulting in more accurate measurements (Panametrics 1996).

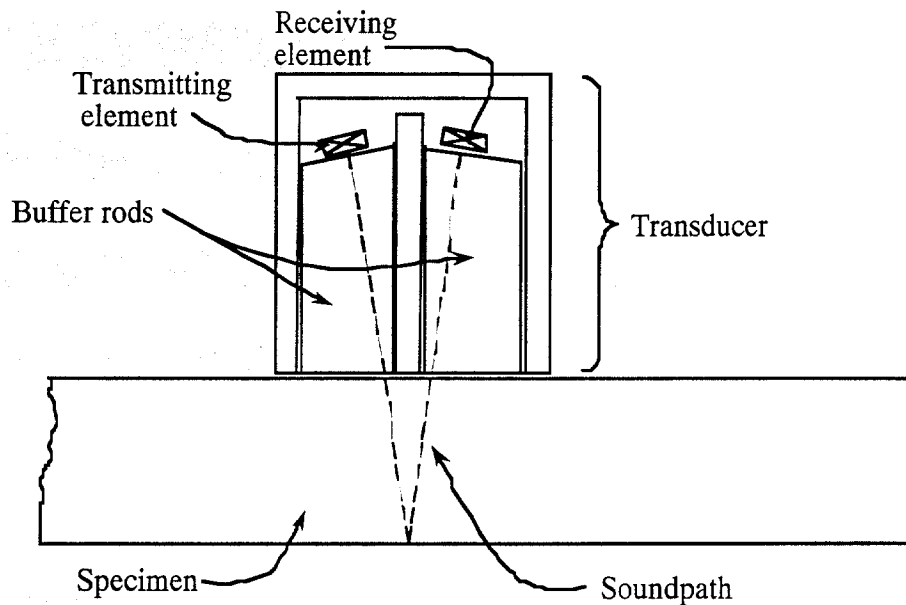


FIG. 2.1. Dual Transducer Sound Paths

Echo-to-echo capability

This allows the UT device to measure the thickness of steel underneath paint or other coatings without measuring the thickness of the coating. Many of the structural members in this study have paint, light to heavy scaling and other non-structural additions to wall thickness. With the echo-to-echo feature the device measures the time from one backwall echo to the next backwall echo and does not include the time penetrating paint or any other coatings that may be present (Panametrics 1996).

Precision and Accuracy

Before any useful conclusions could be drawn about the corrosion of members within a structure, it was necessary to obtain statistical evidence to show that the UT device would give consistent results with a sufficiently small associated error. Tests were conducted to evaluate the accuracy and precision of the device. In this study, a

distinction is made between precision and the resolution of the instrument, since it was found that repeated measurements did not give repeatability in agreement with the resolution. Accuracy, on the other hand, is used in the standard way as an indication of the nearness of a measurement to a "true" value. A consistent bias in the measurements, in particular, would lower the accuracy, but not affect the precision.

The practical precision of a measurement device can be considered to be given by the repeatability of the results of identical measurements, rather than by the resolution available in any one measurement. That is, apparent precision that is not reproducible is really of no value. The practical precision of the Panametrics 26 DL Plus ultrasonic thickness-measuring (UT) device was investigated both for clean bar stock and for corroded tubular members similar to those in the structures to be investigated in this study. This was done since the practical precision of the measurement, as defined here, depends on the specimen as well as the instrument. For measurements made on clean bar stock the surface of the specimen may well have little effect on the results, so that the observed discrepancy can be considered to be only that inherent to the instrument. When the instrument was used on corroded tubular members there was a much larger variation in the results of repeated measurements. This significant decrease in repeatability can be attributed to a combination of two effects. Most obvious is the fact that the transducer could not be perfectly aligned with the front surface of the specimen, since that surface was not smooth and planar. Possibly more important, though, is the fact that the reflecting surface on the back of the specimen was also not planar, and not aligned with the front surface. It is not surprising that these two factors introduced considerable random discrepancy into the measurements.

After the UT device had been calibrated on bar stock, data were taken on seven specimens with varying states and forms of corrosion damage. The specimens were sections that had been removed from tubular members from a previous JIP. The members

in that study sustained various forms of damage from service in the Gulf of Mexico, however care was taken in choosing the specimens to only include corrosion damage. UT data were taken at 36 points on each of the seven specimens without removing any scale or loose surface corrosion. Measurements with a micrometer with 0.0001 inches resolution were also taken at the same locations after the specimens had been thoroughly cleaned with a wire brush to remove any loose surface corrosion, in order to provide the best possible measurement of sound steel remaining.

The results of the calibration measurements are as follows. The practical precision of the UT measurements was characterized by an apparently random discrepancy of each measurement away from the average of many such measurements. For measurements on clean bar stock the standard deviation of this discrepancy was approximately 0.0008 inches. On corroded tubular members the standard deviation was approximately 0.009 inches. Regarding accuracy, it was found that there was no significant bias between the results of micrometer measurements on a cleaned specimen and the UT measurements at the same location on the original, uncleaned specimen. In fact, the average difference between these measurement results was approximately 10% of the standard deviation of the UT measurement. Thus, it was concluded that the UT device gives good accuracy, and that the only significant error to consider in any measurement is the random discrepancy, which is primarily related to the condition of the surface of the specimen. Furthermore, the fact that the standard deviation of the random discrepancy was less than 0.01 inches does allow relatively good precision in making UT measurements on corroded specimens. Section 2.3 includes information on the statistical procedures used in determining the numerical values associated with the precision.

2.2 Specimen Coordinates and Nomenclature

To eliminate ambiguity in the results, certain nomenclature is important. A typical cylindrical member is shown in Fig. 2.2, along with two coordinates Z and θ , which can be

used to describe any point on the surface. Two key terms in describing the measurements will be *rays* and *rings*. Note that a ray is a longitudinal reference line along the specimen at a constant angle θ , as shown. A ring, on the other hand, is a circumferential reference line measured at a constant longitudinal distance Z . These terms are used throughout the description of the experimental investigations, but they are also important to an understanding of some of the statistical techniques described in the following section.

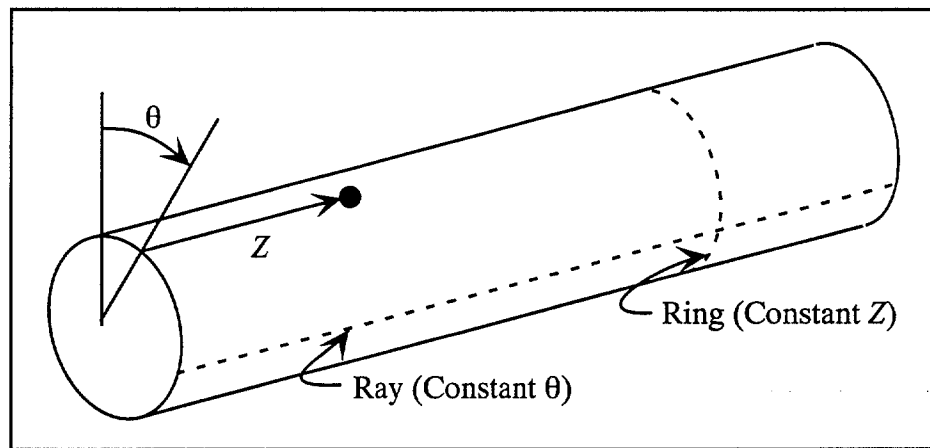


FIG. 2.2. Specimen Coordinates

2.3 Statistical Studies

The first of the statistical procedures described here was used in determining the precision and accuracy of the UT measurements, for which numerical values were given in Sec. 2.1. The other two procedures will be used in analyzing the data from the field measurements of wall thickness within offshore structures. The techniques are accumulated here in one location as background information for their application in the analyses.

Precision and Accuracy of UT Measurements

For any measurement on any specimen, the measured value was regarded as being the "true" measurement value (including any bias or inaccuracy) for the given specimen and instrument plus a discrepancy that was modeled as a random variable. The discrepancies in any two repetitions of a measurement were considered to be statistically independent.

One could determine the standard deviation of the measurement discrepancy term by making many measurements at a given location on a specimen, but this value would be dependent on any peculiarities in the specimen at that location. In this study a more general value was obtained by using an alternate approach in which two or three measurements were made at each of a large number of locations with generally similar surface conditions. The statistical analyses were then performed on the differences between repeated measurements at each location. The variance of the sum or difference of two independent random variables is the sum of the variances of the individual random variables, so that the variance of the difference of two "identical" measurements is simply twice the variance of any one measurement. Thus, the standard deviation of the measurement discrepancy was determined as $1/\sqrt{2} \approx 0.707$ times the standard deviation of the difference of two measurements, and this was used to characterize the magnitude of any one measurement discrepancy.

Detection of Patterns of Corrosion

It can be difficult to detect patterns within a data set when each individual value in the set contains a random error added to the true value. The object, of course, is to ignore the random measurement errors and uncover patterns in the true (but unknown) values. In the current study, for example, it was difficult to tell whether a member was thicker near one end than near the other, or whether it was thicker on the side toward the center of the structure than on the side more exposed to waves. Analysis of variance (ANOVA) is a standard statistical tool developed precisely for making this type of decision. In

particular, ANOVA is a hypothesis test of the null alternative that the variations in measured values are strictly random against the alternative hypothesis that there is some underlying pattern. Typically one rejects the null hypothesis in favor of the alternative if there is less than a 5% probability that a pattern as significant as the one actually observed would have occurred due to random measurement error. Essentially, this amounts to a conclusion that there is a pattern if the so-called p value of the ANOVA test is less than 0.05. ANOVA was used in this study to determine whether or not the apparent variations along the length and around the circumference of the members were significant, or were likely to be due to random variations. As suggested, a p value smaller than 5% was considered to be statistically significant, and, in addition, a p value between 5% and 10% was considered to have marginal statistical significance.

Strictly speaking, the ANOVA procedure tests hypotheses concerning the mean values of two or more subsets of the data (Weiss and Hassett 1982). For the present case, the subsets consisted of data along given rings or given rays for any member. The statistical test is based on computed values of the means and variances of each subset, as well as the variation between the means of the subsets. If the variation between subsets is much larger than the variations within subsets, then the true means for the subsets probably are not the same. However, if the variation between subsets is small compared to that within subsets, then the subsets may have the same true means. Thus, the latter case is consistent with the null hypothesis, while the alternative agrees with the hypothesis that the subsets do not all have the same true mean value. The computation of the probability p that the variation would have occurred by random chance is based on the underlying assumption that the data have a normal (Gaussian) distribution (Wike 1985). The statistic used is a ratio between an estimate of variance based on the variation among the subsets and another estimate of variance based on the variation within subsets. The probabilities are found from the well-known F distribution commonly tabulated in statistics texts.

In this study the variations among mean values for different rings (or different rays) were observed in order to conclude either that at least one of the rings (rays) had a mean value which was significantly different than the others or that the apparent pattern could be explained by random variability (Wike 1985, Freund 1984). The data for any given member from a structure was arranged in a table with one column for each ray and one row for each ring. The ANOVA analysis was then run comparing rows to see if there was a significant variation of wall thickness along the length of the member, then it was run again by columns to see whether there was a significant variation of wall thickness around the circumference of the member.

The data related to longitudinal thickness variation were also analyzed for linearity. This was done by performing linear regression on the set of mean values obtained by averaging thicknesses over all rays for a given member. The linear regression procedure amounts to finding a best-fit straight line for a set of data points. The adequacy of the linear fit is measured by a quantity R^2 that can be considered to give the fraction of the total variation of the independent variable that can be explained as a linear dependence on the dependent variable. In particular, the variance of a set of data is the mean-squared deviation of the data points away from the mean value and $(1 - R^2)$ times this variance is the mean-squared deviation of the data points away from the regression line. One can establish some rules as to what value of R^2 indicates a significant linearity in the data, but such rules are certainly arbitrary. For the purposes of this study, we will say that R^2 greater than 80% indicates a quite strong linear variation of the measurements, a value greater than 50% indicates a significant linear variation, and a value greater than 30% is evidence of a weak linear relationship.

Additional statistical tests were also conducted in an effort to learn more about the circumferential variation of thickness around the rays of each member. This was done by

grouping some of the data in order to form larger, and more reliable, subgroups. In particular, the three rays nearest the top of a member were compared (as one new subgroup) with the three rays nearest the bottom. Also, the three rays toward the center of the structure were compared with the three rays toward the perimeter of the structure. In this case each statistical comparison involved only two of the new, enlarged subgroups, so that it was possible to use an alternate statistical procedure called the *t*-test. This procedure is somewhat different than ANOVA, but involves the same basic ideas. If the observed means of the two subgroups are sufficiently different from each other, then one can reject the null hypothesis that there is no significant pattern. However, if the observed means are not significantly different, then one must conclude that the apparent difference could have occurred due to random variation in the measurements.

The statistic used in the *t*-test is found by dividing the difference in mean values by a standardized form of the variance estimated from the combined data. For normally distributed data with both subgroups having the same mean and variance values, this statistic has the so-called *T* distribution, which is also tabulated in most statistics books. If the null hypothesis is true, then the mean of the statistic is zero. The alternative hypothesis can be taken to be that the two subgroups do not have the same mean, then a significant pattern can be indicated by either a positive or a negative value of the statistic. As with ANOVA, it is common to use a 5% significance level in deciding whether a significant difference has been observed. That definition of significance was used in this study, but a marginal significance was also attributed to *t* values between 5% and 10%. The search for top-bottom differences and inside-outside differences can be viewed as a substitute for the linear regression used in seeking for a simple longitudinal pattern of corrosion. It is not possible to have a linear circumferential pattern, but it would be possible to have the top-bottom or inside-outside patterns.

Choice of Sample Size

One of the goals in this study was to determine the extent to which it is important to have a large sample in drawing any conclusions about the importance of corrosion on a member. For predicting the remaining strength of a member, in particular, it is probably most important to determine the mean value of the extent of corrosion, either over the entire member or possibly only on the thinnest side if such a side can be identified. The problem, then, is to determine the effect of sample size on the reliability of mean-value estimates obtained from finite sets of data.

This problem also was investigated by using the t -distribution, but the application is somewhat different than the standard approach alluded to in the previous section. Since the process is not standard, it will be explained in slightly more detail. Let m denote the true, but unknown, mean value of all possible thickness measurements on a given specimen (or portion of a specimen). Each observation will then be considered to be a random variable t_i and the sample mean \bar{t} and sample variance s will be computed from these n random variables. If the t_i are independent and identically normal, then the random variable $(\bar{t} - m)/(s/\sqrt{n})$ will have the t -distribution with $n-1$ degrees of freedom. This is also stated as

$$P\left[\frac{\bar{t} - m}{s/\sqrt{n}} > T_{\alpha, n-1}\right] = \alpha \quad (2.1)$$

in which $T_{\alpha, n-1}$ is a number which can be found in a statistics table for given values of n and α . This probability statement can now be rearranged as

$$P(m < t_0) = \alpha \quad \text{in which} \quad t_0 \equiv \bar{t} - s \frac{T_{\alpha, n-1}}{\sqrt{n}} \quad (2.2)$$

The value of this relationship becomes apparent when α is given some small value. For example, if $\alpha = 0.05$, then there is only a 5% probability that the quantity t_0 computed from a sample of size n will be greater than the true mean value of m . After the t_i values have been observed they are no longer random, so neither are \bar{t} , s , or t_0 . Thus, after the

measurements have been made it is more appropriate to say that one has $(1 - \alpha)$ confidence that the true mean m is at least as great as the computed value t_0 . Based on knowledge of the possible failure modes of the specimen, this allows the computation of a strength that is also exceeded with high confidence.

In order to determine the effect of the sample size n , it is convenient to combine the two terms in t_0 which involve n . Thus, Table 2.1 shows the ratio $T_{\alpha, n-1} / \sqrt{n}$ versus n for $\alpha = 0.05$ and a variety of possible sample sizes. It can be seen that the ratio decays quickly as n is increased from 2 to 4 or 8, but that the change is much more gradual beyond that point. This demonstrates that the gain from using a large sample size is not as great as one might expect. Viewed in a more positive way, it indicates that the penalty of using a small sample size may not be very severe unless the sample is very small, such as less than 4 or 5. This matter will be discussed further in Chapter VII, using observed values for \bar{t} and s .

TABLE 2.1. Effect of Sample Size ($\alpha = 0.05$)

n	$T_{0.05, n-1}$	$T_{0.05, n-1} / \sqrt{n}$
2	6.314	4.465
3	2.920	1.686
4	2.353	1.177
5	2.132	0.953
6	2.015	0.823
7	1.943	0.734
8	1.895	0.670
9	1.860	0.620
10	1.833	0.580
20	1.729	0.387
40	1.685	0.266
60	1.671	0.216

CHAPTER III

EFFECT OF THICKNESS ON STRENGTH

The purpose of UT measurements on either an in-situ structure or a structure being refurbished would be to detect any loss of wall thickness that was sufficient to cause a significant loss in member strength. Thus, it is important to relate the loss of wall thickness to the loss of strength that it would be likely to cause. Of course, the actual strength is a complicated function of the overall thickness of the tubular member, as a function of both Z and θ , but some information on this matter can be obtained by studying simplified situations. Two such special cases will be considered in this chapter. The first situation represents a uniform corrosion, such that the remaining wall thickness does not vary with Z or θ . The second special case has a maximally unsymmetric cross-section due to nonuniform corrosion. The reduction of section properties is smaller in this second situation, but there is a bending moment induced by the eccentricity of the corrosion, so that the resulting stresses might be larger than for uniform corrosion.

Throughout this analysis it will be presumed that the wall thickness t is small in relation to the member diameter D .

3.1 Uniform Loss of Wall Thickness

Multiple failure modes will be considered for the symmetric situation. For relatively long-slender members the strength will be controlled by the occurrence of elastic Euler buckling, while the mode of failure for short-stubby members will involve some yielding of the cross-section. For very short members this may be global plastic yielding of the entire cross-section, but more typically it is so-called inelastic buckling. All three of these modes of failure will be considered here.

The global yielding force can be written as

$$P_{yield} = A\sigma_{yield} \quad (3.1)$$

in which A denotes the cross-sectional area of the member, and σ_{yield} is the yield stress

level. Similarly, the Euler buckling load for a symmetric loading is

$$P_{Euler} = \frac{\pi^2 EI}{(kL)^2} \quad (3.2)$$

in which E is the modulus of elasticity, I is the centroidal moment of the cross-section, and kL denotes the effective length of the member (i.e., the distance between inflection points in the buckling mode). Thus, it is apparent that A and I are the two properties of the cross-section which are needed for the strength analysis.

Now the section properties A and I will be related to the loss of wall thickness due to corrosion. The symbols t_0 and ε will be used to denote the original wall thickness (before corrosion) and maximum loss of wall thickness, respectively. Thus, $t_0 - \varepsilon$ will be the minimum wall thickness after corrosion has taken place. The member diameter will be denoted by D , and no distinction will be made between the inside diameter and the outside diameter of the member, since they are nearly the same for $t_0 \ll D$.

For a circular member with a diameter D and a uniform, small wall thickness t , the cross-sectional area can be taken as the circumference times t :

$$A = \pi D t \quad (3.3)$$

Thus, the area prior to corrosion is

$$A_{original} = \pi D t_0 \quad (3.4)$$

and the area after uniform corrosion causes a loss of wall thickness ε around the circumference is

$$A_{reduced} = \pi D(t_0 - \varepsilon) = A_{original} \left(1 - \frac{\varepsilon}{t_0}\right) \quad (3.5)$$

Similarly, the moment of inertia about the central axis for the original member can be written as

$$I_{original} = \int_0^{2\pi} \left[\frac{D}{2} \cos(\theta) \right]^2 \frac{D}{2} t_0 d\theta = \frac{\pi D^3 t_0}{8} \quad (3.6)$$

and the uniform corrosion gives a reduced moment of inertia of

$$I_{reduced} = \frac{\pi D^3 (t_0 - \varepsilon)}{8} = I_{original} \left(1 - \frac{\varepsilon}{t_0} \right) \quad (3.7)$$

Experimental testing of compression members indicates that they often reach an unstable condition under axial forces that are significantly less than either the yield load or the elastic Euler buckling load. This is particularly true for members that have a slenderness ratio giving nearly equal values for the yield and Euler buckling loads. This discrepancy is due to residual stresses and imperfections in the specimens, which lead to yielding not initiating simultaneously over the entire cross-section. This condition is called inelastic buckling. Various approximate and empirical formulas have been suggested for improving the design formulas. For the approximation selected by the American Petroleum Institute (API 1993), the nominal capacity for shorter members can be written as

$$P_{capacity} = \left(1 - \frac{P_{yield}}{4P_{Euler}} \right) P_{yield} \quad \text{for} \quad P_{yield} < 2P_{Euler} \quad (3.8)$$

while P_{Euler} from (3.2) is used as the nominal capacity for $P_{yield} \geq 2P_{Euler}$.

For the sake of convenience, it is useful to rewrite the P_{yield}/P_{Euler} ratio in terms of a slenderness ratio. In particular, (3.1) and (3.2), along with the formulas for area and moment of inertia of a circular member give

$$\frac{P_{yield}}{P_{Euler}} = \frac{(kL)^2 A \sigma_{yield}}{\pi^2 EI} = \frac{8}{\pi^2} \left(\frac{kL}{D} \right)^2 \frac{\sigma_{yield}}{E} \quad (3.9)$$

The API (1993) suggests using $\sigma_{yield} = 33$ ksi and $k = 0.8$ for jacket braces, and substituting these values, along with $E = 29,000$ ksi for steel, into (3.9) gives

$$\frac{P_{yield}}{P_{Euler}} = \frac{1}{1694} \left(\frac{L}{D} \right)^2 \quad (3.10)$$

Thus, the $P_{yield} = 2P_{Euler}$ transition point between the domains for use of (3.2) and (3.8) for the member capacity is approximately given by $L/D = 58.2$. For larger values of L/D one uses (3.2), while (3.8) is appropriate for smaller values. In practice it will be rare that a bracing member will have $L/D > 58.2$, so (3.8) will usually be the controlling

formula.

It should also be noted that both the reduced yield load and the reduced Euler buckling load are obtained by multiplying the original values by the same factor of $(1 - \varepsilon/t_0)$, since this is the reduction factor for both area and moment of inertia. The inelastic buckling formula in (3.8) now shows that this factor also applies to the nominal capacity in all situations. Thus, one can say that

$$P_{capacity, reduced} = P_{capacity, original} \left(1 - \frac{\varepsilon}{t_0}\right) \quad (3.11)$$

for a member with uniform loss of wall thickness of amount ε , regardless of the mode of failure.

One can now combine (3.1), (3.8), (3.10) and (3.11) to give the normalized capacity of a short member as

$$\frac{P_{capacity}}{P_{yield}} = \left[1 - \frac{1}{6776} \left(\frac{L}{D}\right)^2\right] \left(1 - \frac{\varepsilon}{t_0}\right) \quad \text{for } L/D < 58.2 \quad (3.12)$$

in which the normalization factor, P_{yield} , denotes the yield load of the uncorroded cross-section. This choice of the normalization is arbitrary, but is a commonly used form in presenting capacity studies of imperfect members. Similarly, the normalized capacity of a long member is found from (3.2), (3.10), and (3.11) as

$$\frac{P_{capacity}}{P_{yield}} = 1694 \left(\frac{D}{L}\right)^2 \left(1 - \frac{\varepsilon}{t_0}\right) \quad \text{for } L/D > 58.2 \quad (3.13)$$

3.2 Unsymmetric Loss of Wall Thickness

A similar method to that used in Sec. 3.1 can be used to evaluate the effect of having a reduced wall thickness that varies around the circumference. This type of section would result from corrosion that was greater on one side of the tubular member and lesser on the opposite side. The reason for considering this type of section is that the lack of symmetry of the section may induce a bending moment in the specimen. In particular, if the unsymmetric corrosion varies along the length of the member, then there will be an

eccentricity between the line of action of the axial force and the centroidal axis of the cross-section. As in a curved member, the eccentricity will induce a bending moment, which can cause the section to fail inelastically. Note that the Euler buckling model is inappropriate for this situation, since it is based on elastic buckling due to a centroidal load.

The deflected shape of an initially straight, axially loaded member experiencing classical Euler buckling is sinusoidal. If it has effective length kL then it has points of inflection at a distance of $(1 - k)L/2$ from each end. Since the bending moment is zero at any point of inflection, it is clear that the line of action of the axial force must pass through the centroid of the section at each of these points. Let x be a longitudinal coordinate measured from one of the points of inflection, and let $w(x)$ be the deflection of the member away from the line passing through these two points. That is, let $w(0) = w(kL) = 0$. The deflected shape in these coordinates can be written as

$$w(x) = w_m \sin\left(\frac{\pi x}{kL}\right) \quad (3.14)$$

in which w_m is the maximum deflection, occurring at mid-length.

The eccentricity of the member will be characterized by a quantity $e(x)$ that gives the distance between the centroid of the cross-section and a straight line passing through the centroid at both points of inflection. Thus, the eccentricity at mid-length, for example, depends not only on the corrosion at mid-length, but also on the corrosion at the points of inflection. For this study it will be assumed that the corrosion is distributed in the worst possible way. In particular, it will be assumed that the centroidal axis at mid-length is shifted a distance $+e_m$ from the original central axis, and that at the points of inflection it is shifted $-e_m$ (the same amount in the opposite direction). Thus, the total eccentricity at mid-length is $2e_m$. This particularly undesirable pattern of corrosion is illustrated in Fig. 3.1. For the sake of simplicity, it will be assumed that the shape of the eccentricity is then given by

$$e(x) = 2e_m \sin\left(\frac{\pi x}{kL}\right) \quad (3.15)$$

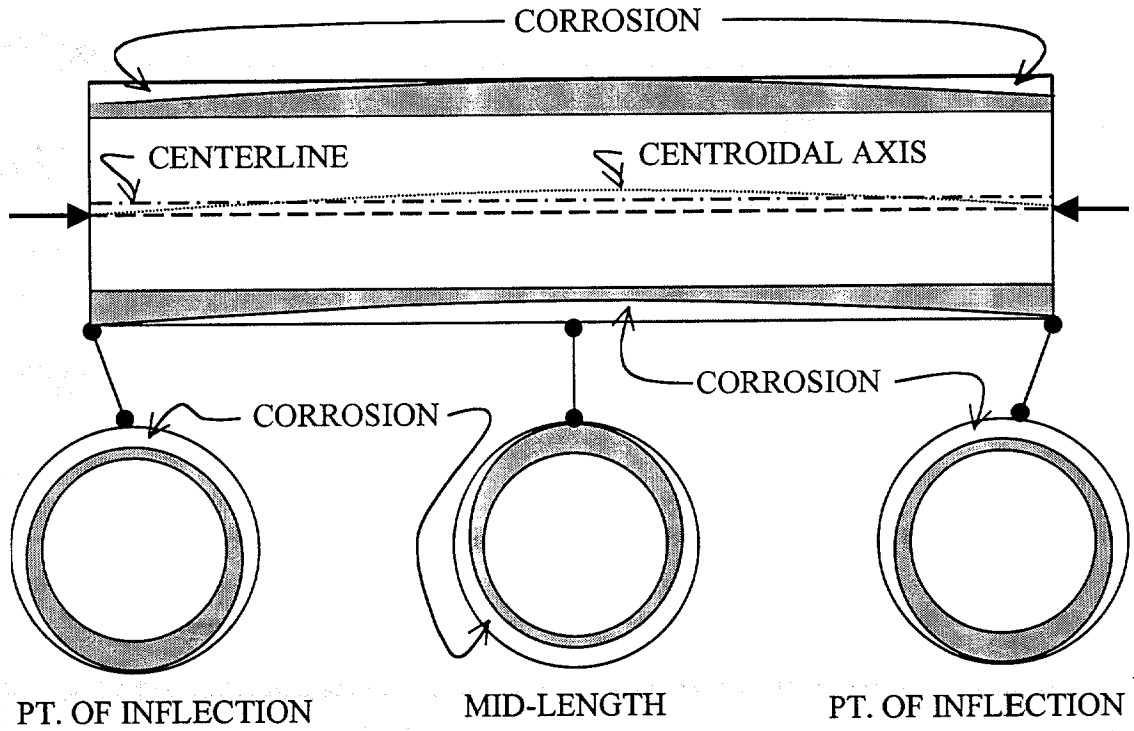


FIG. 3.1. Worst-Case Unsymmetric Corrosion

It will also be assumed that the deflected shape for the eccentrically loaded member will still be well approximated by (3.14). It would certainly be unusual if the pattern of corrosion in a particular member exactly agreed with (3.15), but this “worst case” situation may be useful as a limiting design situation.

The bending moment in the member is now related to the deflected shape as

$$M(x) = -EI(x) \frac{d^2 w(x)}{dx^2} = EI(x) w_c \frac{\pi^2}{(kL)^2} \sin\left(\frac{\pi x}{kL}\right) \quad (3.16)$$

in which $I(x)$ denotes the variable centroidal moment of inertia of the cross-section. In addition, the bending moment is related to the axial load P as

$$M(x) = P[e(x) + w(x)] = P(2e_m + w_m) \sin\left(\frac{\pi x}{kL}\right) \quad (3.17)$$

Equating (3.16) and (3.17) then simplifying and solving for P gives

$$P = EI(x) \frac{\pi^2}{(kL)^2} \frac{w_m}{(2e_m + w_m)} \quad (3.18)$$

If one now chooses w_m to be the deflection that causes incipient yielding at the outer surface of the cross section at mid-length of the member and $I(x)$ to be the moment of inertia at that location, then P in (3.18) gives the elastic capacity of the member.

In finding the stress in the member, it is important to include the effect of the bending moment, as well as that of the axial load. The equation for the maximum combined stress at mid-length of the member is

$$\sigma = \left[\frac{M(x)D}{2I(x)} + \frac{P}{A(x)} \right]_{x=kL/2} = P \left(\frac{(2e_m + w_m)D}{2I_m} + \frac{1}{A_m} \right) \quad (3.19)$$

in which A_m and I_m are based on the cross-section at mid-length of the member. Substituting σ_{yield} for the magnitude of the maximum stress, then solving for w_m gives

$$w_m = \frac{2I_m}{D} \left(\frac{\sigma_{yield}}{P} - \frac{1}{A_m} \right) - 2e_m \quad (3.20)$$

It is now possible to obtain an explicit expression for the capacity of the member by substituting (3.20) into (3.18), then solving for P :

$$P = \frac{A_m \sigma_{yield}}{2} + \frac{\pi^2 EI_m}{2(kL)^2} + \frac{\pi^2 DE e_m A_m}{2(kL)^2} - \sqrt{\left(\frac{A_m \sigma_{yield}}{2} + \frac{\pi^2 EI_m}{2(kL)^2} + \frac{\pi^2 DE e_m A_m}{2(kL)^2} \right)^2 - \frac{\pi^2 EI_m A_m \sigma_{yield}}{(kL)^2}} \quad (3.21)$$

The cross-sectional properties A_m , I_m and e_m must now be related to the amount of corrosion in the member. Note, though, that all these section properties can be evaluated at mid-length of the member. Thus, it is only necessary to investigate that one location. The wall thickness for the thin-walled unsymmetric member will be written as $t(\theta)$, to emphasize the fact that it varies around the circumference of the member. The results presented here will be based on the assumption that $t(\theta) = t_0 - \varepsilon |\theta|/\pi$ for $-\pi \leq \theta \leq \pi$, so that the thickness varies linearly with the circumferential distance. At

$\theta = 0$ the thickness is t_0 , indicating no corrosion, while at $\theta = \pm\pi$ the thickness is $t_0 - \varepsilon$, indicating that ε is the maximum loss of wall thickness (as it was for the symmetric situation). Using these same extreme values of wall thickness, the problem has also been analyzed for a thickness that varies linearly with distance from the original centroidal axis, but the results for a thin-walled member are very similar to those presented here.

The mid-length area of the unsymmetric, corroded cross-section is given by

$$A_m = \int_0^{2\pi} t(\theta) \left(\frac{D}{2} \right) d\theta = \pi D \left(t_0 - \frac{\varepsilon}{2} \right) = A_{original} \left(1 - \frac{\varepsilon}{2t_0} \right) \quad (3.22)$$

Similarly, the reduced moment of inertia about the original central axis is

$$I_0 = \int_0^{2\pi} t(\theta) \left[\frac{D}{2} \cos(\theta) \right]^2 \left(\frac{D}{2} \right) d\theta = \frac{\pi D^3}{8} \left(t_0 - \frac{\varepsilon}{2} \right) = I_{original} \left(1 - \frac{\varepsilon}{2t_0} \right) \quad (3.23)$$

This can be used in finding the centroidal moment of inertia, but first it is necessary to evaluate the eccentricity e_m , which is the distance between the original central axis and the centroidal axis. This eccentricity, can be written as

$$e_m = \frac{1}{A_m} \int_0^{2\pi} t(\theta) \left[\frac{D}{2} \cos(\theta) \right] \left(\frac{D}{2} \right) d\theta = \frac{D^2 \varepsilon}{\pi A_m} \quad (3.24)$$

Using the parallel axes transfer for moments of inertia now gives the centroidal moment of inertia as

$$I_m = I_0 - A_m e_m^2 = \frac{\pi D^3}{8} \left(t_0 - \frac{\varepsilon}{2} \right) - \frac{D^3 \varepsilon^2}{\pi^3 (t_0 - \varepsilon/2)} \quad (3.25)$$

The section properties in (3.22), (3.24), and (3.25) now allow evaluation of the capacity of the corroded member by using (3.21).

3.3 Determination of Controlling Condition

The next step is to determine which form of corrosion is worse. That is, to find out whether the load capacity is lower when the symmetric corrosion of Sec. 3.1 gives the maximal loss of wall thickness, or when the unsymmetric corrosion of Sec. 3.2 gives some loss of wall thickness along with an induced bending moment. This is established by using (3.21) to find the capacity P_{unsym} of the unsymmetrical member and (3.12) and

(3.13) to find P_{sym} for the symmetric situation. In particular, (3.12) gives the capacity of a symmetric member with $L/D < 58.2$, and (3.13) gives the capacity of a longer symmetric member.

Numerical investigations have been carried out in order to compare the P_{unsym} and P_{sym} values. In particular, the ratio P_{unsym}/P_{sym} has been evaluated for a wide range of the dimensionless quantities L/D and ε/t_0 , which give the slenderness of the member and the maximum loss of wall thickness. The other parameters have been taken as $E = 29,000$ ksi, $\sigma_{yield} = 33$ ksi, and $k = 0.8$, as in Sec. 3.1. It has been found that in most situations the P_{unsym}/P_{sym} ratio is greater than unity. That is, the capacity computed from (3.21) is usually greater than that computed from (3.12) and (3.13), so that it is conservative to evaluate the strength of the member by using the symmetric formulas from Sec. 3.1. There are a few situations, though, in which the P_{unsym}/P_{sym} ratio is slightly less than unity. Figure 3.2 shows a contour plot of the ratio only for the situations with $P_{unsym} < P_{sym}$. It is seen that the unsymmetric situation may be worse than the symmetric situation for corrosion which removes approximately 35% to 40% of the wall thickness at selected locations ($\varepsilon/t_0 = 0.35$ to 0.40), particularly for slenderness ratios of $L/D = 40$ to 50 . Note, though, that P_{unsym} is never as much as 7% below P_{sym} in these worst situations.

Recall that the unsymmetric situation which has been analyzed is a very unusual type of corrosion, in which the loss of wall thickness is on one side of the member at the points of inflection and the opposite side of the member at mid-length (Fig. 3.1). Numerical results have also been obtained for a slightly more realistic situation in which there is no corrosion at the points of inflection, and maximum non-symmetry at mid-length. In this case, the maximum eccentricity is e_m [one half of that in (3.15)], and the capacity of the eccentric member is always greater than that calculated from (3.12) and (3.13) for symmetric corrosion.

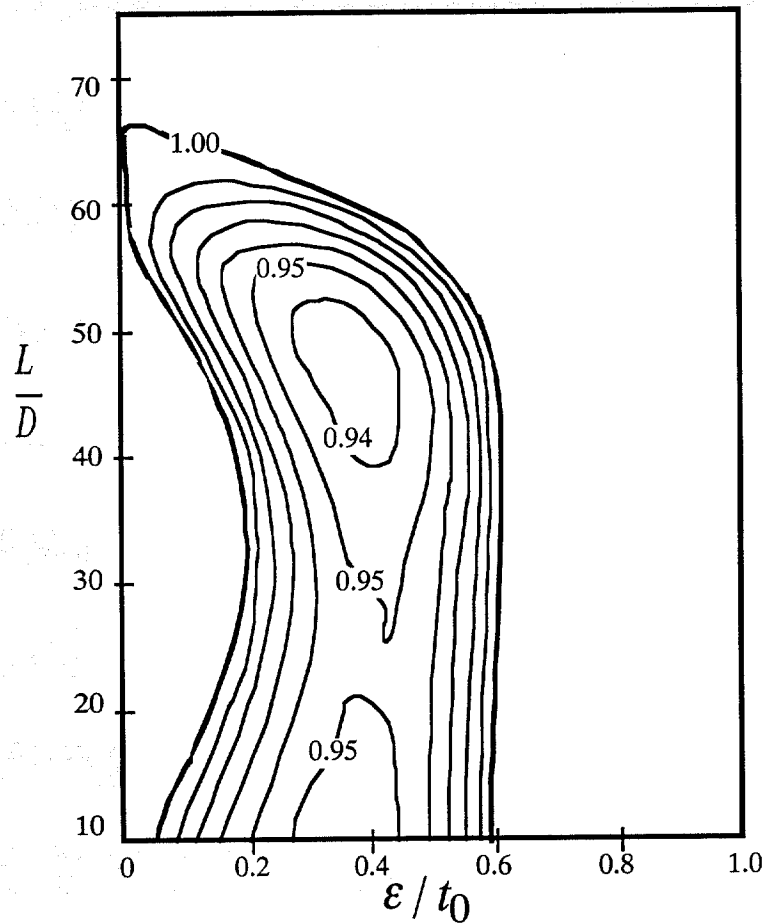


FIG. 3.2 Values of P_{unsym}/P_{sym} for $P_{unsym} < P_{sym}$

Overall, it is seen that for almost all combinations of L/D and ϵ/t_0 , it is worse to have a uniform corrosion of amount ϵ around the entire circumference and over the entire length than it is to have a pattern of corrosion which induces eccentricity in the member. Even for a pattern of corrosion that is very severe and has a very low likelihood of occurrence, the nonconservatism of the formulas from Sec. 3.1 is less than 7%. Taking all this into account, it is reasonable to neglect this small discrepancy, and simply use the formulas of Sec. 3.1 to estimate the strength of a corroded member with these values of ϵ/t_0 and L/D . The stresses caused by the eccentricity-induced bending moment are generally not as significant as the effect of the additional loss of wall thickness for the symmetric corrosion. The approximation used by API to account for

inelastic buckling of the symmetric member is sufficiently conservative to provide adequate strength estimation for any realistic pattern of unsymmetric corrosion. It is recommended that (3.12) and (3.13) be used for strength estimation for any corroded member.

CHAPTER IV

FIELD STUDY

The major focus of this research is the field study, in which new UT measurements were made on recently salvaged offshore structures. In order to meet the project objectives it was necessary to locate platforms that had recently been *in-situ*, with members that had sustained various levels of corrosion damage and for which complete histories were available.

4.1 Description of Site

The first step in the field study was to select a site for taking such measurements. The goal was to find yards with salvaged platforms where work could be performed with a minimum of interruptions for the regular workers. The participants in this project had initially indicated possible sites in Louisiana, near New Orleans, as well as along the Gulf coast in Texas.

Through telephone conversations and various other referrals, a site was finally selected at the J. Ray McDermott, Inc. Fabrication Division in Morgan City, Louisiana. Knowledge of the condition of the members was a key factor in site selection. The Morgan City yard was chosen primarily because it offered damaged members with obvious corrosion and dents. The members selected for study and discussed in the next section were not removed from the structures. As such, it was easy to document the precise location and orientation within the structure of each member. In addition, records were available regarding the duration of service, and the location and orientation of each structure prior to removal from the Gulf of Mexico.

The main contact at McDermott was Larry Verzwylt, who made the necessary arrangements for the research team to take measurements. Information concerning the accessibility of the members was provided prior to travel. Plans of a few offshore platforms were received before travelling to Louisiana. Since the recently salvaged

platforms were at the yard in a horizontal position, it was convenient to make measurements only on members near the ground, eliminating the need for lifts and harnesses.

4.2 Description of Specimens

Two graduate research assistants (B. Kirk Ellison and Keith Konen) made a trip to the Morgan City yards in late March 1999. Six specimens were identified on what appeared to be three separate structures. In fact, the six members came from only two different jacket structures. One of them, an 8-pile jacket, had been cut in two prior to removal from its offshore environment, and after refurbishing will be sold as two separate 4-pile jackets. As such, there were three different structures from two different jackets. Both jackets had been removed from the Gulf of Mexico in late 1998. Descriptions of these three structures are detailed in Table 4.1.

TABLE 4.1. Jacket Structure Histories

Platform*	Block	Configuration	Vintage	Leg Spacing (ft)	Water Depth (ft)	Grouted Piles?	Weight (tons)	Piles in Leg?
Forest I	SMI 143	4-Pile	1979	40x40	240	No	678	No
Forest II	SMI 143	4-Pile	1979	40x40	240	No	641	No
Santa Fe	MP 186	Lean-To	1989	20x20	150	No	148	No

* Note, all platforms salvaged in late 1998.

Table 4.2 provides a description of the members investigated in each platform. Members 01, 02, and 03 were diagonal members while Members 04, 05, and 06 were horizontal. Members 01 through 05 each had two different values of nominal wall thickness, as noted in the table. Only the diagonal members were equipped with anodes, since the horizontal members were above the mean water level. All members were of the welded, rather than the seamless, variety. Although there were no visible holes or cracks in any of the members, it was not possible to determine if any of them had been flooded.

TABLE 4.2 Member Descriptions

Member*	Platform	Diameter (in)	Nominal Thickness (in)**	Location Relative to MWL (0 ft)	Length Used for Data Acquisition (ft)	No. of Anodes
1	Forest I	28	0.750, 0.625	-51 to +12 ft	65	2
2	Forest II	28	0.875, 0.750	-51 to +12 ft	60	2
3	Santa Fe	24	0.750, 0.375	-27 to +10 ft	30	1
4	Forest I	18	0.750, 0.500	+14.5 ft	33.3	0
5	Forest II	18	0.750, 0.500	+14.5 ft	33.3	0
6	Santa Fe	14	0.375	+12.5 ft	16	0

* Members 1-3 are diagonal members, Members 4-6 are horizontal members

** Multiple values represent more than one nominal thickness along section length

The "Platform" designations shown in Tables 4.1 and 4.2 identify the structure within which each member was located. The "Block" column of Table 4.1 refers to the Gulf of Mexico offshore block from which the structure was salvaged. Fig. 4.1 shows the location of these two structures on a map of part of the Gulf coast near Louisiana. For Forest Structures I and II (Forest Oil Corporation), "SMI 143" refers to South Marsh Island Block 143. The structure previously owned by Santa Fe came from "MP 186," or Main Pass Block 186. Note that the Forest structures had been in the Gulf of Mexico for 20 years, and the Santa Fe structure had been salvaged after 10 years of service.

The notation introduced in Sec. 2.2 was used in marking the specimens throughout the field study. Fig. 4.2 describes the location around the circumference of each ray (eight θ angles). Note that ray A is at the top (toward deck) of every member, while ray E is at the bottom (toward seafloor). Rays B, C, and D were always toward the "outside" of the structure, while F, G, and H were toward the "inside," or center. For diagonal bracing members, ring 1 was always taken to be near the upper end (toward the deck) of the member.

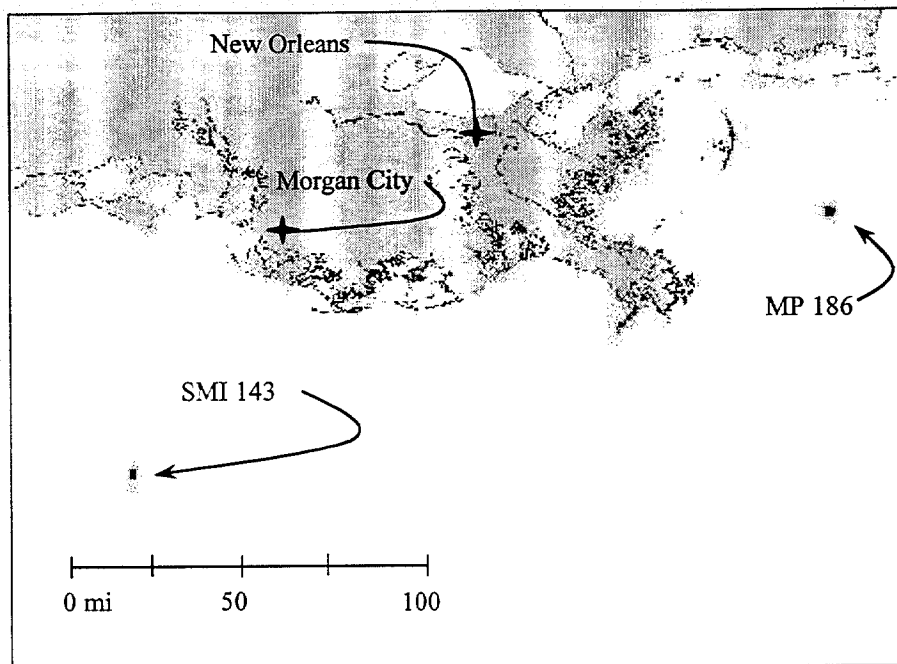


FIG. 4.1. Gulf of Mexico Structure Locations

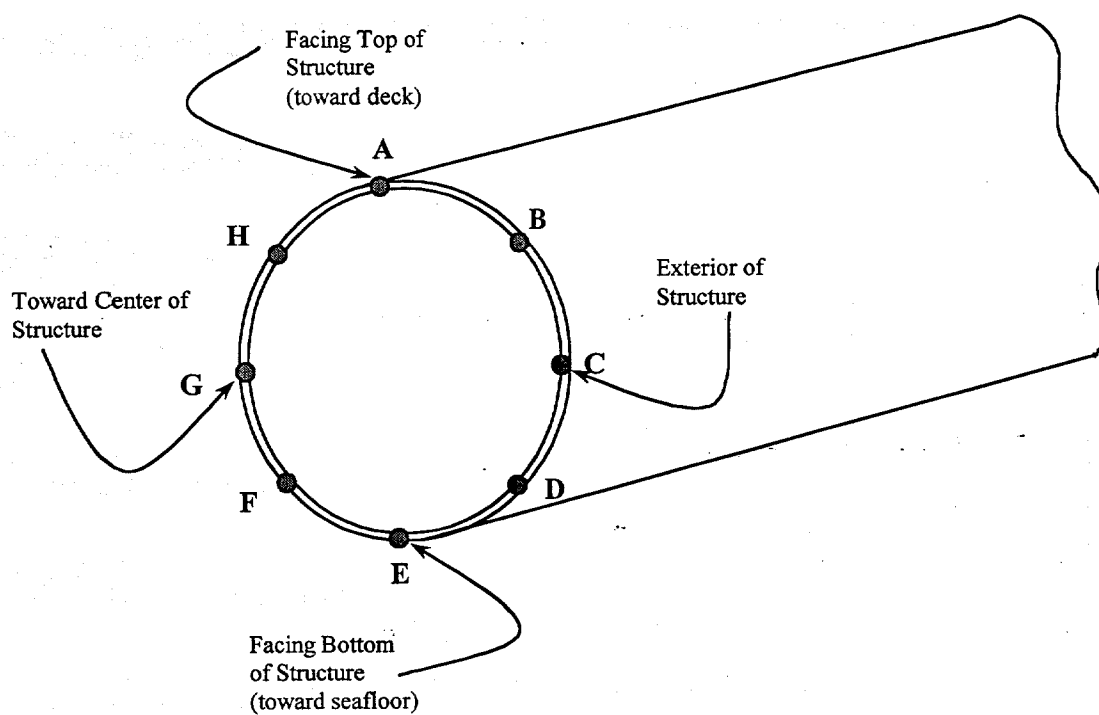


FIG. 4.2. Circumferential Ray Location

As mentioned earlier, both Forest jackets originally came from the same structure, but were separated into two structures during salvage operations. Fig. 4.3 shows a schematic drawing of the 8-pile jacket intact, with the measured members identified. "A" refers to an anode, and their locations are shown on Members 01 and 02. One anode is located 26 feet from ring 1, while the other is located 53 feet from ring 1. Additionally, the mean water level (MWL) is shown to be approximately 14 feet, 6 inches below the top of the jacket structure. The dimension given for each member represents the length of the member that was subjected to UT measurements, not the overall member length. These are also the lengths that are shown in Table 4.2.

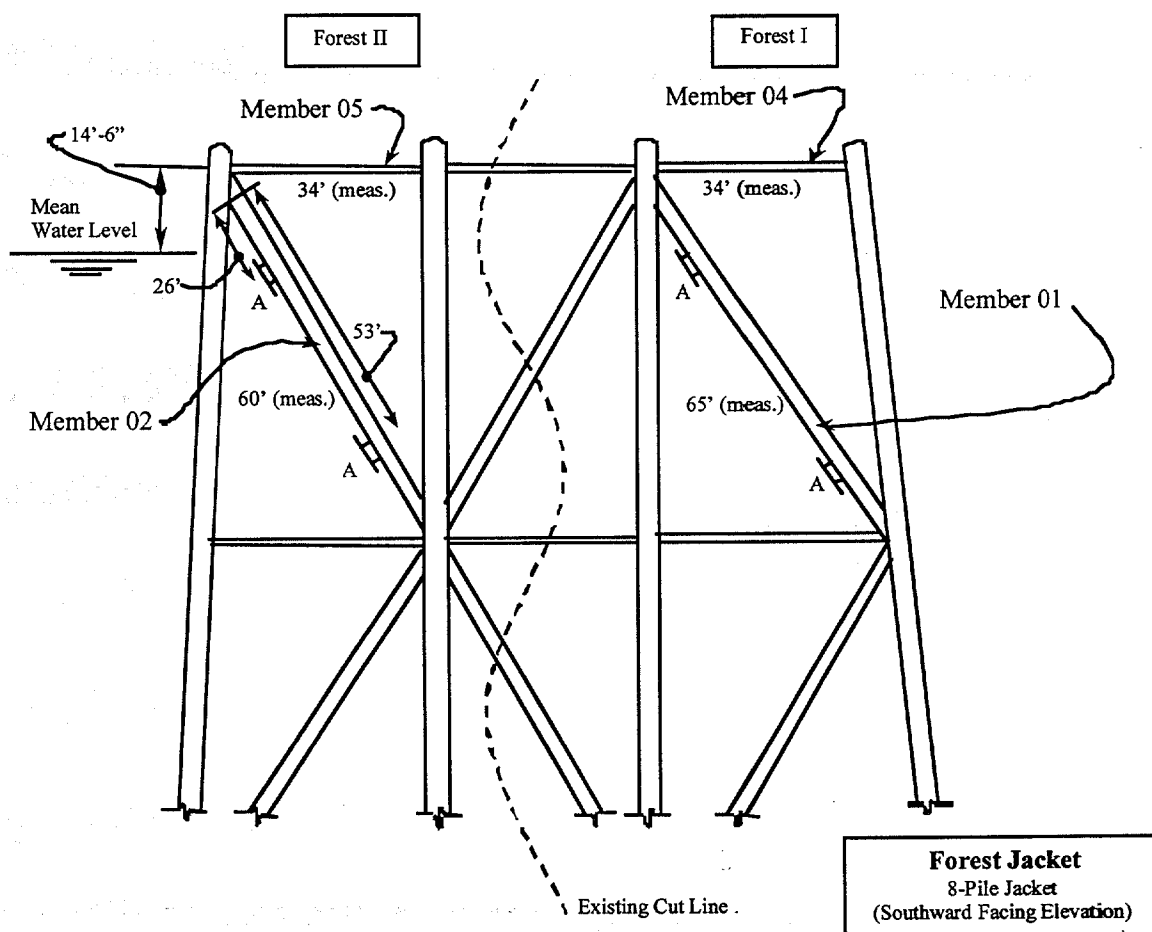


FIG. 4.3. Forest Jacket Schematic Drawing

Figs. 4.4 and 4.5 show the two jacket structures lying in the Morgan City yard. As stated earlier, the members nearest the ground were selected for study. Fig. 4.6 shows the Forest jacket structure orientation in the Gulf of Mexico. Thus, the elevation shown in Fig. 4.3 was facing due south in the Gulf.

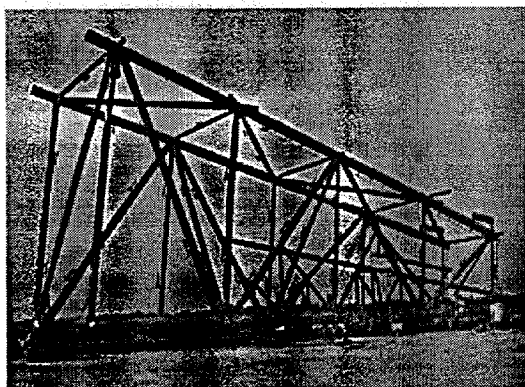


FIG 4.4. Forest I Jacket

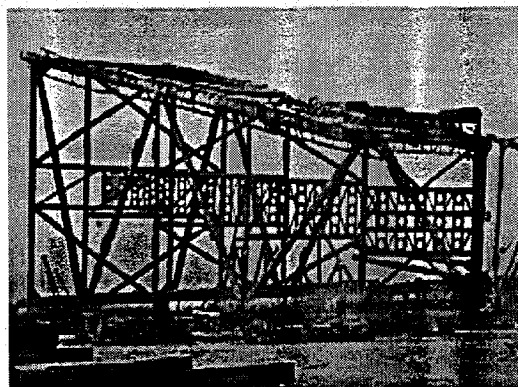


FIG. 4.5. Forest II Jacket

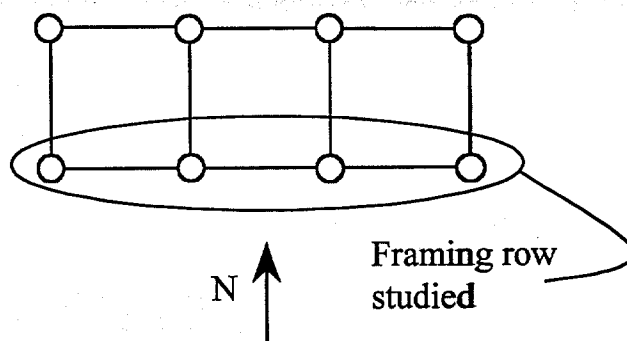


FIG. 4.6. Forest Jacket Orientation (Plan View)

A schematic drawing of the Santa Fe structure is shown in Fig. 4.7. This lean-to structure is smaller than a typical steel jacket, and is classified as a “minimal structure” by the offshore industry. Minimal structures are used in smaller oil and gas fields where large multi-leg space frame platforms or floating systems would only be marginally

economic. Fig. 4.8 shows the Santa Fe structure orientation in the Gulf of Mexico. Thus, the elevation shown in Fig. 4.7 was facing approximately 29° West of South.

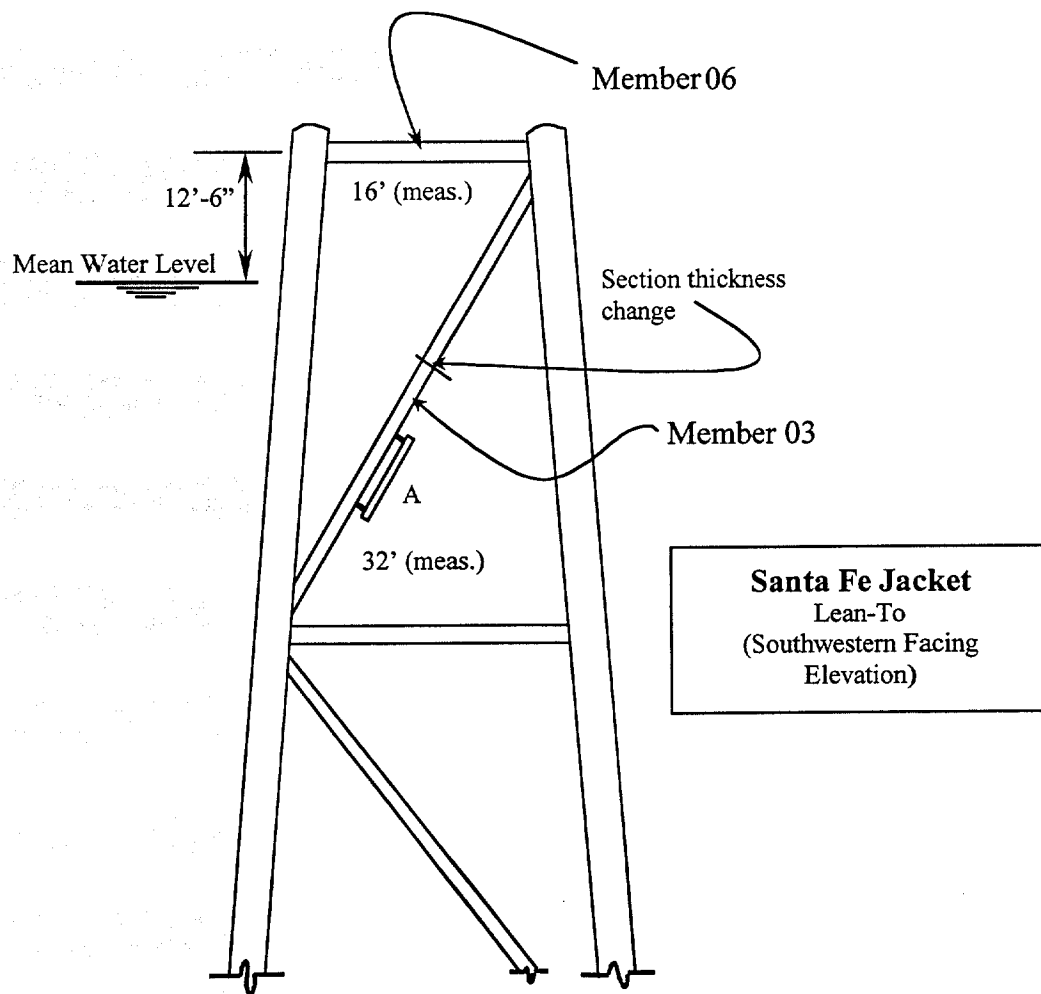


FIG. 4.7. Santa Fe Lean-to Structure Schematic Drawing

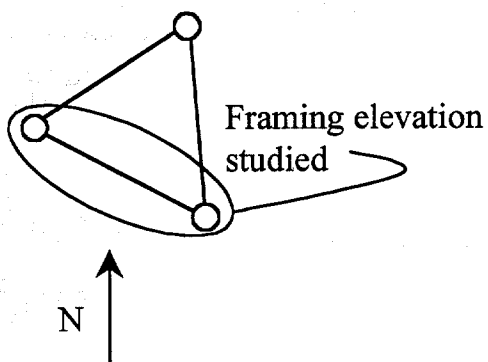


FIG. 4.8. Santa Fe Jacket Orientation (Plan View)

As shown in Figs. 4.3 and 4.7, Members 01, 02, and 03 were the diagonal braces from the Forest I, Forest II, and Santa Fe structures, respectively, while Members 04, 05, and 06 were the corresponding horizontal bracing members. Each of the diagonal members extended through the mean water level and each of the horizontal members was above the mean water level, but within the splash zone.

4.3 Specimen Analysis – UT Thickness Data

A preliminary tour of the fabrication yards, revealed there were four unfurnished jackets available that were lying on their sides. However, only two of these (Forest structures I and II) did not have “tideguard”, a form of corrosion protection that could hinder proper UT measurements. The Santa Fe structure was also identified. It had already been partially refurbished, requiring minimal preparation before taking data.

The subsurface portions of the two Forest structures were heavily covered with marine growth. The two diagonal Forest members (Members 01 and 02) were sandblasted at selected areas to facilitate data acquisition. Fig. 4.9 and 4.10 show overall and close up views of Member 01. Member 02 was very similar and is not shown here. Fig. 4.11 and 4.142 are schematic drawings of Members 01 and 02 showing the size of the members and locations of the rings.

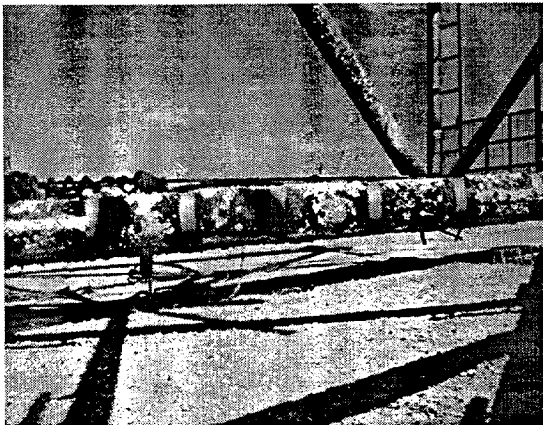


FIG. 4.9. Member 01 (Facing Ray E)

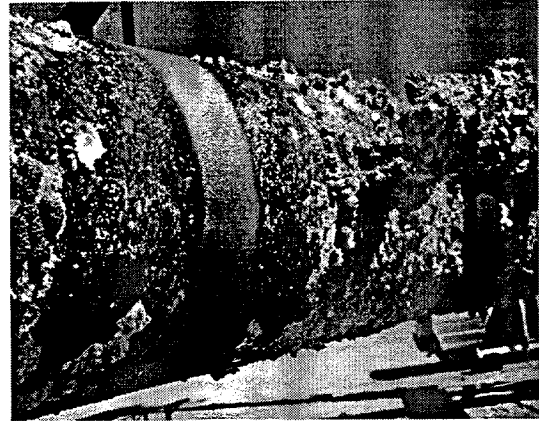


FIG. 4.10. Member 01 (Marine Growth Removed at Ring)

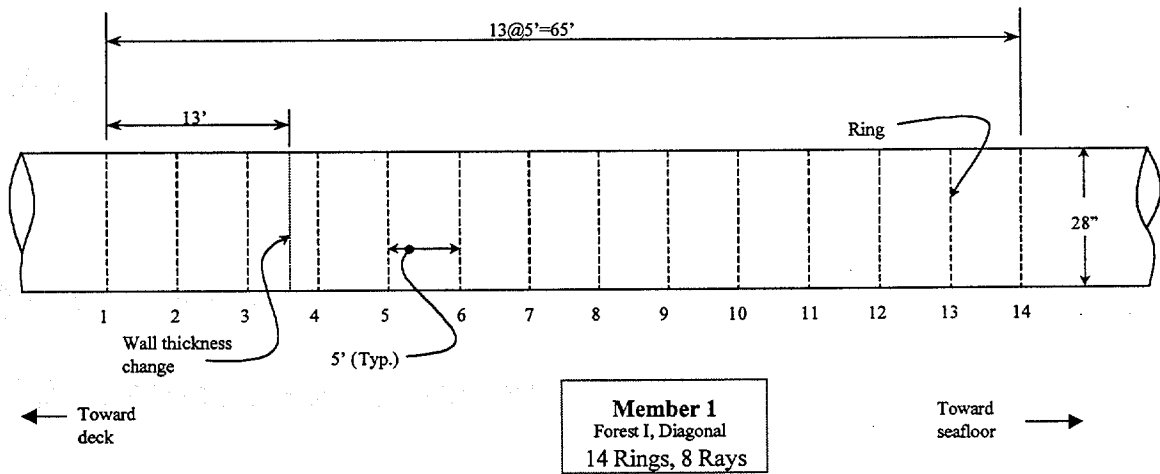


FIG. 4.11. Member 01 Schematic Drawing

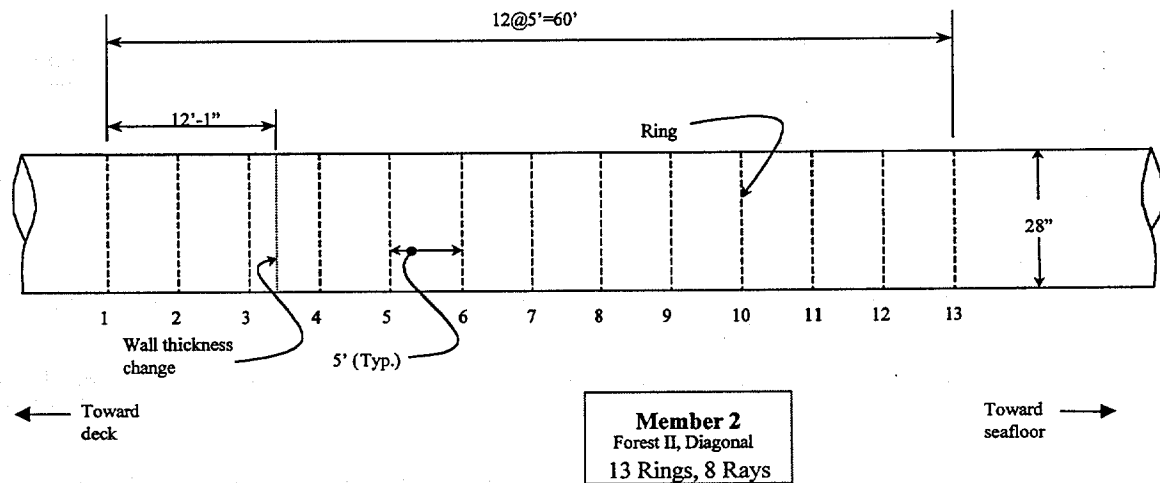


FIG. 4.12. Member 02 Schematic Drawing

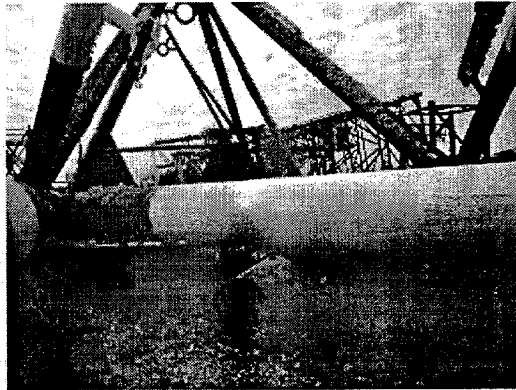


FIG. 4.13. Member 03 (Facing Ray A)

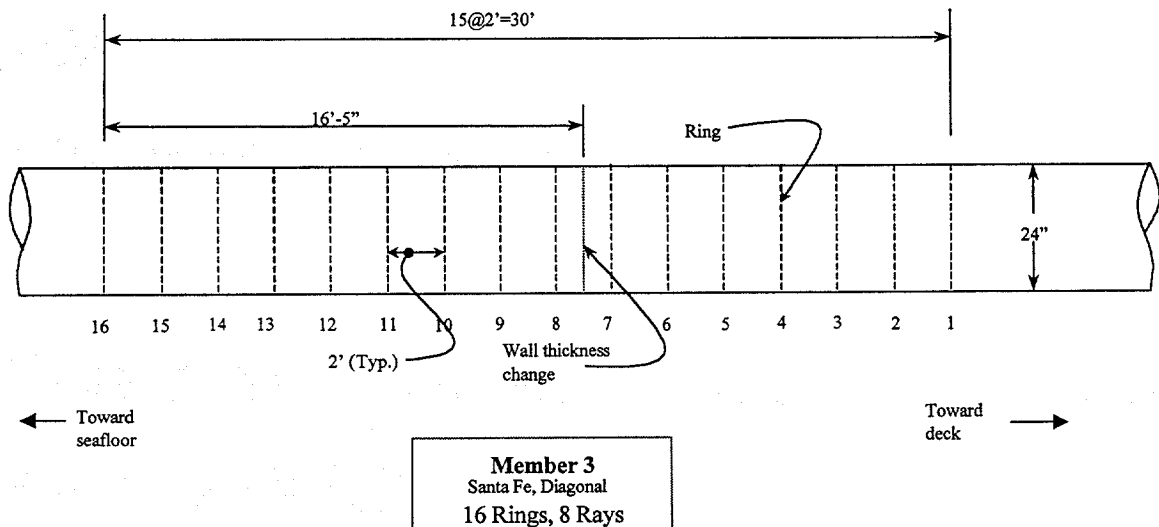


FIG 4.14. Member 03 Schematic Drawing

A photograph and schematic drawings of Member 03 are shown in Figs. 4.13-4.15. As can be seen in the two photograph, most of the member had been refurbished (white paint). This member had one anode as shown in Fig. 4.15. The results of these thickness measurements for Members 01, 02, and 03 are given in Tables 4.3 to 4.5. Detailed analyses of these data are presented in Chapters V and VI.

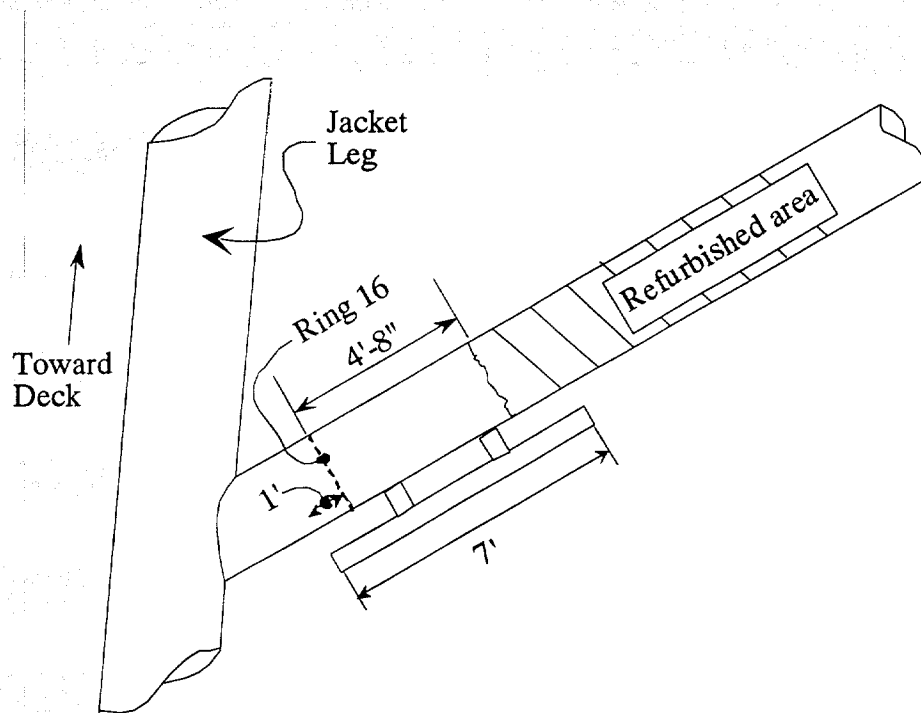


FIG. 4.15. Member 03 Subsection Schematic Drawing

TABLE 4.3. UT Thickness Measurements for Member 01

Member 01 3/24/99 (Forest I, diagonal)											
Ring/Ray	A	B	C	D	E	F	G	H		Mean	St. Dev.
1	0.499	0.506	0.498	0.491	0.525	0.569	0.573	0.515		0.522	0.032
2	0.463	0.463	0.459	0.462	0.465	0.462	0.462	0.460		0.462	0.002
3	0.467	0.442	0.445	0.445	0.448	0.443	0.445	0.442		0.447	0.008
4	0.588	0.585	0.563	0.560	0.559	0.558	0.556	0.553		0.565	0.013
5	0.578	0.553	0.552	0.550	0.555	0.552	0.550	0.549		0.555	0.010
6	0.555	0.550	0.553	0.556	0.558	0.550	0.570	0.576		0.559	0.010
7	0.556	0.557	0.560	0.556	0.586	0.560	0.558	0.582		0.564	0.012
8	0.582	0.557	0.552	0.554	0.578	0.578	0.579	0.589		0.571	0.014
9	0.555	0.554	0.557	0.549	0.577	0.554	0.579	0.578		0.563	0.013
10	0.570	0.569	0.567	0.567	0.570	0.569	0.574	0.566		0.569	0.003
11	0.586	0.581	0.581	0.586	0.585	0.584	0.578	0.580		0.583	0.003
12	0.598	0.572	0.571	0.569	0.573	0.568	0.572	0.573		0.575	0.010
13	0.568	0.567	0.565	0.569	0.595	0.595	0.598	0.592		0.581	0.015
14	0.596	0.558	0.585	0.559	0.568	0.560	0.585	0.588		0.575	0.015
Mean	0.554	0.544	0.543	0.541	0.553	0.550	0.556	0.553		0.549	
St. Dev.	0.045	0.043	0.044	0.043	0.044	0.043	0.045	0.048			0.043
Mean (1-3)	0.476	0.470	0.467	0.466	0.479	0.491	0.493	0.472		Mean (1-3)	0.477
St. Dev. (1-3)	0.020	0.033	0.027	0.023	0.040	0.068	0.070	0.038		St. Dev. (1-3)	0.038
Mean (4-14)	0.576	0.564	0.564	0.561	0.573	0.566	0.573	0.575		Mean (4-14)	0.569
St. Dev. (4-14)	0.016	0.012	0.011	0.011	0.013	0.014	0.014	0.014		St. Dev. (4-14)	0.014

TABLE 4.4. UT Thickness Measurements for Member 02

Member 02 (Forest II, diagonal) 3/25/99										
Ring/Ray	A	B	C	D	E	F	G	H	Mean	St. Dev.
1	0.547	0.572	0.561	0.561	0.565	0.573	0.559	0.535	0.559	0.013
2	0.491	0.492	0.489	0.489	0.489	0.491	0.492	0.497	0.491	0.003
3	0.488	0.488	0.483	0.485	0.486	0.487	0.490	0.486	0.487	0.002
4	0.771	0.738	0.732	0.739	0.745	0.734	0.734	0.735	0.741	0.013
5	0.744	0.734	0.734	0.734	0.738	0.758	0.757	0.771	0.746	0.014
6	0.744	0.756	0.730	0.729	0.732	0.728	0.743	0.753	0.739	0.011
7	0.746	0.745	0.739	0.739	0.745	0.737	0.739	0.742	0.742	0.003
8	0.748	0.745	0.738	0.743	0.770	0.739	0.744	0.746	0.747	0.010
9	0.751	0.712	0.715	0.715	0.725	0.718	0.718	0.712	0.721	0.013
10	0.725	0.734	0.718	0.726	0.731	0.721	0.716	0.715	0.723	0.007
11	0.727	0.725	0.752	0.725	0.733	0.728	0.720	0.721	0.729	0.010
12	0.726	0.726	0.725	0.728	0.764	0.730	0.725	0.727	0.731	0.013
13	0.736	0.731	0.730	0.737	0.746	0.733	0.729	0.729	0.734	0.006
Mean	0.688	0.684	0.680	0.681	0.690	0.683	0.682	0.682	0.684	
St. Dev.	0.104	0.098	0.099	0.098	0.103	0.097	0.098	0.102		0.097
Mean (1-3)	0.509	0.517	0.511	0.512	0.513	0.517	0.514	0.506	Mean (1-3)	0.512
St. Dev. (1-3)	0.033	0.047	0.043	0.043	0.045	0.049	0.039	0.026	St. Dev. (1-3)	0.035
Mean (4-13)	0.742	0.735	0.731	0.732	0.743	0.733	0.733	0.735	Mean (4-13)	0.735
St. Dev. (4-13)	0.014	0.012	0.011	0.008	0.015	0.011	0.013	0.018	St. Dev. (4-13)	0.013

TABLE 4.5. UT Thickness Measurements for Member 03

Member 03 (Santa Fe, diagonal) 3/24/99										
Ring/Ray	A	B	C	D	E	F	G	H	Mean	St. Dev.
1	0.723	0.742	0.733	0.726	0.740	0.749	0.755	0.746	0.739	0.011
2	0.721	0.733	0.732	0.733	0.753	0.732	0.737	0.734	0.734	0.009
3	0.729	0.735	0.728	0.728	0.723	0.724	0.727	0.728	0.728	0.004
4	0.732	0.743	0.742	0.728	0.749	0.735	0.741	0.731	0.738	0.007
5	0.738	0.741	0.743	0.739	0.725	0.736	0.732	0.730	0.736	0.006
6	0.728	0.740	0.747	0.737	0.741	0.739	0.735	0.733	0.738	0.006
7	0.727	0.736	0.752	0.741	0.734	0.735	0.740	0.733	0.737	0.007
8	0.414	0.390	0.390	0.376	0.388	0.401	0.398	0.398	0.394	0.011
9	0.381	0.386	0.374	0.363	0.378	0.379	0.385	0.378	0.378	0.007
10	0.386	0.386	0.382	0.384	0.377	0.382	0.388	0.381	0.383	0.003
11	0.379	0.380	0.383	0.383	0.370	0.382	0.374	0.376	0.378	0.005
12	0.379	0.379	0.385	0.363	0.380	0.406	0.391	0.378	0.383	0.012
13	0.375	0.369	0.371	0.372	0.370	0.397	0.377	0.369	0.375	0.009
14	0.353	0.357	0.351	0.352	0.339	0.348	0.365	0.347	0.352	0.008
15	0.353	0.334	0.363	0.366	0.351	0.351	0.336	0.396	0.356	0.020
16	0.356	0.358	0.347	0.355	0.366	0.359	0.349	0.354	0.356	0.006
Mean	0.530	0.532	0.533	0.528	0.530	0.535	0.533	0.532	0.532	
St. Dev.	0.182	0.189	0.189	0.187	0.190	0.184	0.187	0.184		0.181
Mean (1-7)	0.728	0.739	0.740	0.733	0.738	0.736	0.738	0.734	Mean (1-7)	0.736
St. Dev. (1-7)	0.006	0.004	0.009	0.006	0.011	0.008	0.009	0.006	St. Dev. (1-7)	0.008
Mean (8-16)	0.375	0.371	0.372	0.368	0.369	0.378	0.374	0.375	Mean (8-16)	0.373
St. Dev. (8-16)	0.019	0.018	0.015	0.011	0.015	0.021	0.020	0.017	St. Dev. (8-16)	0.017

After data were taken on the diagonal members (01, 02, and 03), UT thickness measurements were made on the three horizontal members (Members 04, 05, and 06). Since these members were all above the mean water level, they had less marine growth than submerged diagonal members. The possibility of sandblasting Members 04 and 05 was first explored, because they both had painted surfaces that might have hindered thickness readings. Five or six trial measurements revealed that reliable UT data could be taken without sandblasting the two members, however. Although Member 04 had no visible dents, cracks or holes, it did have significant corrosion. A railing system with an attached grating was located where ray A would be, so measurements could not be made along that ray. Figs. 4.16 through 4.18 show Member 04 (Forest I, horizontal). Fig. 4.19 and 4.20 are schematic drawings of the member with ring locations and further details of the railing system. It was decided to make measurements around Member 04 at each railing attachment, which were spaced at approximately one meter. This resulted in 11 rings and 7 rays.

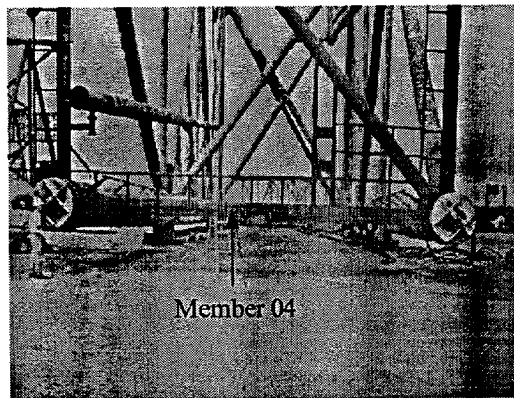


FIG. 4.16. Member 04 (Full-length)

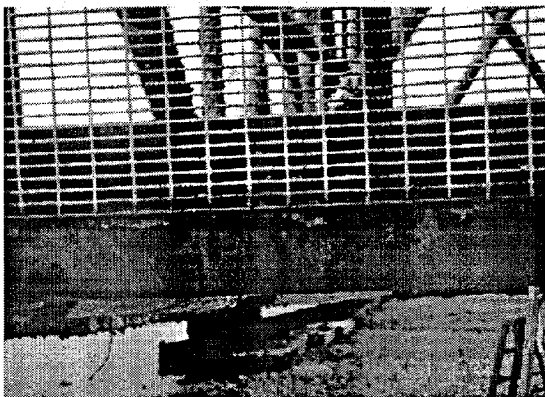


FIG. 4.17. Member 04 (Corrosion at Grate, View from Deck)



FIG. 4.18. Member 04 (Heavy Corrosion, View toward Deck)

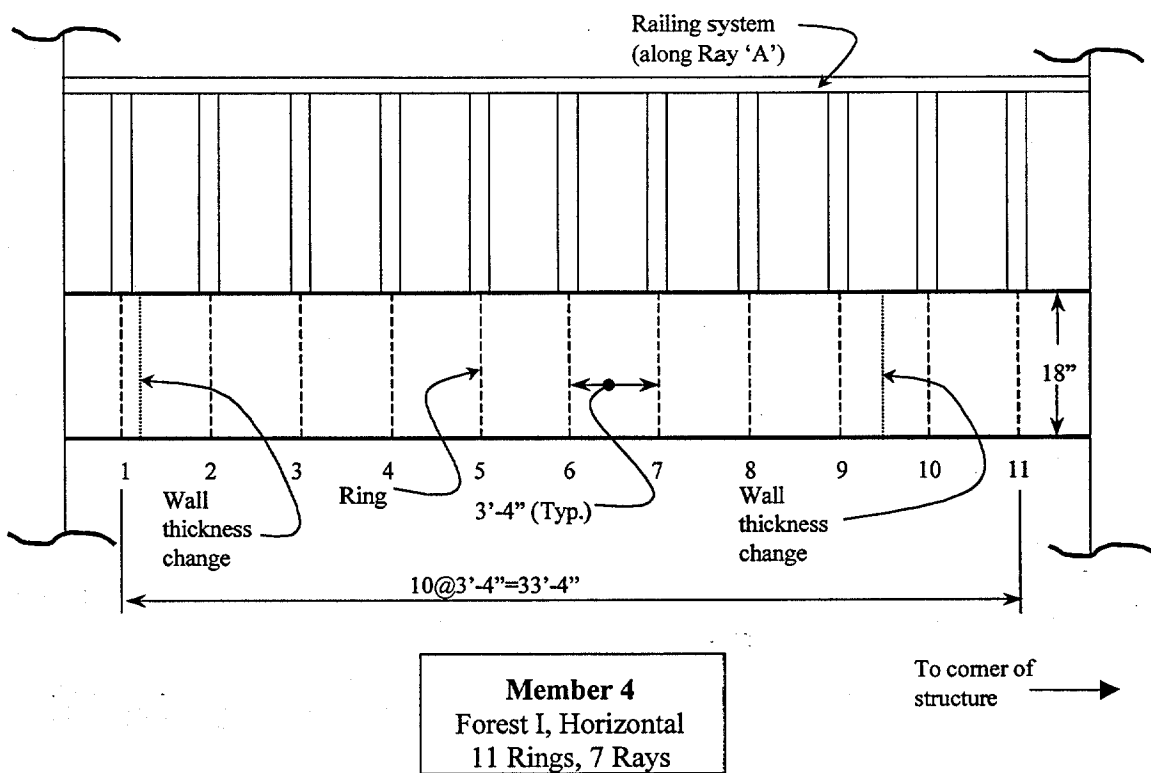


FIG. 4.19. Member 04 Schematic Drawing (View toward Deck)

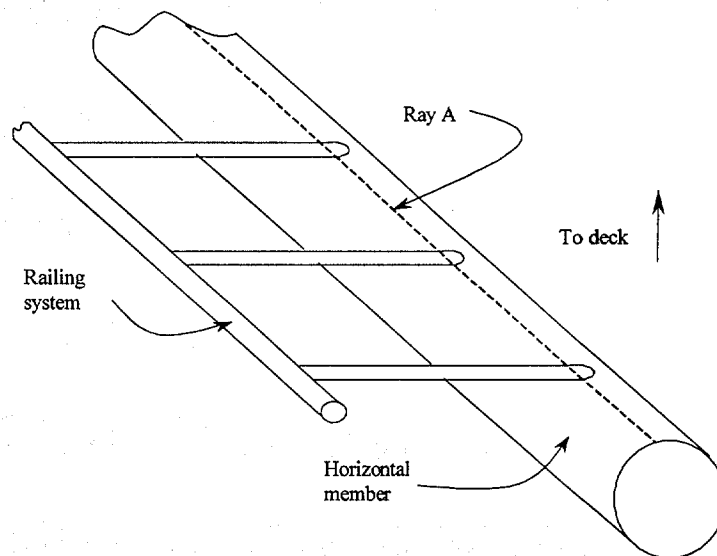


FIG. 4.20. Member 04 Railing System Detail

Member 05 (Forest II horizontal) was very similar to Member 04 including a railing system. Again, no UT measurements could be taken along ray A. Longitudinal seams were noted at rays C and G. Two dents were also present in this member, one of them was very severe (bending the member), resulting in extreme corrosion. Figs. 4.21 through 4.23 show an overall view and close up views of the dented area of Member 05. A schematic drawing of this member showing ring location, dent location and rail orientation is presented in Fig. 4.24.

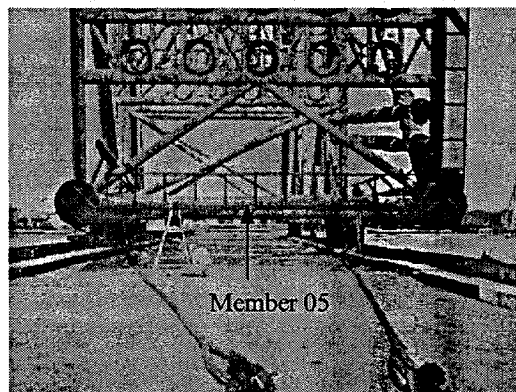


FIG. 4.21 Member 05 (Full-length)

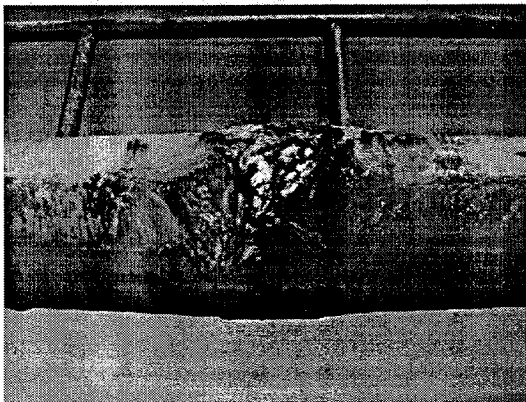


FIG. 4.22. Member 05 Dent
(View toward Deck)

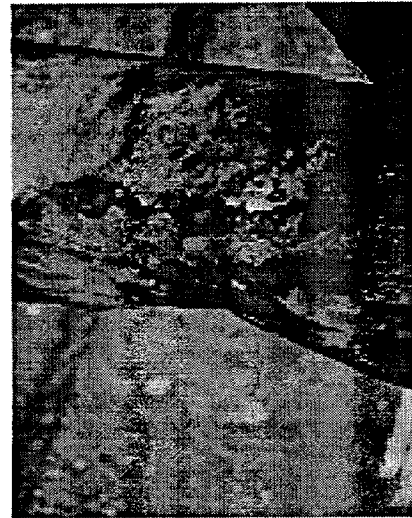


FIG. 4.23. Member 05 Dent (View
from Center of Structure)

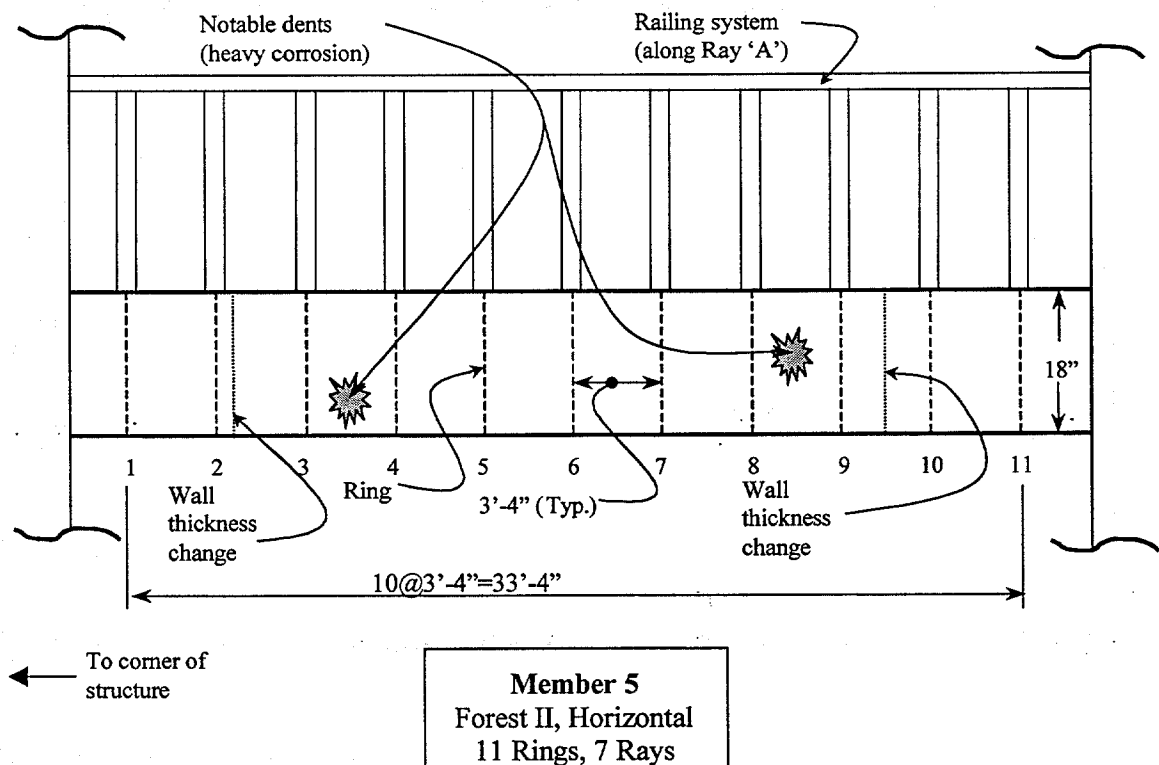


FIG. 4.24. Member 05 Schematic Drawing
(View toward Deck)

Member 06, from the Santa Fe lean-to, was a totally refurbished member. Again, a grate along ray A prevented the taking of any data there. A photo and schematic drawing of this member are shown in Fig. 4.25 and 4.26.

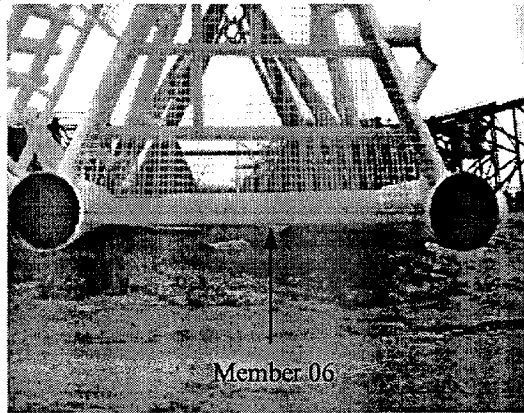
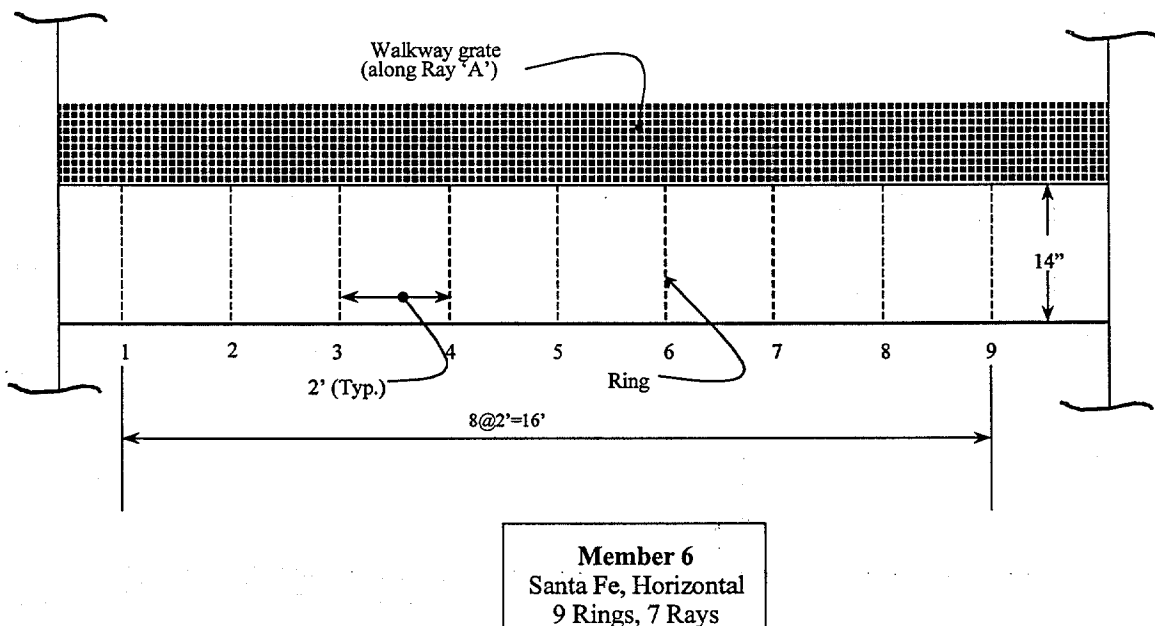


FIG. 4.25. Member 06 (View from Deck)



**FIG. 4.26. Member 06 Schematic Drawing
(View toward Deck)**

All UT thickness data for the horizontal members (Members 04, 05, and 06) are given in Tables 4.6 to 4.8. Tables 4.6 and 4.7 show changes in nominal thickness at each end of Members 04 and 05, respectively, while Table 4.8 shows a constant thickness throughout the length of Member 06. Detailed analyses of these data are presented in Chapters V and VI.

TABLE 4.6. UT Thickness Measurements for Member 04

Member 04 3/25/99 (Forest I, horizontal)										
Ring/Ray	A	B	C	D	E	F	G	H	Mean	St. Dev.
1	-	0.769	0.765	0.755	0.779	0.783	0.795	0.760	0.772	0.014
2	-	0.509	0.480	0.524	0.512	0.539	0.526	0.515	0.515	0.018
3	-	0.538	0.515	0.505	0.499	0.499	0.496	0.519	0.510	0.015
4	-	0.528	0.498	0.517	0.516	0.505	0.497	0.493	0.508	0.013
5	-	0.522	0.526	0.485	0.502	0.498	0.497	0.520	0.507	0.016
6	-	0.530	0.505	0.493	0.503	0.518	0.519	0.511	0.511	0.012
7	-	0.552	0.512	0.485	0.532	0.485	0.491	0.508	0.509	0.025
8	-	0.483	0.499	0.521	0.517	0.505	0.498	0.485	0.501	0.015
9	-	0.477	0.478	0.507	0.525	0.523	0.526	0.500	0.505	0.021
10	-	0.754	0.770	0.756	0.774	0.766	0.760	0.768	0.764	0.007
11	-	0.777	0.766	0.758	0.765	0.780	0.757	0.766	0.767	0.009
Mean	-	0.585	0.574	0.573	0.584	0.582	0.578	0.577	0.579	
St. Dev.	-	0.119	0.125	0.118	0.122	0.126	0.124	0.121		0.117
Mean (1,10,11)	-	0.767	0.767	0.756	0.773	0.776	0.771	0.765	Mean (1,10,11)	0.768
St. Dev. (1,10,11)	-	0.012	0.003	0.002	0.007	0.009	0.021	0.004	St. Dev. (1,10,11)	0.011
Mean (2-9)	-	0.517	0.502	0.505	0.513	0.509	0.506	0.506	Mean (2-9)	0.508
St. Dev. (2-9)	-	0.026	0.017	0.016	0.012	0.017	0.015	0.013	St. Dev. (2-9)	0.017

TABLE 4.7. UT Thickness Measurements for Member 05

Member 05 3/25/99 (Forest II, horizontal)										
Ring/Ray	A	B	C	D	E	F	G	H	Mean	St. Dev.
1	-	0.737	0.720	0.711	0.735	0.728	0.721	0.760	0.730	0.016
2	-	0.735	0.727	0.736	0.744	0.732	0.736	0.765	0.739	0.012
3	-	0.519	0.507	0.482	0.515	0.479	0.481	0.504	0.498	0.017
4	-	0.477	0.524	0.463	0.480	0.543	0.495	0.492	0.496	0.028
5	-	0.494	0.516	0.459	0.469	0.535	0.493	0.482	0.493	0.026
6	-	0.465	0.507	0.470	0.458	0.476	0.499	0.473	0.478	0.018
7	-	0.485	0.495	0.451	0.450	0.464	0.464	0.485	0.471	0.018
8	-	0.460	0.461	0.460	0.482	0.485	0.483	0.497	0.475	0.015
9	-	0.480	0.476	0.446	0.452	0.458	0.484	0.513	0.473	0.023
10	-	0.731	0.783	0.755	0.722	0.746	0.725	0.735	0.742	0.021
11	-	0.726	0.704	0.709	0.713	0.728	0.730	0.756	0.724	0.017
Mean	-	0.574	0.584	0.558	0.565	0.579	0.574	0.587	0.575	
St. Dev.	-	0.127	0.122	0.135	0.131	0.125	0.123	0.133		0.123
Mean (1,2,10,11)	-	0.732	0.734	0.728	0.729	0.734	0.728	0.754	Mean (1,2,10,11)	0.734
St. Dev. (1,2,10,11)	-	0.005	0.034	0.022	0.014	0.009	0.006	0.013	St. Dev. (1,2,10,11)	0.018
Mean (3-9)	-	0.483	0.498	0.462	0.472	0.491	0.486	0.492	Mean (3-9)	0.483
St. Dev. (3-9)	-	0.020	0.022	0.012	0.023	0.034	0.012	0.014	St. Dev. (3-9)	0.023

TABLE 4.8. UT Thickness Measurements for Member 06

Member 06 (Santa Fe, horizontal) 3/25/99										
Ring/Ray	A	B	C	D	E	F	G	H	Mean	St. Dev.
1	-	0.335	0.346	0.347	0.350	0.362	0.368	0.348	0.351	0.011
2	-	0.344	0.348	0.343	0.350	0.360	0.359	0.345	0.350	0.007
3	-	0.339	0.351	0.337	0.361	0.354	0.360	0.350	0.350	0.009
4	-	0.344	0.346	0.347	0.361	0.362	0.354	0.353	0.352	0.007
5	-	0.374	0.344	0.347	0.355	0.362	0.348	0.351	0.354	0.010
6	-	0.363	0.345	0.347	0.358	0.365	0.356	0.346	0.354	0.008
7	-	0.359	0.340	0.345	0.365	0.348	0.359	0.347	0.352	0.009
8	-	0.377	0.343	0.336	0.349	0.359	0.349	0.359	0.353	0.013
9	-	0.341	0.336	0.350	0.365	0.370	0.359	0.347	0.353	0.013
Mean	-	0.353	0.344	0.344	0.357	0.360	0.357	0.350	0.352	
St. Dev.	-	0.016	0.004	0.005	0.006	0.006	0.006	0.004		0.009

4.4 Comment on Measurement Accuracy

Recall that the practical precision of the Panametrics 26 DL Plus UT thickness-measuring device was studied in Section 2.1. It was shown that the reproducibility of any measurement depended on the amount of corrosion on the surfaces. Repeated measurements on clean bar stock gave variations in measured values having a standard deviation of 0.0008 inches, while measurements on badly corroded members gave a standard deviation of 0.009 inches. It is reasonable to assume that these two values are approximately lower and upper bounds of the standard deviations that would be obtained in practical applications of the device on members within offshore structures. In particular, it is reasonable to assume that the measurements on the structures studied in Morgan City had more consistency than those on the badly corroded members previously studied, since the Morgan City members seemed to have less corrosion. It should also be noted that the accuracy of a statistical average of several measurements can be greater than the accuracy of any of the individual measurements, due to cancellation of errors. Thus, some of the statistical data in the following chapters may be considered to be more accurate than would be indicated by the standard deviation values given here.

CHAPTER V

LONGITUDINAL VARIATIONS OF THICKNESS

The data from the field study were analyzed graphically and by using the ANOVA procedure described in Section 2.3. Recall that the p value from ANOVA can be interpreted as the probability that the actual observed pattern of corrosion measurements would have occurred due to random variations, even if there really was no underlying phenomenon causing the corrosion to have a pattern of occurrence. A p value of less than 5% is generally considered to indicate a high likelihood that there is a non-random pattern of corrosion. Thus, the graphs of observed values will be used to seek patterns, and the ANOVA results will be used to determine whether these variations are statistically significant, with a small p value being an indication of significance.

For purposes of simplicity, these searches for patterns in the data will be separated into a study of longitudinal variations, presented in this chapter, and a study of circumferential variations, presented in the following chapter.

Within the search for longitudinal variations it is crucial to eliminate variation patterns which are not due to corrosion. In particular, several of the members were fabricated using different wall thickness at different locations along the length. Such a fabrication, obviously, does give a non-random longitudinal variation of the wall thickness, and it would definitely give a very small p value if it were allowed to influence the ANOVA study of the member. This problem has been avoided in this study by performing longitudinal ANOVA studies only on data obtained from segments (rings) of the member with the same nominal fabrication thickness. In any ANOVA test a p value less than 5% has been considered to have statistical significance, and a p value between 5% and 10% has been considered to have marginal significance. It should be noted, though, that these 5% and 10% values are quite arbitrary. The only point that can be asserted with certainty is that a smaller p value corresponds to a smaller probability that the perceived pattern occurred due to random variations.

5.1 Member 01 (Forest I, Diagonal)

The plans for the Forest I structure indicated that the nominal wall thickness for Member 01 should change at a circumferential seam (weld) between ring 3 and ring 4. In particular, the nominal wall thickness was indicated to be 0.750 inches for rings 1-3 and 0.625 inches for rings 4-14. A set of data from only three rings was judged not to be sufficient to allow a search for longitudinal variation of wall thickness. Thus, it was concluded that the study of longitudinal variation for this member should be confined to rings 4-14. Nonetheless, some of the plots will show measurements taken at all 14 rings.

Figure 5.1 shows all the thickness measurements made on Member 01. The data are plotted versus the longitudinal parameter Z , with a separate curve for each ray (i.e., each θ angle). The plot clearly shows that there was a change in thickness between rings 3 and 4, as predicted. The measured thickness for rings 1-3, though, was not at all in agreement with the value of 0.750 inches shown on the plans. In fact the data from rings 2 and 3, would suggest that the nominal thickness might have been 0.500 inches. It is presumed that this discrepancy is due to an undocumented modification of the design during construction of the platform. The discrepancy is of no significance to this study, since it was already concluded that rings 1-3 should not be used for seeking longitudinal corrosion patterns in this member. Note also that the data from ring 1 on this member show very considerable variation around the circumference, and are not generally in good agreement with the data from rings 2 and 3. For reasons not apparent to the researchers, it was difficult to obtain readings at this ring for Member 01 (and the same was also true for Member 02) even after sanding the surface and applying more transducer couplant. These data were therefore not considered to be reliable, and were not used in any further analysis.

Figure 5.2 shows a curve that is the average of the 8 curves in Fig. 5.1. That is, all the data from any given ring were averaged to give a mean thickness value for that ring. In order to investigate these mean values more thoroughly, though, rings 1-3 have been excluded. Focusing in this way on only rings 4-14, which have the same nominal

thickness, allows the scale of the plot to be expanded, so that any longitudinal variation of the mean thickness values is more evident. A linear trend line has also been inserted to see if perhaps the trend, if any, followed a linear pattern. It is important to remember, though, that trends could follow any pattern, rather than necessarily being linear. The trend line shown was obtained by linear regression, as discussed in Sec. 2.3. As explained there, the rather arbitrary judgement has been made that an R^2 value greater than 80% indicates a strong linear variation of the measurements, a value greater than 50% indicates a significant linear variation, and a value greater than 30% is evidence of a weak linear relationship. Thus, the R^2 value of 0.6425 for Member 01 indicates that there is a significant linear trend, even though there is other variation as well.

The ANOVA test of the data from Rings 4-14 gave a very small p value of 2.59×10^{-5} . Thus, it seems extremely unlikely that the longitudinal variations in the values observed could have occurred as a strictly random occurrence. There definitely does seem to be a longitudinal pattern in Member 01, and as noted above, this trend is relatively linear. Note that the mean wall thickness was observed to increase from ring 4 to ring 14, which is from the upper portion to the lower portion of the member, and from the inner leg to the corner leg of the original Forest structure.

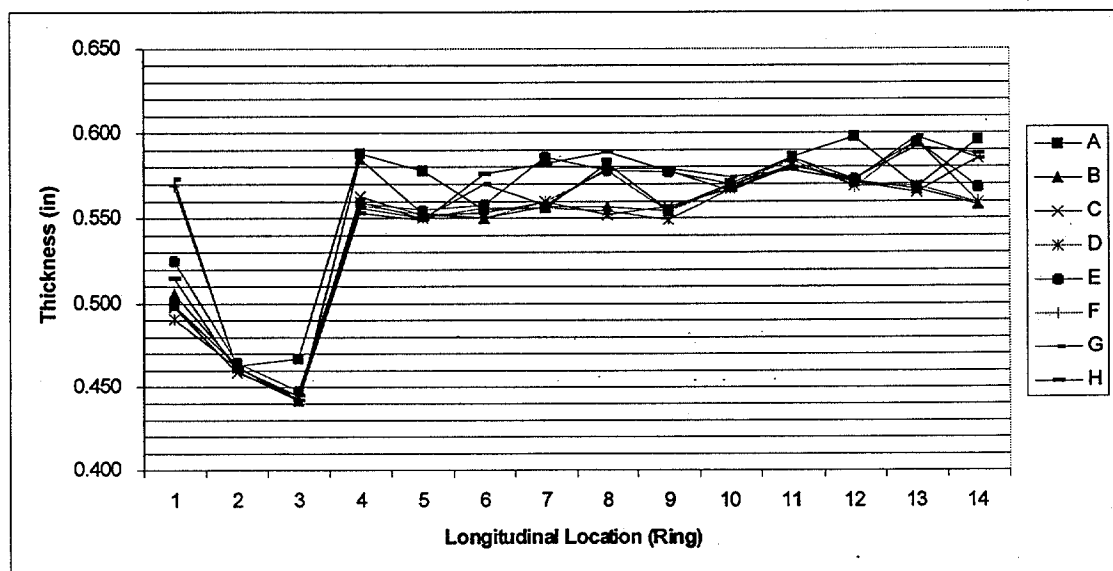


FIG. 5.1. Longitudinal Relationships for Member 01, Showing All Rings

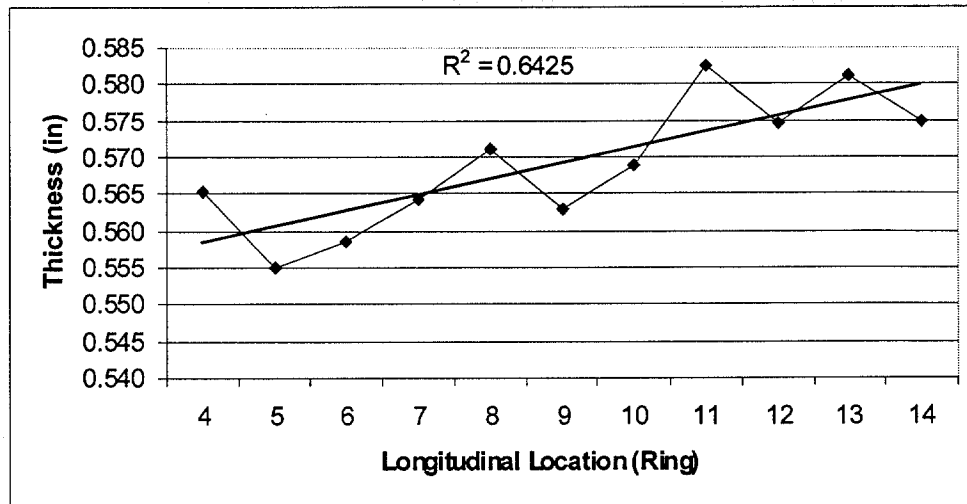


FIG. 5.2. Longitudinal Relationships for Member 01, Showing Rings 4-14 (Average over All Rays)

5.2 Member 02 (Forest II, Diagonal)

The plans and the measurements confirmed that Member 02 also had a change in wall thickness at a circumferential seam between rings 3 and 4, similar to the situation in Member 01. The plans gave the nominal wall thickness as 0.875 inches for rings 1-3 and 0.750 inches for rings 4-13. Figures 5.3, presenting all the measured thickness values, shows that again there was a major discrepancy between the nominal wall thickness and the measured wall thickness for rings 1-3. As for Member 01, this discrepancy did not affect the search for patterns of longitudinal variations in wall thickness, since those studies concentrated on rings 4-13. From Fig. 5.3 it can also be seen that the readings at ring 1 were not quite as varied as those for that ring on Member 01, but they were still considered to be unreliable.

Figure 5.4 shows the same mean thickness data for each ring, but including only rings 4-13, and has an enlarged scale to allow better identification of longitudinal trends within this segment with a constant value of nominal wall thickness. As before, a linear trend line from regression analysis is included. Somewhat surprisingly, the linear trend shown in Fig. 5.4 represents thickness decreasing from ring 4 to ring 13, which is from

the top to the bottom of member within the structure. This is in direct contrast to the results for Member 01 for which the thickness increased from the top to the bottom of the member. Since Members 01 and 02 were actually similar parts of the same structure while in the Gulf of Mexico, they were exposed to the same corrosive environment. Thus, it was expected any corrosion patterns would be the same in both members. The significance of this anomaly will be discussed more later. There may or may not be any significance to the fact that in both Members 01 and 02 the thickness did increase from the end near the inner leg of the original structure to the end near the corner leg.

It should be noted that the R^2 value in Fig. 5.4 is only 0.3663, indicating that a straight line is not a very good approximation of the actual variation of thickness along the length of Member 02. The ANOVA test for this variation, though, was only 4.11×10^{-6} , which is a strong indication that there is a non-random longitudinal variation of thickness. From Fig. 5.4 it appears that the maximum corrosion occurred in the vicinity of ring 9, rather than near either end of the specimen. Thus, there was a significant longitudinal trend, but it was not very strongly linear.

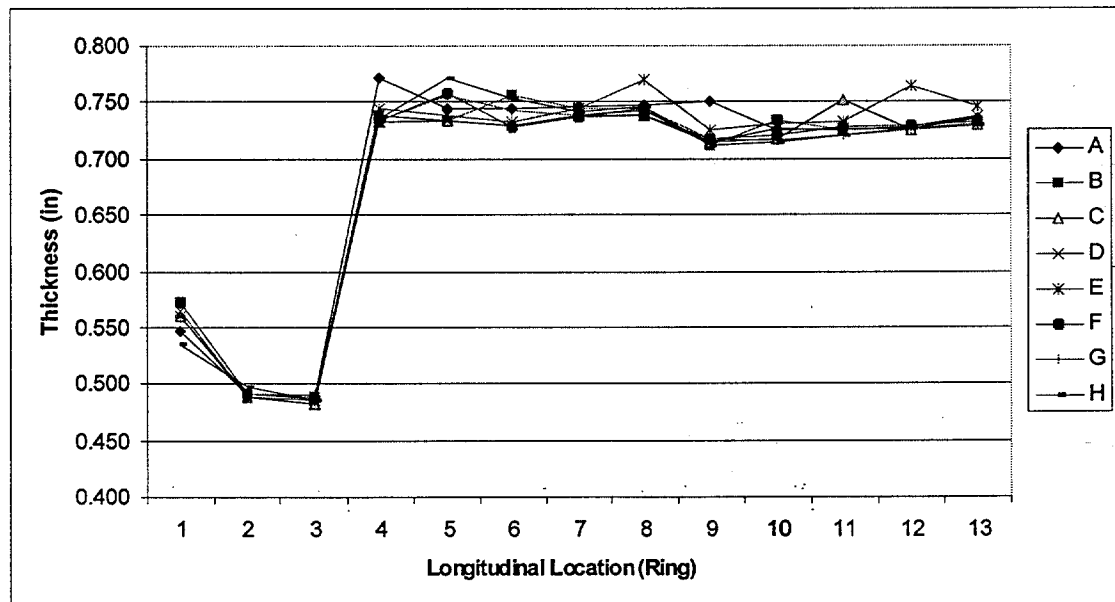


FIG. 5.3. Longitudinal Relationships for Member 02, Showing All Rings

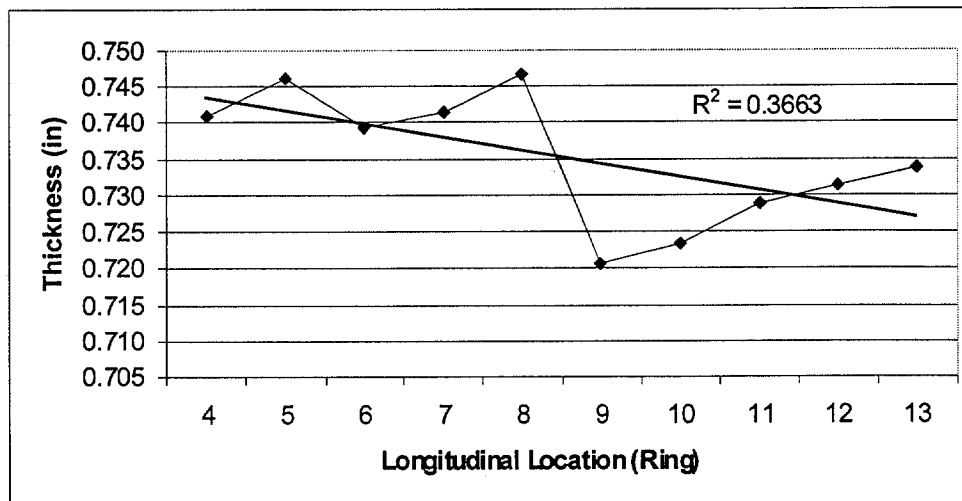


FIG. 5.4. Longitudinal Relationships for Member 02, Showing Rings 4-13 (Average over All Rays)

5.3 Member 03 (Santa Fe, Diagonal)

Member 03, from the Santa Fe lean-to, also had a change in nominal wall thickness, but this time it was near mid-length. There were seven rings on one side of the change, and nine on the other. This provided sufficient data on each side of the change in wall thickness for a separate ANOVA procedure. The presentation of all the thickness measurements in Fig. 5.5, shows that the thickness change occurred between rings 7 and 8. Rings 1-7 had a nominal wall thickness of 0.750 inches, while rings 8-16 had a nominal wall thickness of 0.375 inches.

The form of plots used here is generally the same as for Members 01 and 02, but with slightly more information. Figure 5.5 shows a longitudinal plot with all thickness measurements for Member 03. Because of the change in nominal wall thickness, the scale of Fig. 5.5 largely hides the scatter of the thickness values at the individual rings. Thus, Figs. 5.6 and 5.7 have been added to display this scatter. Finally, Figs. 5.8 and 5.9 show the mean values for the two segments of the beam along with the trend lines obtained by linear regression. It is seen that there is a fairly constant thickness in the first section and a decrease in thickness between rings 8 and 16 in the second section.

ANOVA studies were performed separately for rings 1-7 and rings 8-16, in order to seek longitudinal variations within either subset of the data. The p values found were 0.075 and 3.41×10^{-7} , respectively. The p value of 7.5% for rings 1-7 may be considered to be marginally significant. This suggests that there may or may not be a significant longitudinal thickness variation within the range of these rings. The variations observed might have occurred as a random event even if the probability distributions over the set of all possible thickness values were the same at every one of these rings, but the probability of this random event is 7.5%. The very small p value for the second segment suggests that there definitely is a significant thickness variation within the range of rings 8-16. From the R^2 value of 0.0263 in Fig. 5.8 it is clear that there is not a significant linearity to the thickness variation within rings 1-8, while the R^2 value of 0.7829 in Fig. 5.9 confirms the graphical evidence that this significant longitudinal variation for rings 8-16 is quite strongly linear. The plot in Fig. 5.9 also shows that the thickness decreases from the top end to the bottom end of Member 03, within the range of rings 8-16. This trend agrees somewhat with that in Member 02, but disagrees with the result for Member 01. Note that the thickness data for rings 8-16 show a decrease in thickness closer to the leg, and recall that all legs of the Santa Fe platform are corner legs. The trend observed, though, seems to be the opposite of the results for Members 01 and 02, for which the greatest thickness occurred near the corner leg of the original Forest structure.

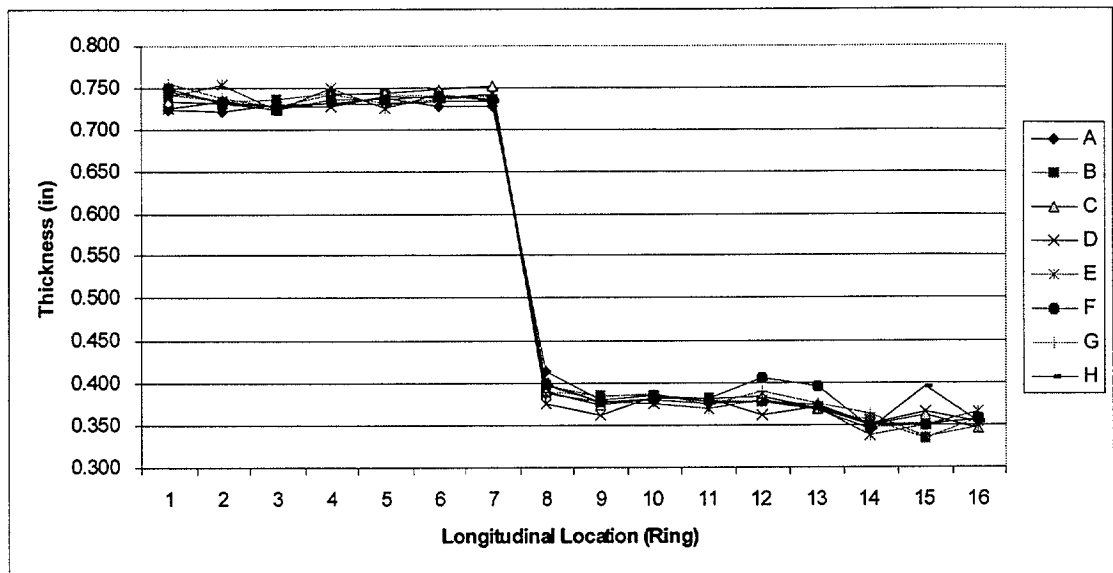
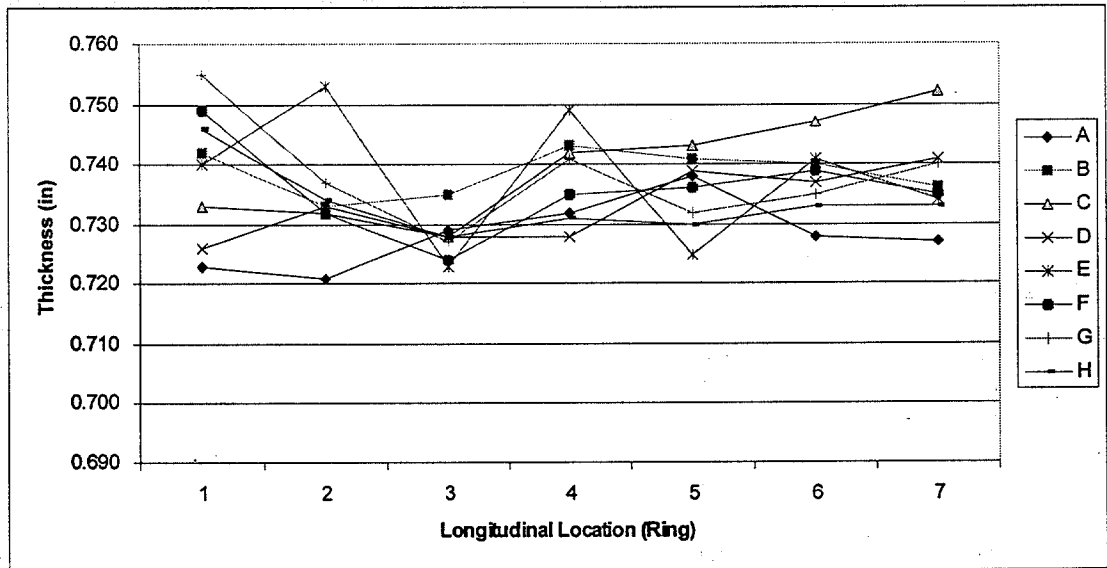
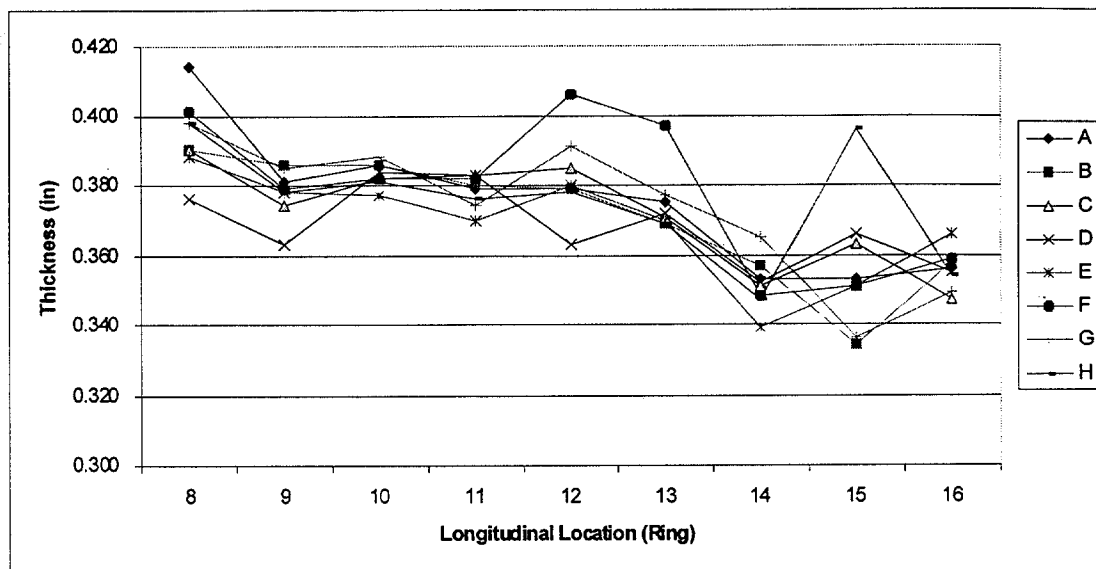


FIG. 5.5. Longitudinal Relationships for Member 03, Showing All Rings



**FIG. 5.6. Longitudinal Relationships for Member 03
Showing Rings 1-7**



**FIG. 5.7. Longitudinal Relationships for Member 03,
Showing Rings 8-16)**

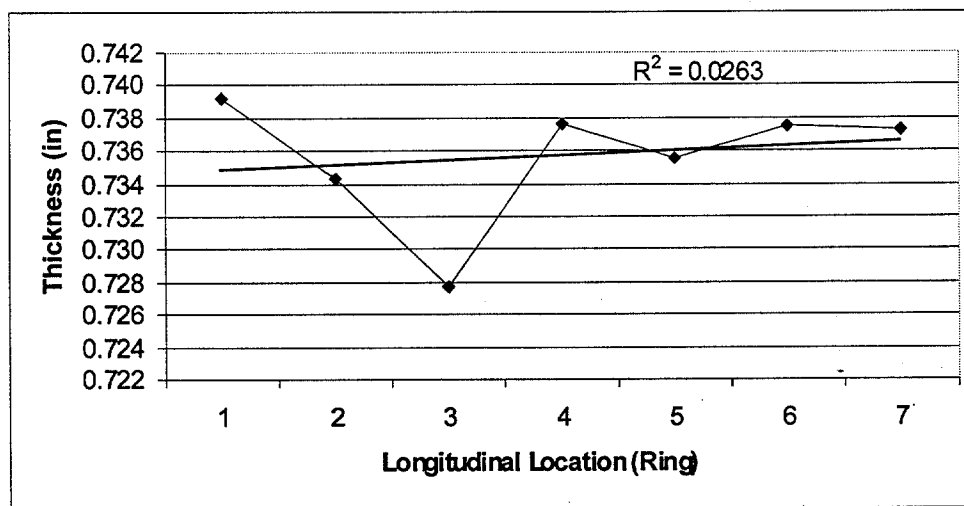


**FIG. 5.8. Longitudinal Relationships for Member 03,
Showing Rings 1-7 (Average over All Rays)**

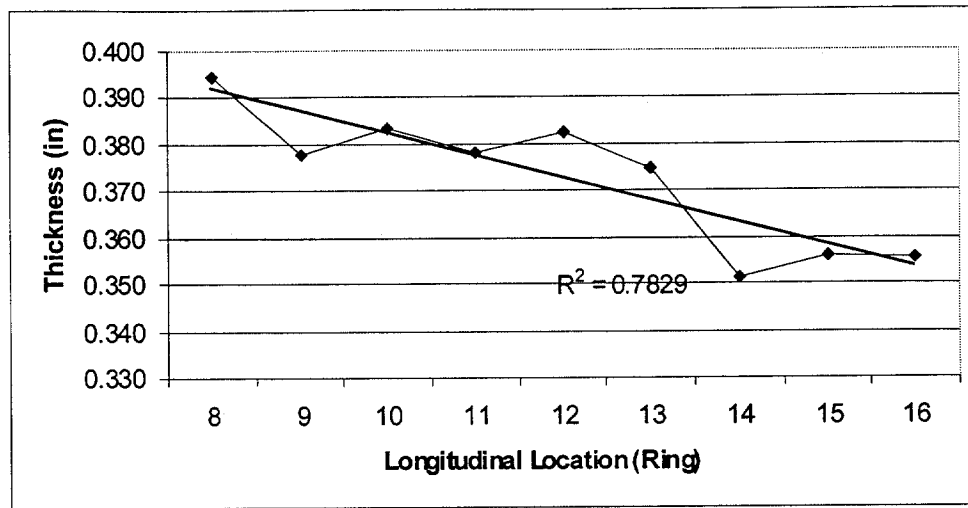


**FIG. 5.9. Longitudinal Relationships for Member 03,
Showing Rings 8-16 (Average over All Rays)**

5.4 Member 04 (Forest I, Horizontal)

Member 04 had nominal changes in thickness at each end. That is, rings 2-9 were of different thickness than rings 1, 10 and 11. This is common practice in the design of such members, as a means of increasing the capacity at the connections. Rings 1, 10, and 11 had a normal thickness of 0.750 inches while the nominal thickness of rings 2-9 was 0.500 inches. The analysis of longitudinal variation corrosion was limited to rings 2-9. Recall that no data were obtained for ray A for this specimen, because of the presence of a railing system attached at that location. Thus, any average over "all rays" refers to rays B-H.

The two thicker ends of Member 04 are evident in Figs. 5.10, which includes all data for the member. The relevant data from rings 2-9 are plotted alone as an average over all rays in Fig. 5.11. From Fig. 5.11 it is clear that there is a general decreasing trend in thickness from ring 2 to ring 9. This represents a decrease in thickness moving towards the corner leg of the *in-situ* structure. Figure 5.9 also shows the linear regression trend line, with an R^2 value of 0.5437, which indicates significant linearity to the observed longitudinal variation of thickness. The p value for the ANOVA test of these data was 0.8985, though. This large value clearly indicates that the degree of thickness variation shown in Fig. 5.11 could very likely have occurred simply as a random event.

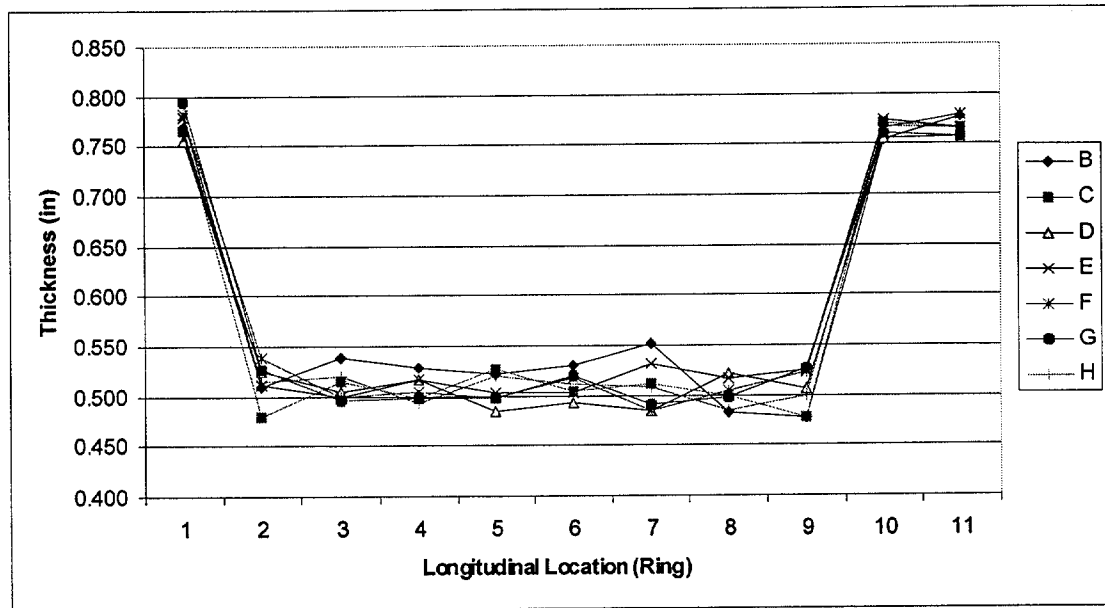


FIG. 5.10. Longitudinal Relationships for Member 04, Showing All Rings

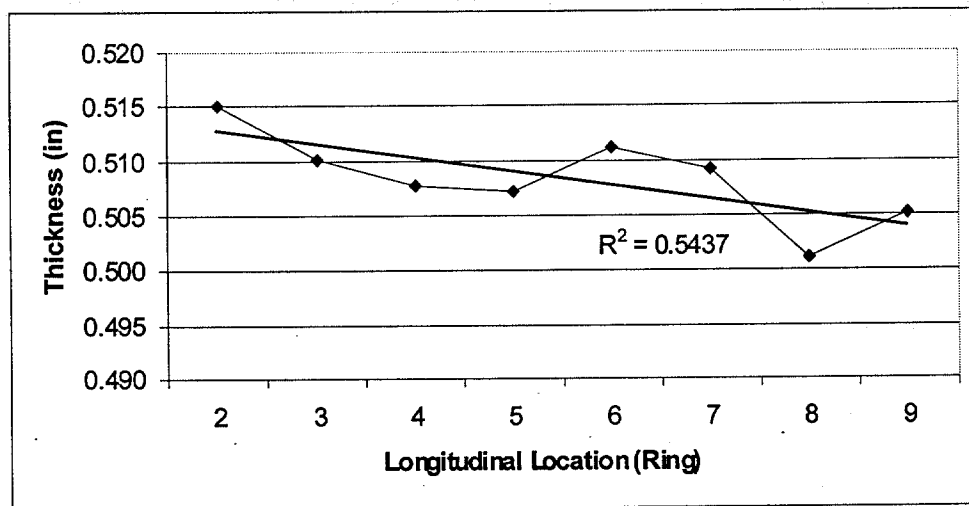


FIG. 5.11. Longitudinal Relationships for Member 04, Showing Rings 2-9 (Average Over All Rays)

5.5 Member 05 (Forest II, Horizontal)

Member 05, like Member 04, had thickness changes at each end. The data were therefore analyzed from ring 3 to ring 9. For this section, the nominal wall thickness was 0.500 inches, the same as Member 04. Nominal wall thickness for rings 1, 2, 10, and 11 was

again 0.750 inches. As with Member 04, a railing system prevented the taking of measurements at Ray A, so that any average over "all rays" refers to rays B-H.

Figure 5.12, showing all rings for Member 05, is similar to Fig. 5.10 for Member 04, as expected. The data relevant to the search for longitudinal dependence are replotted in Fig. 5.13 as an average over all rays, only for rings 3-9, along with the linear regression trend line. The trend in Fig. 5.13 seems to be decreasing thickness from ring 3 to ring 9. This represents a decrease in thickness from the corner leg to the inner leg of the original Forest structure. The R^2 value of 0.8374 for this regression line indicates a significant linearity to this longitudinal variation. Furthermore, the p value for the ANOVA test was 0.06646, indicating at least a marginal statistical significance of the longitudinal variation in Member 05. The trend in the data for Member 05 of being thickest nearest the corner leg of the original platform is the opposite of the trend for Member 04, but it should be recalled that the trend from Member 04 was clearly not statistically significant.

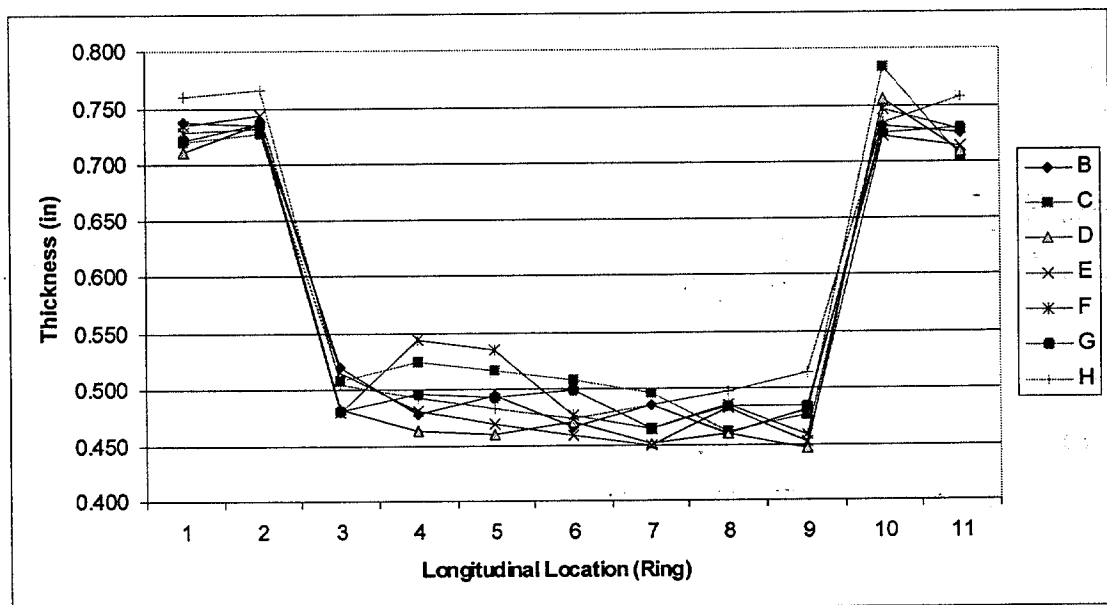


FIG. 5.12. Longitudinal Relationships for Member 05, Showing All Rings

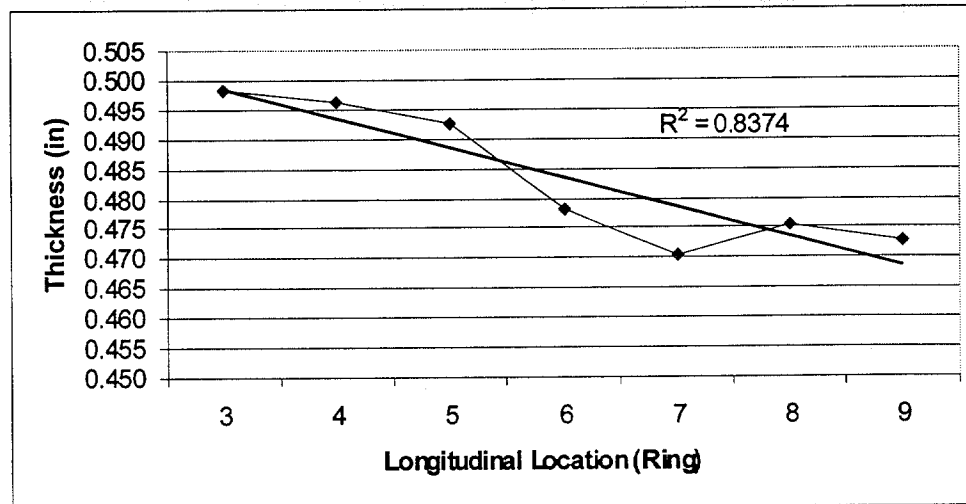


FIG. 5.13. Longitudinal Relationships for Member 05, Showing Rings 3-9 (Average Over All Rays)

5.6 Member 06 (Santa Fe, Horizontal)

Member 06 had the same nominal thickness (0.375 inches) throughout its entire length, so that all rings could be used in the statistical analysis. As in the other horizontal specimens, though, there was a walkway attachment, which prevented the making of measurements at Ray A.

Figs. 5.14 and 5.15 present the data in the same form used for the other members. From the plot of all data in Fig. 5.14 it is difficult to detect any longitudinal pattern to the corrosion, but a trend does seem more clear in the plot of averaged values in Fig. 5.15. The R^2 value of 0.366 for the linear regression line in Fig. 5.15 shows that there is not a strong linear pattern to the longitudinal variation. In fact, Rings 5 and 6 seem to be the thickest, with thinner values toward each leg of the platform. The ANOVA test, though gave a p value of 0.0992, indicating that this longitudinal variation of thickness has only marginal statistical significance.

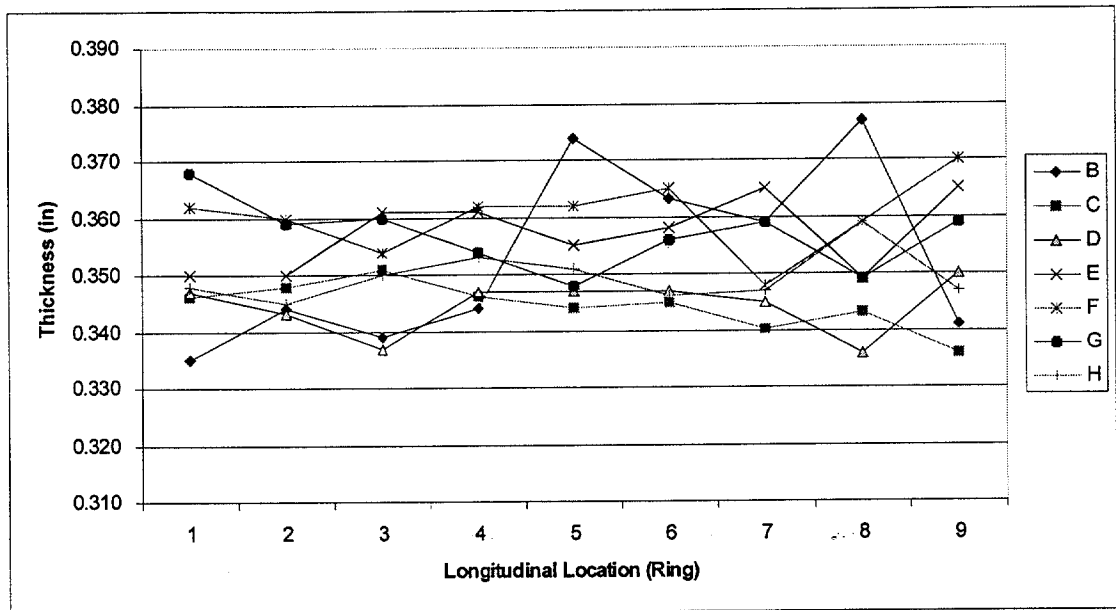
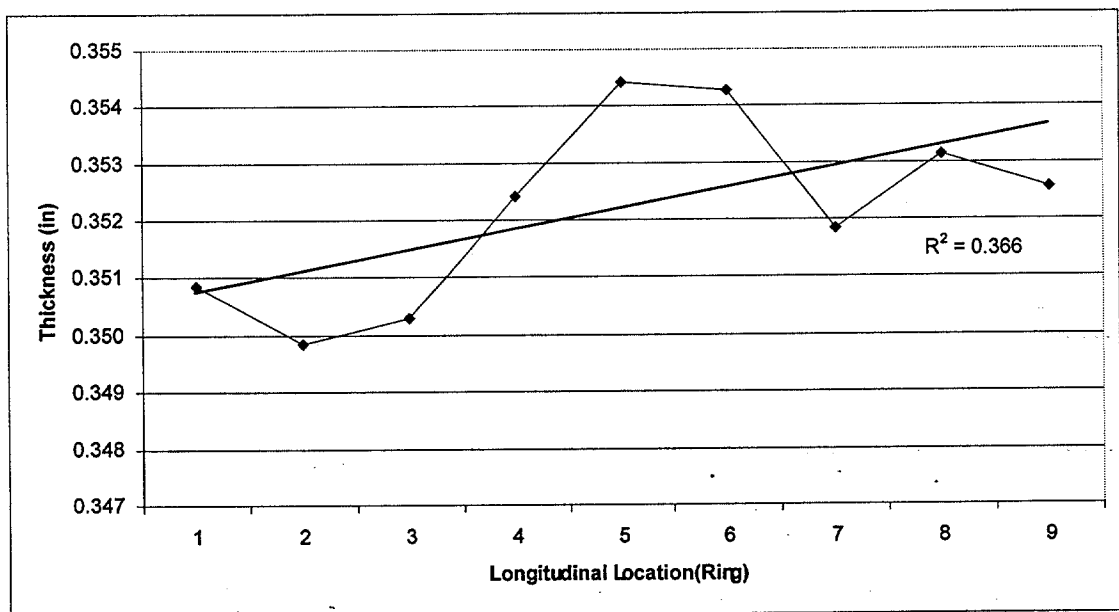


FIG. 5.14. Longitudinal Relationships for Member 06, Showing All Rings



**FIG. 5.15. Longitudinal Relationships for Member 06,
Showing All Rings (Average Over All Rays)**

5.7 Summary of Observations

Table 5.1 summarizes the results found regarding the possibility of longitudinal patterns in the corrosion in the six members. From the column of p values, it is clear that three sets of data [Members 01, 02, and 03 (8-16)] had clear statistical evidence of a significant longitudinal variation in thickness. All three of these members were diagonals. For two of these three sets of data, the significant variation in thickness had a quite strong linear trend, as indicated by the R^2 values. For Member 02 the variation was only weakly linear. The p values for the other sets of data indicated marginal statistical significance of the thickness variation in two cases [Members 03 (1-7) and 05] and no statistical significance in the other two [Members 04 and 06]. For one of the sets with marginal statistical significance, the variation was strongly linear, while for the other it clearly was not linear. The final two columns in the table give some crude information about the location along the length of the member of the ring having the maximum corrosion/minimum thickness. The horizontal locations are best understood by referring to Figures 4.3 and 4.7. In particular, "Corner Leg" for the Forest jacket refers to one of the legs at the corner of the original *in situ* structure. "Inner Leg" refers to a leg that was not at a corner of the structure, although it was still on the outer perimeter of the structure. Since the Santa Fe structure is a lean-to, it only has corner legs.

TABLE 5.1. Summary of Results for Longitudinal Variation of Thickness

Member (Rings)	p	R^2	Loc. of Minimum Thickness (Maximum Corrosion)	
			Horizontally	Vertically
01	2.592×10^{-5}	0.6425	Inner Leg	Upper End
02	4.111×10^{-6}	0.3663	Away from Legs	Away from Ends
03 (1-7)	0.0741	0.0263	Away from Legs	Away from Ends
03 (8-16)	3.411×10^{-13}	0.7829	Corner Leg	Lower End
04	0.8985	0.5437	Corner Leg	----
05	0.0665	0.8374	Inner Leg	----
06	0.9918	0.3660	Both Legs	----

Figures 5.16 and 5.17 present the results for the loss of wall thickness in a schematic way. The wall thickness values analyzed are plotted along the length of each

of the six members studied. Overall, it seems that this information indicates that the longitudinal pattern of the corrosion is highly variable, and does not have any simple correlation with geometric position within the offshore structure. It should be noted, though, that there is no scale for the wall thickness in these figures. The purpose of these figures is only to show the locations having substantial corrosion.

Recall that the first three members studied also had attached sacrificial anodes to provide corrosion protection. Members 01 and 02 each had two anodes, attached in the vicinity of rings 6 and 11, while Member 03 had one anode attached in the vicinity of rings 14 and 15. These anode locations are indicated by a circled A on the schematics in Figures 5.16 and 5.17. For these particular members there does not seem to be any consistent, significant correlation between the extent of corrosion and the longitudinal proximity to an anode.

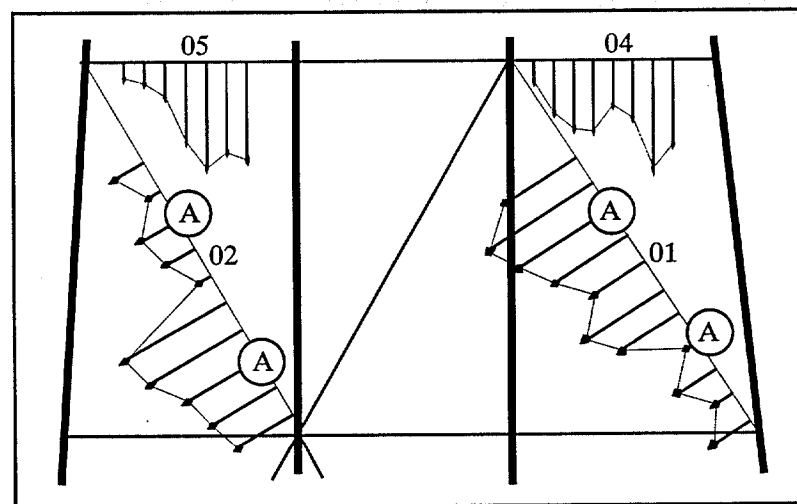


FIG. 5.16. Wall Loss in Forest Structure (Schematic)

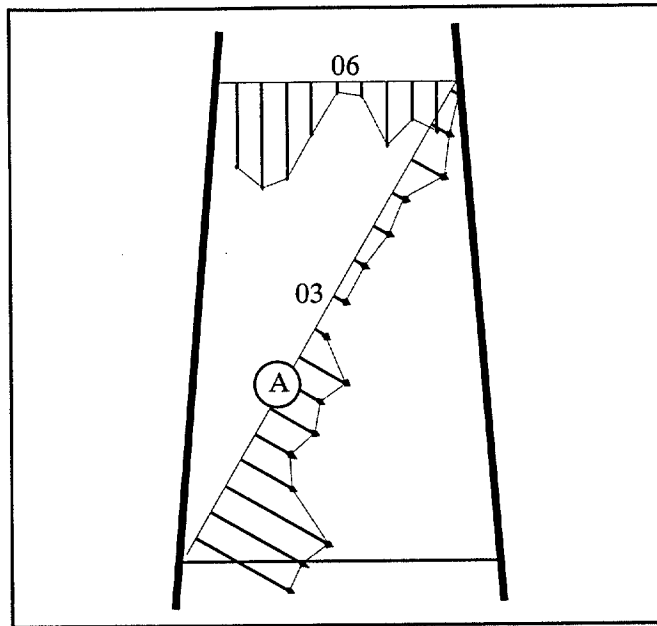


FIG. 5.17. Wall Loss in Santa Fe Structure (Schematic)

CHAPTER VI

CIRCUMFERENTIAL VARIATIONS OF THICKNESS

The data presented in Chapter V are here analyzed to determine whether the corrosion had patterns around the circumference of the members. The initial studies use exactly the same procedures as were employed in Chapter V – namely, graphical presentations to seek trends and ANOVA analysis to determine whether the trends are statistically significant. These studies are also supplemented with similar studies using “lumped” versions of the data, and a *t*-test to check for statistical significance. Linear regression is not used in this chapter, since it is virtually impossible to have a linear variation of thickness with respect to θ . In particular, $\theta = 0$ and $\theta = 2\pi$ are the same location on the member, so the thickness cannot vary linearly from one to the other.

6.1 Plots and ANOVA Results

The sets of data that could be analyzed with ANOVA were the same as in Chapter V: rings 4-14 of Member 01, rings 4-13 of 02, rings 1-7 of 03, rings 8-16 of 03, rings 2-9 of 04, rings 3-9 of 05, and rings 1-9 (all rings) of 06. As explained in the preceding chapter, the omission of some of the rings from the statistical analysis was because of changes in thickness in the tubular members as they were fabricated. In addition, it should be remembered that there were no data from ray A for members 04, 05 and 06, since these three were horizontal members with a walkway/railing attached at ray A.

Figures 6.1 to 6.7 show the variations of wall thickness for the seven sets of data that were extensive enough to warrant ANOVA analysis. The individual thickness values are not plotted here, since they were shown in Chapter V. Rather, each plotted point, for a given ray on a given member, gives the average thickness over all rings within the given set of data. Figure 6.1 also includes the average over rings 1-3 for Member 01. This is done only to illustrate the clear difference between the wall thickness for these three rings near the upper end of the member and the thickness for the other eleven rings. ANOVA analysis was not performed for rings 1-3, or any other small set of data.

Table 6.1 gives the p values for the ANOVA analyses of the seven sets of data shown in Figs. 6.1 – 6.7. It is seen that only Members 05 and 06 have patterns that are statistically significant according to the rather arbitrary standard of $p \leq 5\%$. Member 01, with $p \approx 6\%$, meets the standard suggested in Chapter V for marginal significance (5% to 10%), while the p value of 12% for rings 1-7 of Member 03 narrowly misses that standard. The ANOVA results for Member 02, rings 8-16 of Member 03, and Member 04 do not seem to indicate any possibility of statistically significant patterns.

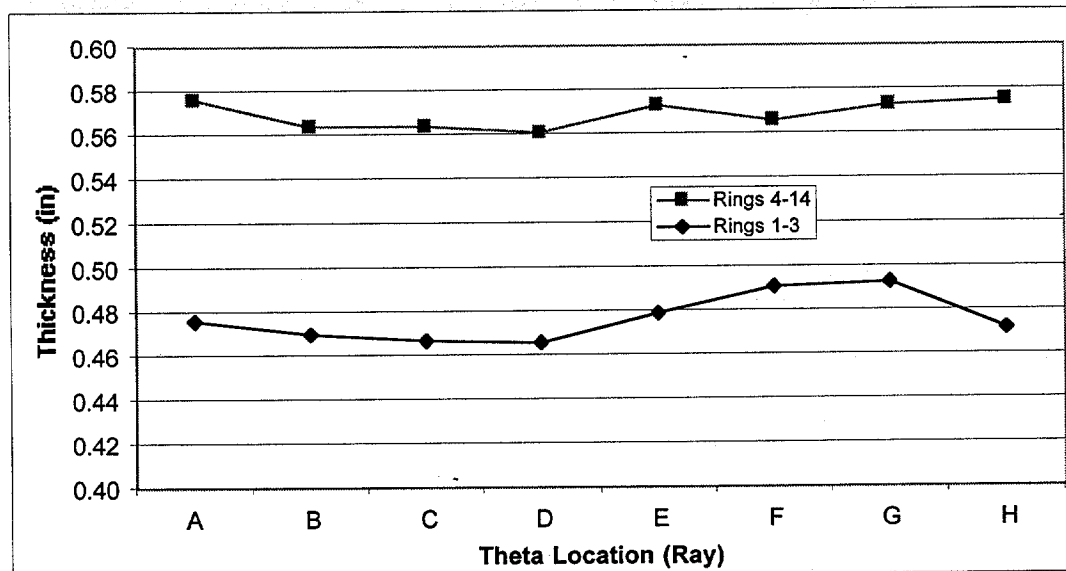


**FIG. 6.1. Circumferential Relationships for Member 01,
Average over Rings 1-3 and Average over Rings 4-14**

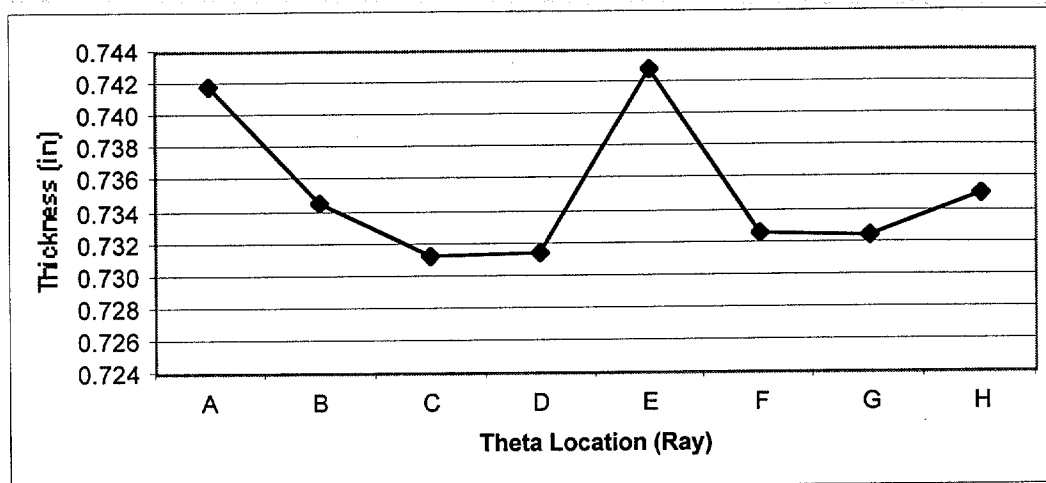


FIG. 6.2. Circumferential Relationships for Member 02, Average Over Rings 4-13

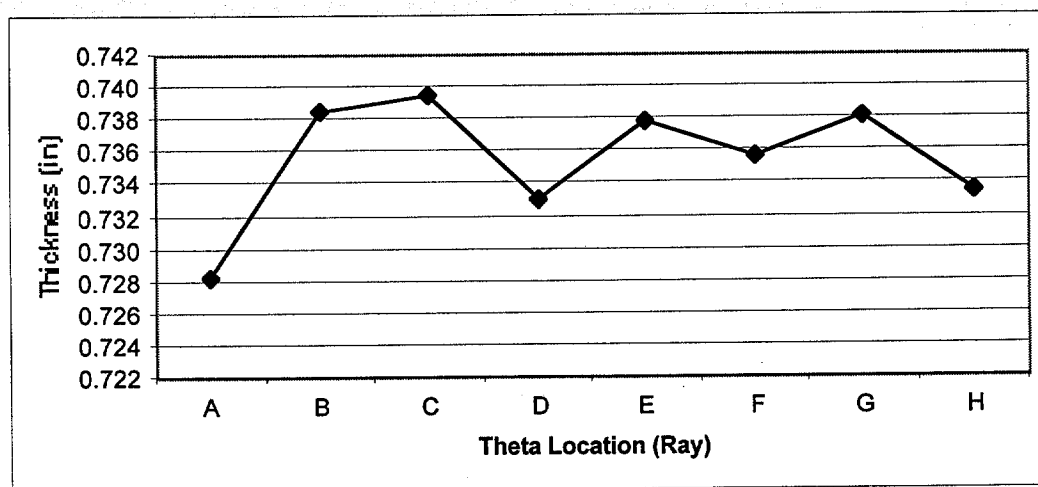


FIG. 6.3. Circumferential Relationships for Member 03, Average Over Rings 1-7

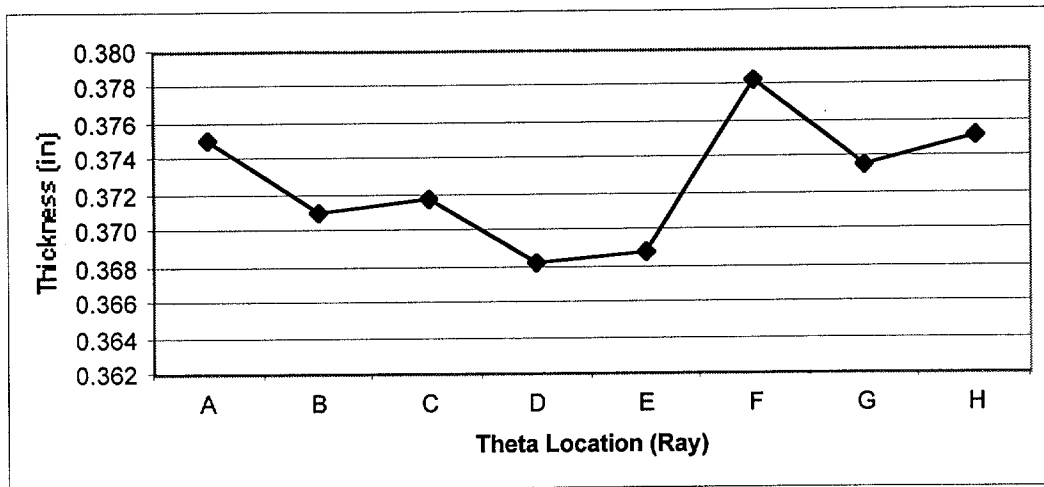


FIG. 6.4. Circumferential Relationships for Member 03, Average Over Rings 8-16

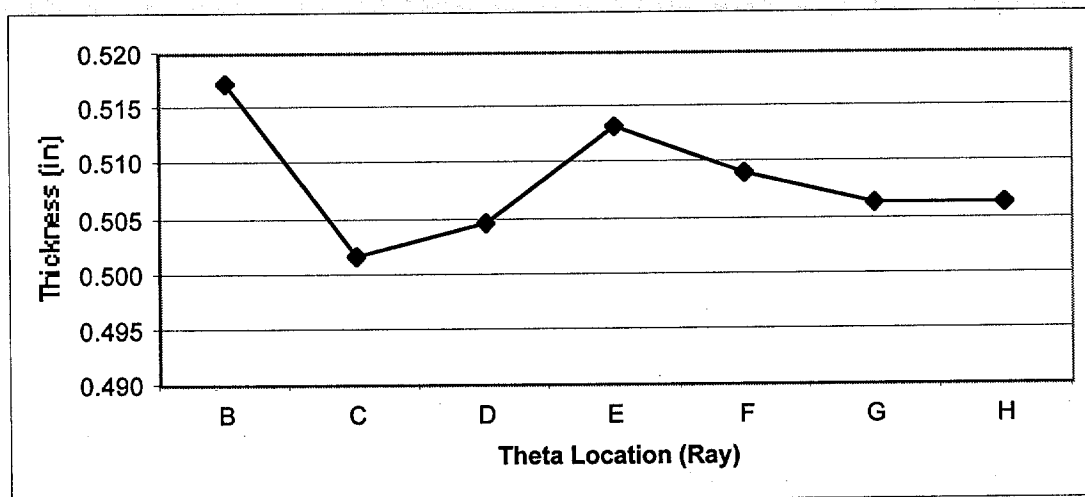


FIG. 6.5. Circumferential Relationships for Member 04, Average Over Rings 2-9

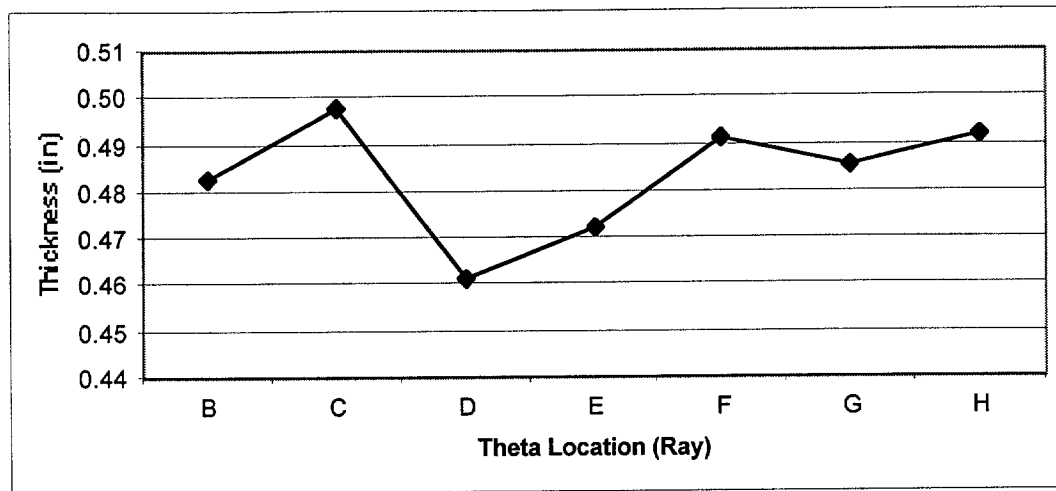


FIG. 6.6. Circumferential Relationships for Member 05, Average Over Rings 3-9

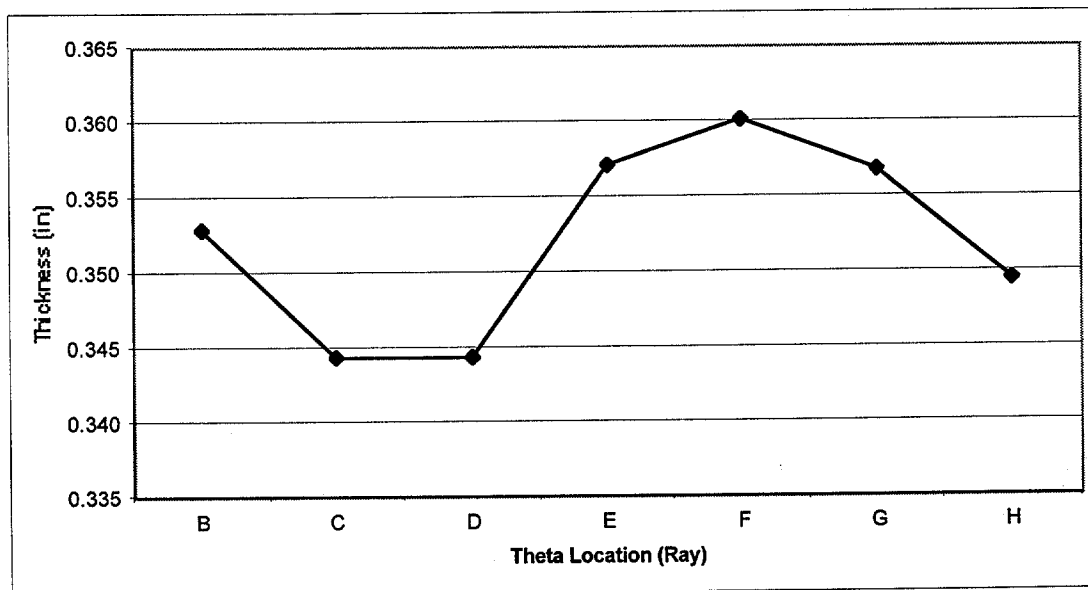


FIG. 6.7. Circumferential Relationships for Member 06, Average Over All Rings

which does not lump data from segments of the member with different nominal thickness values. In particular, the seven sets of rings included in Table 6.3 and the t -test are identical to those used in the ANOVA tests described in Chapter V and Section 6.1. It should also be noted that the data from ring 1 has been excluded for both Member 01 and Member 02, since there seemed to be a measurement error for that ring on the two diagonal Forest members.

TABLE 6.2. Mean Thickness Values for Grouped Data, Using All Rings

Member	Top	Bottom	Outside	Inside
01	0.5538	<u>0.5495</u>	<u>0.5462</u>	0.5530
02	0.6960	<u>0.6944</u>	<u>0.6917</u>	0.6929
03	0.5311	<u>0.5309</u>	<u>0.5308</u>	0.5333
04	0.5811	<u>0.5797</u>	<u>0.5775</u>	0.5790
05	0.5805	<u>0.5678</u>	<u>0.5718</u>	0.5802
06	<u>0.3512</u>	0.3539	<u>0.3472</u>	0.3556

Note: The underlined value indicates the smaller thickness in each comparison.

**TABLE 6.3. Mean Thickness Values for Grouped Data,
Grouping Only Rings with the Same Nominal Thickness**

Member (Rings)	Top		Bottom		Outside		Inside	
	Mean	St Dev	Mean	St Dev	Mean	St Dev	Mean	St Dev
01(4-14)	0.5715	0.0147	<u>0.5669</u>	0.0132	<u>0.5632</u>	0.0110	0.5713	0.0142
02(4-13)	0.7372	0.0150	<u>0.7357</u>	0.0124	<u>0.7325</u>	0.0104	0.7334	0.0141
03(1-7)	<u>0.7335</u>	.00065	0.7356	0.0084	0.7371	0.0068	<u>0.7358</u>	0.0074
03(8-16)	0.3738	0.0177	<u>0.3718</u>	0.0166	<u>0.3703</u>	0.0148	0.3757	0.0190
04(2-9)	0.5119	0.0207	<u>0.5090</u>	0.0147	0.5079	0.0204	<u>0.5072</u>	0.0143
05(3-9)	0.4876	0.0170	<u>0.4751</u>	0.0265	<u>0.4808</u>	0.0233	0.4898	0.0212
06(All)	<u>0.3512</u>	0.0133	0.3529	0.0090	<u>0.3472</u>	0.0103	0.3556	0.0071

Note: The underlined value indicates the smaller thickness in each comparison.

In Tables 6.2 and 6.3, the smaller mean value has been underlined for each member for both the top versus bottom and the inside versus outside comparisons. Thus, the underlined value, in each case, indicates the rays that seemed to exhibit more corrosion. From this underlining, it is apparent that there may be some tendency for corrosion to be somewhat more pronounced on the bottom of the member and on the outside perimeter of the structure. It is hypothesized that these trends may be plausible since the wave action may be more significant on the bottom and outside sections of the members. Experienced engineers working at the Morgan City yard also expressed a belief that there is a common trend for corrosion to be more evident on the outside perimeter of a structure (Landrum 1999).

The trends shown in Tables 6.2 and 6.3 are from simple observation alone, and do not necessarily reflect statistical significance. In particular, it is noted that the differences in mean thickness are quite small for most members, so that it is not easy to rule out the possibility that the apparent trends are only an artifact of random occurrences. The *t*-test

is used here to search for statistical significance, in much the same way as the ANOVA test was used for the ungrouped data. As explained in Section 2.3, the basic procedure tests the null hypothesis that there is no difference in the statistics of two sets of data against the alternative that there is a difference. The statistic used is found by dividing the difference in mean values by a standardized form of the variance estimated from the combined data. The underlying assumption is that the data are normally distributed, so that the test statistic has the so-called t -distribution if the two sets do have the same mean and variance values. This is tabulated in most statistics books. If the null hypothesis is true, then the mean of the statistic is zero. The alternative hypothesis can be taken to be that the two subgroups do not have the same mean, then a significant pattern can be indicated by either a positive or a negative value of the statistic. Alternatively, a "one-sided" alternative can be used, such that the null hypothesis is rejected only for a positive value or only for a negative value of the statistic

For each member, t -tables, similar to the ANOVA tables, were set up comparing the top three rays to the bottom three, and the outside three rays to the inside three. For Members 01, 02, and 03 (diagonal members), both samples had the same number of values. For Members 04, 05, and 06, the top and bottom samples had a different number of points since it was not possible to measure along ray A.

As in the ANOVA test, the number of primary interest in the t -test is the p value. In the present case, the p value represents the probability that the differences in the mean values could have occurred as a random event in the absence of a top-bottom or inside-outside pattern. A p value of 5% or less indicates a high probability that there are significant, verifiable differences between top and bottom sections and/or inside and outside sections. A p value between 5% and 10% may be considered to indicate marginally significant variations in the mean values.

As stated above, the two-sided probability corresponds to using the alternative hypothesis that the means are not the same. Based on industry opinion and the tabular results one can also justify consideration of a one-sided test in which the alternative is

that the outside is more corroded (thinner) than the inside. Similarly, the graphical results suggest that one might consider a one-sided alternative that the bottom is more corroded than the top. Caution should be used in selecting such one-sided tests, though. Particularly for the top vs. bottom comparison, the t -test will be performed on the same data as first suggested that the bottom might be more corroded. Using the same data to identify a trend and to test for its significance risks introducing an inappropriate bias in favor of statistical significance. For completeness, the p value results will be shown for both the two-sided and the one-sided tests, but **the two-sided values must be viewed as the more reliable, since they represent a completely unbiased analysis in the absence of any prior knowledge.** Summaries of all p values found in the t -tests are shown in Table 6.4.

The numerical values in Table 6.4 show that there is not any clear, repeated pattern of statistically significant circumferential thickness variation, either with respect to top vs. bottom, or outside vs. inside. The only members showing clear statistical significance were Members 01 and 06, for which the thickness was significantly less on the outer perimeter of the structure than it was toward the center of the structure. One can also consider the outside-inside p value for the one-sided test for Member 05 to have marginal statistical significance, and the corresponding value for rings 8-16 of Member 03 almost makes the 10% limit. The only possible significance of the top vs. bottom variations comes from the rather questionable one-sided test, which indicates only marginal significance for Members 01 and 05. Recall that the ANOVA results in Table 6.1 indicated that there were statistically significant circumferential patterns in Members 05 and 06, and a marginally significant pattern in Member 01. Thus, there is some measure of agreement between the ANOVA and t -test results.

**TABLE 6.4. Summary of *t*-test Results for
Circumferential Relationships**

Member (Rings)	Top vs. Bottom		Outside vs. Inside	
	Two-Sided <i>p</i>	One-Sided <i>p</i>	Two-Sided <i>p</i>	One-Sided <i>p</i>
01(4-14)	0.1792	0.0896	0.0112	0.0056
02(4-13)	0.6739	0.3369	0.7711	0.3856
03(1-7)	0.3716	0.1858	0.6701	0.3351
03(8-16)	0.5611	0.2805	0.2487	0.1244
04(2-9)	0.6043	0.3021	0.8962	0.4481
05(3-9)	0.1287	0.0644	0.2005	0.1003
06(All)	0.3850	0.1925	0.0010	0.0005

Note: The two-sided *p* value is the best unbiased test for a pattern.

In conclusion, then, it seems that there is not strong consistent statistical evidence showing either top-bottom or inside-outside patterns. The consistent differences in mean values shown in Tables 6.2 and 6.3 are usually too small to be statistically significant. In particular, the data do not provide any convincing statistical evidence for increased corrosion on the bottom side of a member, in spite of the relatively consistent pattern to that effect in the tables. The situation is slightly different for the outside-inside comparison, since two of the six members (01 and 06) did show significantly more corrosion on the outside of the structure, and this trend was in agreement with the mean values obtained for all six members, as well as with industry opinion. It seems quite likely that this is a truly repeatable trend, even though the magnitude is relatively small and the statistical evidence is not beyond question.

One can also seek another sort of statistical significance in the results from the grouped data. In particular, recall that the data in Table 6.2 show that each of the six members exhibited more corrosion on the outer side than on the inner side, and five of the six exhibited more corrosion on the bottom than on the top of the member. One can

determine the probability of observing such apparent patterns in the absence of any real pattern. This calculation involves only the binomial distribution, and is simply performed. The result is that there is little to no statistical significance to the apparent top-bottom pattern. There is approximately a 22% probability that at least five out of six measurements would be the same in the absence of any real pattern. On the other hand, there is only a 3% probability that all six measurements would simply happen to be the same in the absence of a true pattern. Thus, it does seem likely that the observed inside-outside pattern is a reflection of a meaningful trend, even though the thickness variation is small.

One can also perform this type of analysis for the reduced data sets of Table 6.3, for which each data set includes only measurements at locations with the same nominal thickness. The statistical evidence for a significant pattern of corrosion is not very strong for these data, though. In particular, five of the seven data sets exhibited more corrosion on the outer side than on the inner side, and five out of seven also exhibited more corrosion on the bottom than on the top of the member. The binomial calculations show, though, that there is over a 45% probability that at least five out of seven measurements would be the same in the absence of any real pattern. Thus, one must decide whether to accept the apparent top-bottom significance from Table 6.2 or the apparent lack of any significance from Table 6.3. Recall that the reason for using Table 6.3 in the t -test was the need of a standard deviation calculation, which would be made meaningless by a change in nominal thickness. Since standard deviation is not used in the present binomial calculation there is no reason not to use the data in Table 6.2. The other difference between the two tables is that the data sets are larger in Table 6.2. In general, of course, one obtains more reliable information from a larger data set. Thus, it is concluded that there does seem to be statistical significance to the perceived tendency for the corrosion to be greater on the outer perimeter of the structure and lesser toward the center of the structure. The evidence for this conclusion, though, must be regarded as relatively weak.

Recall, also, that sacrificial anodes were attached to Members 01, 02, and 03, to inhibit corrosion. It seems pertinent to note that the five anodes attached to these three

members were all attached on the bottom sides, near ray E. Thus, if proximity to an anode were a crucial factor in the corrosion, then one might expect the members to have larger thickness values on the bottom. In fact, though, Members 01, 02, and rings 8-16 of Member 03 all showed greater thickness on the upper rays. Even though there seems to be little if any statistical significance to the observed top-bottom differences, the data do confirm the conclusion reached in Chapter V, that proximity to an anode had no discernible correlation with corrosion in these members.

CHAPTER VII

ISSUES RELATED TO TESTING PROTOCOL

One of the primary goals of this study has been to identify a testing protocol that would be efficient in the sense of yielding a large amount of information about the structural integrity of a member based on a low-cost testing procedure. Two of the important aspects of this protocol can be identified as determination of the locations where thickness measurements should be made, and determination of the number of thickness measurements that are required. This chapter addresses aspects of both of these questions.

The issue of measurement location is addressed in Sec. 7.1 by considering whether and how the results of the statistical studies in Chapters V and VI can be used in identifying optimal measurement sites. In Sec. 7.2, the results from Sec. 2.3 are used in seeking to determine the number of measurements that must be made in order to characterize the condition of a particular member. In particular, statistical tests are used to determine how the accuracy of an estimate of the mean wall thickness obtained from a set of measurements is related to the number of measurements in the set. The discussion of axial load capacity of a corroded member, in Chapter III, is also relevant to both of these discussions, since the goal is to know the strength of the member.

7.1 Review of Corrosion Trends

Recall that the data presented in Chapters V and VI were based on several statistical approaches: ANOVA for both Z and θ dependence, linear regression for Z dependence, and the t -test for θ dependence in grouped data. It should be noted, though, that this information is not all of equal importance in the choice of a testing protocol. For example, it is of little use to know, based on ANOVA analysis, that there is a pattern of θ dependence, unless that pattern is sufficiently simple that it can be used in easily identifying the location at which corrosion is most likely to be large. Thus, the t -test is probably more useful than the ANOVA analysis for identifying θ dependence. In

particular, a pattern determined from the t -test of grouped θ data immediately yields information as to whether the corrosion is likely to be greater on the bottom than the top of the member, or whether it is likely to be greater on the perimeter than on the inside of the structure. The linear regression results regarding Z dependence could be particularly useful, in a similar way. A strong linear dependence, combined with a pattern that is both consistent and statistically significant, could be used to indicate that corrosion is more likely to be large near the bottom end of a diagonal brace, or near a corner leg of the structure, for example. Another useful alternative could be identification of a consistent pattern of having greater (or lesser) corrosion near the mid-length of a member than near the ends. This latter pattern of Z dependence would not be obvious from linear regression, but could be identified from the plots in Chapter V.

Graphical summaries will now be presented, combining the results of the various statistical analyses of the thickness data, as presented in Chapters V and VI, but with the emphasis being placed on the existence of useful trends, rather than simple statistical significance. Fig. 7.1 shows the two Forest structures together, as they were *in-situ*. The corrosion in Member 01, as shown, exhibited possibly useful trends in both Z dependence and θ dependence. First, the wall thickness increased significantly from the top end (inner leg) to the bottom end (outer leg) -- indicated by "more corrosion" and "less corrosion," respectively. Also, the wall thickness was significantly greater on the side toward the center of the structure than it was on the outer perimeter of the structure. Even though the Z dependence of the corrosion in Member 02 was statistically significant, it is not very useful. There was a moderate trend for the corrosion to increase from the top end (outer leg) to the bottom end (inner leg), but the maximum corrosion was not near either end of the member. Member 02 did not exhibit any useful θ dependence of corrosion. Member 04 did not show any useful pattern of either Z or θ dependence, and there was only marginal significance to the trends in Member 05 of having greater corrosion near the inner leg and on the bottom surface.

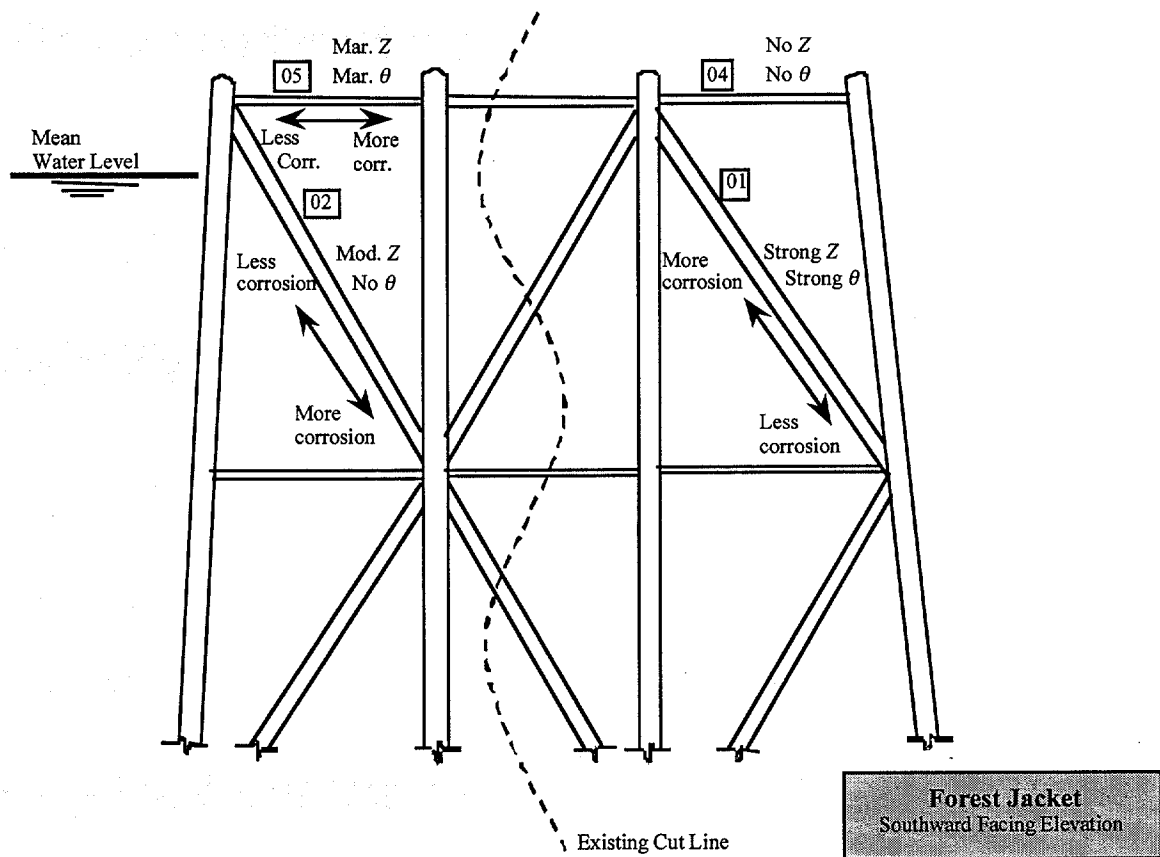


FIG. 7.1. Summary of Corrosion Trends, Forest Jacket

The corrosion trends found in the Santa Fe jacket are summarized in Fig. 7.2. Recall that Member 03 had a nominal change in thickness near mid-length (between rings 7 and 8). The lower section of this member showed strong Z dependence, changing from thicker to thinner from mid-length to bottom. There was no Z dependence evident in the top section, however, and no significant θ dependence along the entire length of the member. Member 06 showed no Z dependence, but a strong θ dependence, with more corrosion appearing on the outer perimeter of the structure.

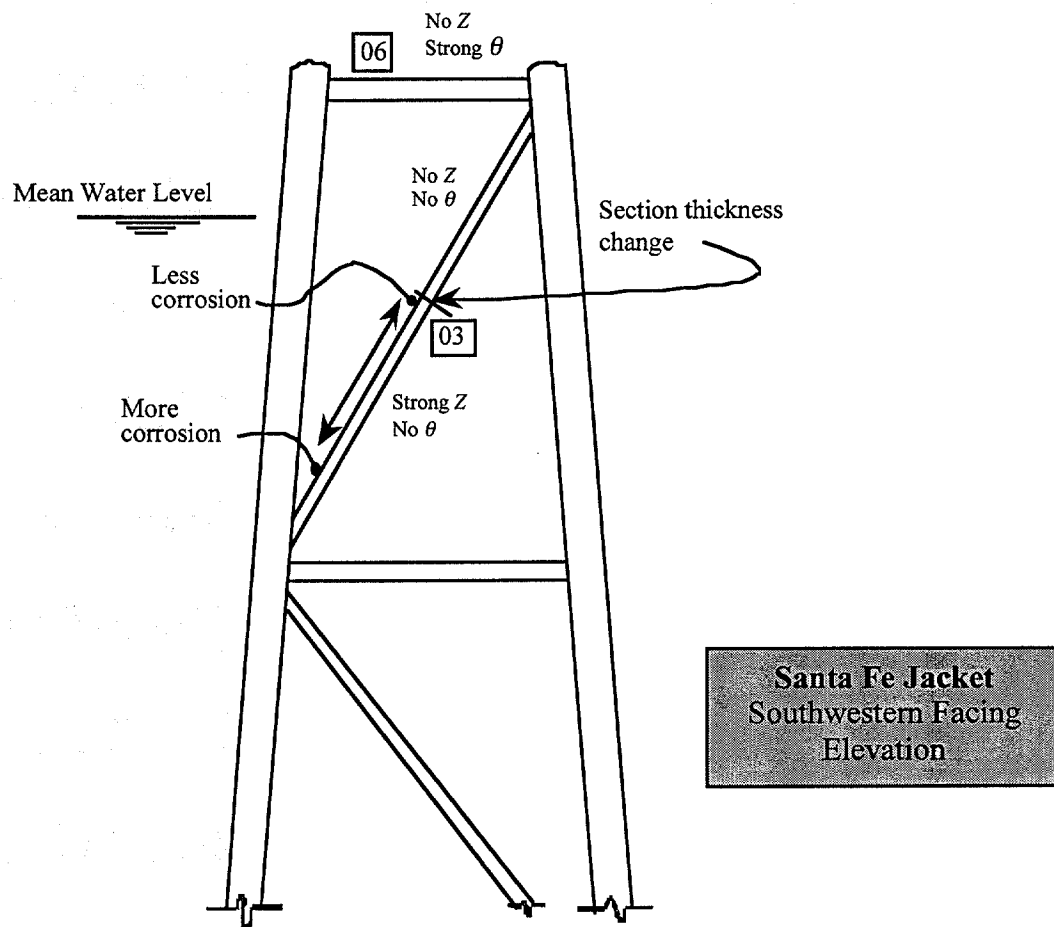


FIG. 7.2. Summary of Corrosion Trends, Santa Fe Jacket

Fig. 7.3 graphically summarizes the circumferential trend found in Chapter VI. It was shown that the thinnest section (more corrosion) tends to be along the outside perimeter of the structure (facing the waves), while the thicker regions (less corrosion) tend to be toward the inside of the structure. However, it is important to note that these conclusions are not very firmly founded on statistical analysis. The trend existed in each of the six members studied, but the *t*-test results were statistically significant for only two of the members (Members 01 and 06).

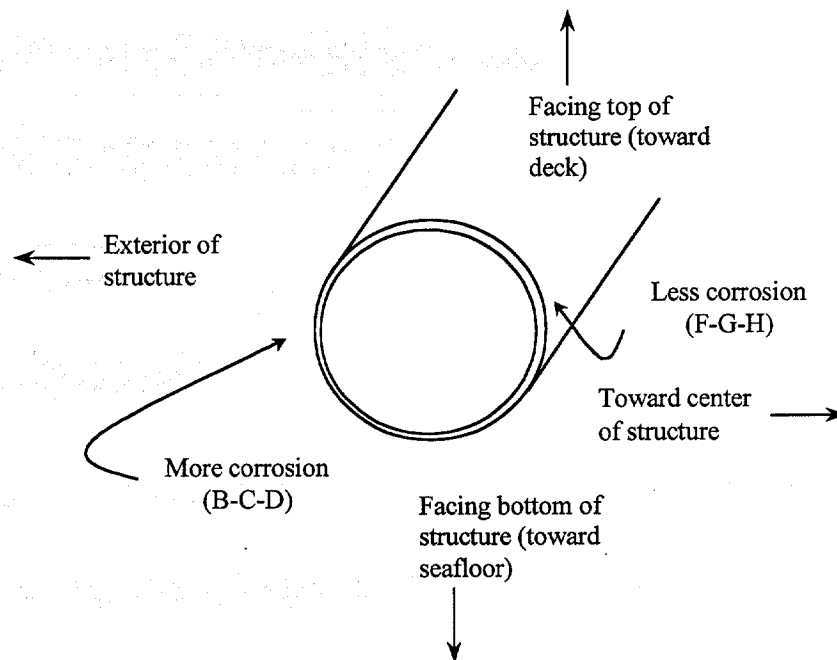


FIG 7.3. Thickness Comparison Summary

7.2 Effect of Sample Size on Detection of Strength Loss

In Chapter III, the loss of strength of members due to loss of wall thickness was presented. The loss of strength has been related to the corrosion ratio ϵ/t and the length to diameter ratio KL/D , where ϵ is the maximum loss of wall thickness, t is the nominal wall thickness, KL is the effective length, and D is the nominal diameter for the member. The reduction in strength due to loss of wall thickness was based on analyses considering incipient yielding, inelastic buckling and Euler buckling. It is now important to consider the matter of determining how many data points (n) are required to "reliably" detect a significant value of the loss ratio ϵ/t . Of course, there are several variables involved in answering this question, such as member length, diameter, nominal wall thickness, and the mean and standard deviation of the thickness data. Not all of this information is available *prior* to a thorough UT study (e.g., data mean and standard deviation). However, based on analysis of the Morgan City data, general information regarding reliable sample sizes may be gained.

Ideally, one would wish to be able to evaluate the correct number of data points to be taken on a given member without prior knowledge of sample mean and standard deviation, so that a decision could be made before taking data. As shown in the probability development in Sec. 2.3, however, this is not feasible. Therefore, the results from the Morgan City data analysis will be used here to make some general observations. In particular, the sample mean and standard deviation values from the data presented in Chapter IV will be used, along with various hypothetical choices for the sample size n , to demonstrate the effects of having fewer data points. The goal is to determine the smallest number of data points that will be sufficient for making the thickness assessment.

As outlined in Sec. 2.3, one can compute a sort of lower bound for the overall average value of the thickness of the member (at all points) by using known values of the sample mean (\bar{t}) and sample standard deviation (s) from a finite sample, along with values for the T -distribution. The number t_0 computed in this way approximates a lower bound for the average thickness in the sense that there is a low likelihood that the true value of the average is less than t_0 . For the purposes of this study, the parameter α has been given the commonly used value of 0.05, so that one has 95% confidence that the true average value is greater than the computed t_0 . Values of \bar{t} and s have actually only been measured for one value of the sample size (n) for each member in this study. Nonetheless, one can obtain some idea of the effect of sample size by assuming that these \bar{t} and s values will also apply for some samples of other sizes. Table 7.1 shows such results for all seven sets of data analyzed in this study, that is, two sets of data for Member 03 and one set of data for each of the other members. These values have been calculated from the values in Table 2.1, using the t -distribution equation given there.

TABLE 7.1. Thickness Bounds from Reduced Samples ($\alpha = 0.05$)

	Member (rings)						
	01 (4-14)	02 (4-13)	03 (1-7)	03 (8-16)	04 (2-9)	05 (3-9)	06 (1-9)
\bar{t}	0.5690	0.7353	0.7356	0.3728	0.5084	0.4834	0.3522
s	0.0137	0.0133	0.0079	0.0170	0.0167	0.0227	0.0095
actual n	88	80	56	72	56	49	63
actual t_0	0.567	0.733	0.734	0.369	0.505	0.478	0.350
Alternative Possibilities							
n	t_0						
2	0.508	0.676	0.700	0.297	0.434	0.382	0.310
3	0.546	0.713	0.722	0.344	0.480	0.445	0.336
4	0.553	0.720	0.726	0.353	0.489	0.457	0.341
5	0.556	0.723	0.728	0.357	0.492	0.462	0.343
6	0.558	0.724	0.729	0.359	0.495	0.465	0.344
7	0.559	0.726	0.730	0.360	0.496	0.467	0.345
8	0.560	0.726	0.730	0.361	0.497	0.468	0.346
9	0.560	0.727	0.731	0.362	0.498	0.469	0.346
10	0.561	0.728	0.731	0.363	0.499	0.470	0.347
20	0.564	0.730	0.733	0.366	0.502	0.475	0.349
40	0.565	0.732	0.734	0.368	0.504	0.477	0.350
60	0.566	0.732	0.734	0.369	0.505	0.479	0.350

The t_0 values in Table 7.1, which are values that are almost surely exceeded by the true average wall thickness, can be compared with some critical thickness that would result in a certain percentage loss in strength of the member, by using the analysis in Chapter III. The discussion here will focus only on the possible accuracy in finding a lower bound for the average wall thickness. For example, the original data set for

Member 01 had measurements at 88 points and gave $t_0 = 0.567$ inches. Thus, one can say with 95% confidence that the true average thickness over the entire member was at least 0.567 inches. The first row in the "Alternative Possibilities" portion of Table 7.1 is for only two data points, and if these two data points had the same \bar{t} and s values as the original data, then one could say with 95% confidence that the true average wall thickness was at least 0.508 inches. Comparing this with the original confidence bound of 0.567 inches shows the penalty paid for use of a smaller data set. Note, for example, that using only 5 data points gives the confidence bound as 0.556 inches, which is quite close to the 0.567 value obtained for $n = 88$.

The pattern observed for Member 01 is basically repeated for each of the other members. In almost all cases, using measurements at only 5 or 6 locations would yield a t_0 lower bound value that was within 0.01 inches of the value obtained for a sample of size 60. Thus, these numbers suggest that little loss in accuracy in the predicted member strength would result from using a quite small number of measurements. The one mild exception to this conclusion is for Member 05, for which one would need 9 measurements to determine t_0 within 0.01 inches of the value found with 60 measurements. This member does serve to illustrate the limitation of the conclusion about the efficacy of small samples. In particular, one notes that the sample standard deviation for Member 05 is larger than that for any of the other members, and the formula in Chapter II gives the error in choosing t_0 (for any given n value) as being proportional to this standard deviation. Thus, the sample size should, ideally, be increased on any member which gives a large value of the sample standard deviation.

It is important to remember the assumptions used in this analysis. Most importantly, these are generalizations, and are not exact, because fixed values for sample mean and standard deviation were assumed in the estimations. In fact, these values would change for each new choice of the random sample. For the present case, they were held fixed at the values given from the original Morgan City data given in Chapter IV. Given these assumptions, however, it is insightful to see that using significantly fewer

measurements would result in only small changes in the estimates of strength loss due to wall corrosion.

The results from Sec. 2.1 can also be used to identify the sample size necessary to give a specified accuracy for a member with a particular observed value of the standard deviation. In particular, the formula in (2.2) makes it clear that the discrepancy between the observed mean thickness, \bar{t} , and the 95% bound on the true mean thickness, t_0 , is equal to $sT_{0.05,n-1}/\sqrt{n}$, in which s denotes the standard deviation of the thickness measurements. Figure 7.4 shows a plot of n versus s for three different values of the "error bound," $(\bar{t} - t_0)$.

To illustrate the use of Fig. 7.4, consider Member 05. Table 7.1 gives the s value for this specimen as 0.0227. From Fig. 7.4, then, one can see that a sample size n of about 15 will give $\bar{t} - t_0 = 0.01$, so that one could have 95% confidence that a sample of 15 measurements would give a \bar{t} value that was within 0.01 inches of the true mean value for the specimen. This agrees with the values in Table 7.1, which also shows that a sample of size 60 for this specimen would give a \bar{t} value that was within 0.004 inches of the true mean. Similarly, if one wants an error bound of 0.02 inches, and if the first five measurements give a standard deviation value of $s = 0.03$ inches, then Fig. 7.4 shows that it would be appropriate to make three more measurements, so that the final sample size would be $n = 8$.

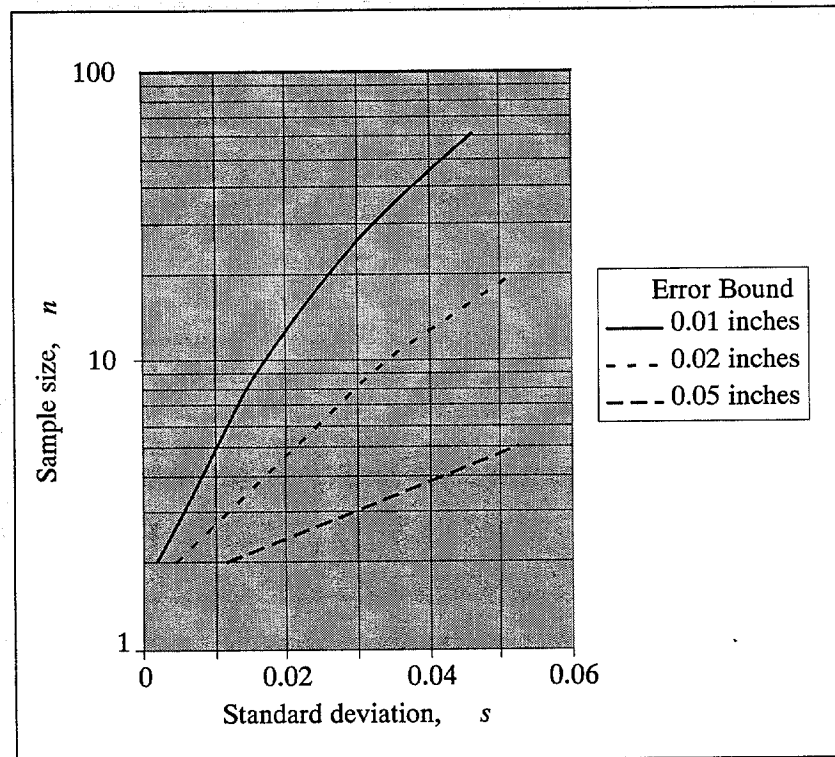


FIG. 7.4. Sample Size to Give Prescribed Error Bound

7.3 Summary

The only consistent corrosion trend identified in Sec. 7.1 was a slight tendency for the loss of wall thickness to be greater on the side of the member that was on the outer perimeter of the structure. In order to obtain a conservative estimate for the strength of a member, based on this observation, it seems desirable to concentrate the thickness measurements on the outer perimeter. This procedure should maximize the probability that the ε/t ratio observed is a good representation of the most corroded portion of the member. It should also be recalled that some of the members exhibited strong longitudinal patterns of corrosion, with the variation sometimes being primarily linear. There was not any consistent pattern allowing reliable prediction of the location of maximum corrosion, but this observation also has significant implications. It seems that measurements should always be distributed along the length of the member, including

some near each end and some near the mid-length. The alternative of measuring only near one end, for example, would allow the possibility of only making measurements on the least corroded portion of a particular member.

Finally one must choose the number of measurements to make on any given member. Based on the data in Sec. 7.2, it appears that an ideal protocol would involve a two-stage decision making process. It appears that a sample of 5 or 6 measurement locations would be an appropriate initial value to use on any member. Then one would calculate the sample standard deviation for this set of measurements. If that standard deviation were found to be small, then that small number of measurements might be judged to be adequate, while a large sample standard deviation would probably suggest the need for a larger set of measurements.

CHAPTER VIII

SUMMARY AND RECOMMENDATIONS

The basic objectives of this research project, as discussed in Chapter I, were:

- determination of the feasibility of using ultrasonic thickness (UT) measurements for assessment of corroded members in offshore structures,
- identification of any common patterns of corrosion in these members, which might be used in designing a more effective assessment protocol, and
- determination of the amount of data needed for meaningful assessment.

These objectives were fulfilled using UT measurements taken with a Panametrics 26DL Plus device on a set of six specimens during a field study in Morgan City, Louisiana. These members were in place within jacket structures that had recently been salvaged from their offshore environment in the Gulf of Mexico. The structures were in the offshore fabrication yards of J. Ray McDermott, Inc. in Morgan City. The six members chosen for study were located within three structures, with one diagonal member and one horizontal member analyzed in each structure. The diagonal members passed through the mean water level, and the horizontal members were within the splash zone. Extensive UT measurements were made on all members, and all data were logged with the UT device. Several statistical tests, including ANOVA, linear regression, and a *t*-test were performed on the data in the search for consistent, significant patterns in the corrosion.

In addition, analyses were performed to relate loss of wall thickness and the remaining compressive strength of a corroded member. These analyses included consideration of Euler buckling, inelastic buckling, and onset of yielding in a member with unsymmetric corrosion.

8.1 Summary

The strength analyses in Chapter III demonstrated that it is acceptable to use the API design formulas to predict member strength, even if the corrosion is not symmetrical. In particular, the API design formula to protect against inelastic yielding is sufficiently conservative that it gives an adequate strength value even for such an unsymmetric member. A limiting condition was analyzed in which the corrosion was unsymmetric and also varied along the length of the member in such a way as to maximize the bending moment due to eccentricity. Even for this extremely unlikely pattern of corrosion, the onset of yielding was for a load that was only 7% below the inelastic buckling load according to the API formula.

Since the API formulas for symmetric members are sufficiently conservative, there is no need to seek patterns of corrosion in the application of UT testing to actual structures. Rather, one should seek a conservative (i.e., lower bound) estimate of the remaining wall thickness of the member, then use the API formulas to predict strength for a member with that value of wall thickness, proceeding as if the thickness were the same everywhere. This does not preclude the use of patterns of corrosion, though, in designing the testing protocol. To the contrary, if the location of maximum corrosion can be predicted, then that is surely the location where UT measurements should be taken in order to obtain the lower bound estimate of wall thickness. Thus, the test results were analyzed for any significant, consistent patterns that could be used in devising an efficient protocol for testing.

No conclusive evidence was found for useful variations of corrosion along the length of the members. The ANOVA analyses did show very small probabilities that the thickness variations with Z could be strictly random for the diagonal members (Members 01 and 02, and the lower half of Member 03), and regression showed that some of these variations had substantial linearity. However, the trends were inconsistent, or contradictory, with one member experiencing maximum corrosion near its top end, one being most corroded near the bottom end, and one having maximum corrosion away from both ends. Thus, it was not possible to conclude that measurements at either end or at the

mid-length would consistently give a conservative lower bound of the member's wall thickness. In fact, the data indicated that the opposite was true, and that one should take measurements along the length of a member. For the horizontal members (Members 04, 05, and 06), the Z dependence was small enough that it had no more than marginal statistical significance. One must accept the possibility that the apparent patterns observed in these members simply occurred as random events. Overall, it is concluded that one should take measurements along the length of each member, including measurements near each end, in order to avoid the possibility of only taking measurements at a location with minimal corrosion.

The variation of corrosion around the circumference of the members was analyzed in two different ways. ANOVA analysis was used to seek for any form of statistically significant θ dependence, and a t -test was used in a search for useful patterns. In particular, the t -test was applied to grouped data, so that the top of a member could be compared with the bottom, and the side toward the center of the structure could be compared with the side on the outer perimeter of the structure. The statistical significance for the existence of useful circumferential patterns of corrosion is not high. Only two of the six members (Members 05 and 06) demonstrated more than marginal significance in the ANOVA tests, and only one of these (Member 06) also had more than marginal statistical significance in the t -test of grouped data.

However, a specific, repeated θ dependence was observed in the grouped data. In particular, each of the six members had more corrosion on the side located on the outer perimeter of the structure than it did on the side toward the center of the structure. Even though, the variations were small, it does appear that this may be a reliable trend that can be used in a testing protocol. Also, five out of six members had more corrosion on the lower side than on the upper side. This top-bottom variation is not statistically significant, though, since there is approximately a 22% probability that at least five out of six measurements would be the same in the absence of any real pattern. The inside-outside trend observed also agrees with an opinion held within at least some segments of

the offshore industry, and may be related to the exposure to waves when the structures are in place in the Gulf of Mexico.

It was suspected that corrosion might be negatively correlated with the proximity to a sacrificial anode. Thus, the anode positions were noted, but it was observed that they had no apparent effect on corrosion thickness trends. The maximum corrosion along the length of the members was sometimes located away from the anode or anodes, but it was sometimes very near an anode. Also, as noted above, the maximum corrosion usually occurred on the lower sides of the members, even though the anodes were all located on the lower sides as well. Apparently the anodes were sufficiently close together on these structures that there were no areas experiencing excessive corrosion because of lack of cathodic protection.

Statistical analyses were also used in an effort to determine the sample size needed to obtain reliable predictions of the strength loss due to corrosion in tubular members. It would be desirable to choose the optimal sample size prior to making measurements on a given member, but the answer is heavily dependent on the standard deviation of the thickness variation for the member. For the purposes of this study, it was assumed that the standard deviation values observed for the Morgan City members were typical, and this allowed some generalization on the problem. A statistical *t*-distribution was used to identify a thickness level that could be treated as lower bound for each member, since there was 95% confidence that the true mean thickness exceeded this value. These lower bounds on wall thickness could then be used to identify bounds on the loss of strength due to corrosion of the member. It was confirmed that detection of corrosion is always less certain as fewer data points are used, but it was also shown that using only five or six points can often give results which may be quite adequate in practice. If this small number of data points detects a large standard deviation in thickness for the member, though, then one may wish to obtain more data points. In particular, a plot has been given that can be used to determine a sample size that will give a prescribed error bound for a member with the observed value of the standard deviation.

Based on the results of this research, it is apparent that UT is a feasible tool for assessment of wall thickness in aging offshore structures. Konen (1999) found that the random errors in the results obtained from such an instrument are small enough to allow reliable measurements of wall thickness. In particular, the standard deviation values for repeated measurements at a given location on a given specimen were less than 0.001 inches for clean bar stock and less than 0.01 inches for badly corroded members. The measurement error is expected to be within these bounds for members of interest within existing structures. Further, with proper knowledge of the instrumentation, readings may be taken quickly and efficiently. The strength analyses showed that there is no need to identify corrosion patterns within the member being assessed, and it was found that estimation of only the average wall thickness can often be done quite reliably with relatively few data points. The pattern observed in the members studied reinforced an existing opinion that it is prudent to concentrate the UT measurements on the side of the member most exposed to waves from the open sea, in order to obtain a conservative estimate of the wall thickness. The measurements should be distributed over the length of the member, since corrosion can have a significant longitudinal variation that cannot be predicted *a priori*.

8.2 Recommendations

It is recommended that UT be seriously considered as a method of assessing the extent of corrosion in members in aging structures. This could be done in inspections of structures *in situ* in the sea, or in determining the condition of members within a structure being rehabilitated onshore before being put back into service. For any given member, it is recommended that five or six measurements be taken initially, and that the measurement locations be distributed over the length of the member, but concentrated on the side of the member most exposed to waves from the open sea. If the standard deviation of the measured wall thickness values is small, then this will yield a good estimate of the lower bound of the average wall thickness for all locations on the member. If the standard deviation is large, then the lower bound may be overly conservative unless more independent measurements are obtained.

Certain recommendations may also be made regarding the possible benefits of future research. Only six specimens were used in the field study described in Chapter IV. A larger data sample might lead to more conclusive results about the existence of significant corrosion patterns. However, this would require a **much** larger sample size. For example, the results here showed some contradictory and some inconclusive results for Z dependence. If twice as many members were used, then it would still be difficult to single out any definite corrosion trend supported by statistical evidence, even if the new members were consistent with each other, since the current data would still be part of the total data set. A sample on the order of 100 members might give substantially more conclusive results, but such a task is probably not justified, since the cost would probably exceed any financial benefit.

Additionally, it is quite possible that more information could be gathered by studying members having more corrosion than was found in the members studied here. In particular, different results might be obtained from flooded members having holes leading to increased corrosion on interior surfaces. Similarly, members with more dents might have more corrosion on both internal and external surfaces. Studying such badly damaged members, though, might have little practical significance, since it would often be obvious that they should be replaced or repaired. For example, there might be little value in knowing the remaining wall thickness of a member if it were already obvious that it should be filled with grout in order to give it greater strength.

REFERENCES

- API (1993). *Recommended Practice for Planning, Designing and Constructing Fixed Offshore Platforms – Load and Resistance Factor Design*, RP 2A-LRFD, American Petroleum Institute, Washington, DC.
- Bea, R., Puskar, F., Smith, C., and Spencer, J. (1988). "Development of AIM (Assessment, Inspection, Maintenance) programs for fixed and mobile platforms," *Proceedings Offshore Technology Conference*, Houston, TX, 2, 193-205.
- Ellison, B.K. (1999). *Ultrasonic Thickness Testing Of Aging Offshore Structures*, Master of Science Thesis, Texas A&M University, College Station, TX.
- Freund, J. (1984). *Modern Elementary Statistics*, 6th ed., Prentice Hall, Englewood Cliffs, NJ.
- James K. Dodson Co. (1993). *DDS RPT-145*. Grapevine, TX.
- Hennegan, N., Abadie, W., Goldberg, L., and Winkworth, W. (1993). "Inspections, surveys and data management," *Proceedings International Workshop for Assessment & Requalification of Offshore Production Structures*, New Orleans, LA, 55-63.
- Holdsworth, R., and Townley, D. (1999). "Corrosion protection of fixed offshore structures," *Proceedings International Workshop on Corrosion Control for Marine Structures and Pipelines*, Galveston, TX (to appear).

Konen, K.F. (1999). *Ultrasonic Thickness Measurements on Corroded Steel Members – A Statistical Analysis of Error*, Master of Science Thesis, Texas A&M University, College Station, TX.

Landrum, T. (1999). Personal Communication, J. Ray McDermott, Inc., Morgan City, LA.

Lewis, J., and Mercer, A. (1984). *Corrosion and Marine Growth on Offshore Structures*, Ellis Horwood Limited, Chichester, West Sussex, England.

Lotsberg, I. (1993). "Requalification of offshore platforms," *Proceedings International Workshop for Assessment & Requalification of Offshore Production Structures*, New Orleans, LA, 5-16.

Moehlman, S. (1990). *Testing and Evaluation of Damaged Tubular Jacket Braces*, Master of Science Thesis, Texas A&M University, College Station, TX.

Panametrics, Inc. (1996). *Ultrasonic Thickness Gage Instruction Manual*, Waltham, MA.

Potter, R. (1994). "Characterization of flaws in erosion corrosion by ultrasonic testing," *Materials Performance*, 33(2), 64-67.

Rubio, V. (1999). "PEMEX experience on corrosion control for offshore facilities at the Bay of Campeche," *Proceedings International Workshop on Corrosion Control for Marine Structures and Pipelines*, Galveston, TX (to appear).

Weiss, N., and Hassett, M. (1982). *Introductory Statistics*, Addison-Wesley Co., Reading, MA.

Wike, E. (1985). *Numbers: A Primer of Data Analysis*, Bell & Howell, Co., Columbus, OH.

Winkworth, W. (1993). "Requalification of offshore installations: A North Sea perspective," *Proceedings International Workshop for Assessment & Requalification of Offshore Production Structures*, New Orleans, LA, 45-51.